MIR-10A AS A MODULATOR OF PROLIFERATION AND CELL CYCLE PROGRESSION IN OVARIAN CLEAR CELL CARCINOMA

Kaitlyn Elizabeth Collins

Submitted to the faculty of the University Graduate School
in partial fulfillment of the requirements
for the degree
Doctor of Philosophy
in the Department of Biochemistry and Molecular Biology,
Indiana University

August 2024

Accepted by the Graduate Faculty of Indiana University, in partial fulfillment of the requirements for the degree of Doctor of Philosophy.

Doctoral Committee

Shannon Hawkins, M.D., Ph.D., Chair

Jaeyeon Kim, Ph.D.

May 30, 2023

Lindsey Mayo, Ph.D.

Kenneth Nephew, Ph.D.

Chi Zhang, Ph.D.

Teresa Zimmers, Ph.D.

DEDICATION

To my parents, Debbie and Jeff, for their unyielding support, sacrifices, and encouragement, which have helped me pursue my dreams.

To my grandparents, David and Helen, for their love and belief in me and for instilling in me my love of learning.

To my Aunt Sandy for helping guide me to my true passion of studying female reproductive tract diseases.

To all the members of the Hawkins Lab who helped me learn and grow over the last five years and will continue to help me throughout my life and career.

Finally, it wouldn't be me if I didn't thank my furry companions who were with me along the way: Buffy, Tiger, Lacey, Sammy (Miss Kitty), Chessie, Beau, Lily, Murphy, Sadie, and Finnegan.

ACKNOWLEDGEMENT

First, I want to acknowledge my career mentor, career model, research mentor, and committee chair, Dr. Shannon Hawkins. Thank you for accepting me into your lab and giving me the room and opportunities to make *many* mistakes and forge my own path while being there to help me all the times I needed it. Thank you for listening to my wild ideas, both good and bad, over the years. I greatly appreciate all your support and mentorship and am glad to have had the opportunity throughout my graduate education to learn from you.

Thank you to current and previous Hawkins Lab members: Dr. Jillian Wendel, Xiyin Wang, Dr. Yuliya Klymenko, and Jessica Kersey and current and past students: Adrienne Sowers, Stacey White, Maria Martinez, Noah Davis, and Hunter Quigley. Each person played a role in my dissertation project both being ears to listen to my ideas, helping troubleshoot experiments, and assisting with data collection.

Thank you to Dr. Chad Creighton and his laboratory at Baylor College of Medicine for miRNA:mRNA targeting software analysis. Thank you to Dr. Chi Zhang and Kaman So at Indiana University School of Medicine for their work on gene enrichment set analysis and pathway activation score analysis to compare the human transcriptomic dataset to OCCC human cell lines.

Thank you to the Medical Scientist Training Program directors and members for their support over the years. I owe Drs. Brittney-Shea Herbert and Maureen Harrington an extra thank you for their feedback and support while writing my dissertation.

Thank you to my committee members, Drs. Kim, Mayo, Nephew, Zhang, and Zimmers, for your encouragement and constructive conversations that improved my project and training.

Kaitlyn Elizabeth Collins

MIR-10A AS A MODULATOR OF PROLIFERATION AND CELL CYCLE PROGRESSION IN OVARIAN CLEAR CELL CARCINOMA

Endometriosis, a benign inflammatory disease whereby endometrial-like tissue grows outside the uterus, is a significant risk factor for endometriosis-associated ovarian cancers. In particular, ovarian endometriomas, cystic lesions of deeply invasive endometriosis, are a potential precursor lesion for ovarian clear cell carcinoma (OCCC). To explore the transcriptomic landscape, OCCC from women with pathology-proven concurrent endometriosis (n=4) were compared to benign endometriomas (n=4) by bulk RNA and small-RNA sequencing. Analysis of protein-coding genes identified 2449 upregulated and 3131 downregulated protein-coding genes (DESeq2, $P<0.05$, log2 fold-change$>|1|$) in OCCC with concurrent endometriosis compared to endometriomas. Gene set enrichment analysis showed upregulation of cell cycle regulation and DNA replication pathways and downregulation in cytokine receptor signaling and matrisome pathways. Analysis of miRNAs revealed 64 upregulated and 61 downregulated mature miRNA molecules (DESeq2, $P<0.05$, log2 fold-change$>|1|$). Hsa-miR-10a-5p represented over 21% of the miRNA molecules in OCCC with endometriosis and was significantly upregulated (NGS: log2 fold change=4.37, P=2.43E-18; QPCR: 8.1-fold change, $P<0.05$). Correlation between miR-10a expression level in OCCC cell lines and IC50 (50% inhibitory concentration) of carboplatin in vitro revealed a positive correlation (R2=0.92). The cellular function of miR-10a was investigated by overexpressing miR-10a in vitro. MiR-10a overexpression revealed a significant decrease in proliferation (n=6; $P< 0.05$), compared to a non-targeting control. Cell-cycle analysis revealed a

significant shift in cells from S and G2 to G1 in (n=6; P<0.0001). MiR-10a overexpression in vitro was correlated with decreased expression of predicted miR-10a target genes critical for proliferation, cell-cycle regulation, and cell survival [SERPINE1 (3.2 downregulated; P<0.05), CDK6 (2.4 downregulated; P<0.05) and, RAP2A (2-3 downregulated; P<0.05)].

Shannon Hawkins, M.D., Ph.D., Chair

Jaeyeon Kim, Ph.D.

Lindsey Mayo, Ph.D.

Kenneth Nephew, Ph.D.

Chi Zhang, Ph.D.

Teresa Zimmers, Ph.D.

TABLE OF CONTENTS

List of Tables x
List of Figures xi
List of Abbreviations xii
Chapter 1: Introduction 1
    1.1 Ovarian Cancer 1
        1.1.1 The Histological and Molecular Heterogeneity of Ovarian Cancers..........4
        1.1.2 Ovarian Cancer Treatment: Imprecise Effectiveness of Therapies 13
    1.2 The Importance of Endometriosis in Ovarian Cancer 16
    1.3 MicroRNAs in endometriosis and ovarian carcinomas 20
    1.4 Summary and Overall Aims of this Study 23
Chapter 2: Materials and Methods..........26
Chapter 3: Bioinformatic Analysis of Poly-A Transcriptomic Profiling of OCCC with Concurrent Endometriosis Compared to Endometrioma..........40
    3.1 Background..........40
    3.2 Results..........41
    3.3 Discussion..........67
Chapter 4: Small RNA Transcriptomic Profiling Identifying MiR-10a Overexpression and Its Relationship to Chemoresistance in OCCC 69
    4.1 Background..........69
    4.2 Results..........69
    4.3 Discussion..........85
Chapter 5: MiR-10a Overexpression Effects on OCCC Proliferation and Cell Cycle 87
    5.1 Background..........87
    5.2 Results..........88
    5.3 Discussion..........110
Chapter 6: Discussion 113
Appendix..........123
Bibliography 137
Curriculum Vitae 168

LIST OF TABLES

Table 2-1: Clinical characteristics of patient samples 27
Table 2-2: Primer Sequences used for qPCR expression..32
Table 2-3: Common characteristics for ovarian carcinoma cell lines used in experiments 36
Table 3-1: RNA Sequencing Reads Summary..44
Table 3-2: Gene Set Enrichment Analysis of upregulated genes 51
Table 3-3: Gene Set Enrichment Analysis of downregulated genes.................................54
Table 3-4: Genes dysregulated in OCCC and involved in cell cycle 57
Table 3-5: Cytokine genes that are dysregulated in OCCC 59
Table 3-6: Common characteristics of ovarian carcinoma cell lines used in experiments 65
Table 4-1: Small RNA Sequencing Summary 71
Table 4-2: Upregulated miRNA in OCCC compared to endometrioma............................73
Table 4-3: Downregulated miRNA in OCCC compared to endometrioma.......................75
Table 4-4: Top ten downregulated mature miRNAs in OCCC with concurrent endometriosis 79
Table 4-5: Top ten upregulated mature miRNA in OCCC with concurrent endometriosis 80
Table 5-1: MiR-10a Target Genes Identified by TargetScan 96
Table 5-2: MiR-10a Target Genes Identified by miRDB 98
Table 5-3: MiR-10a Target Genes Identifies with miRTarBase.....................................100
Table 5-4: WebGesalt miR-10a 103
Table 5-5: WebGesalt miR-10a pathways 104
Table 5-6: Putative miR-10a-5p target genes downregulated in OCCC with concurrent endometriosis within the receptor signaling pathway...................................106
Supplementary Table 1: Clinical characteristics and experimental use of patient samples..124
Supplementary Table 2: Gene Omnibus OCCC transcriptomic datasets cell lines 129
Supplementary Table 3: Gene Omnibus OCCC transcriptomic datasets primary tumor samples 133

LIST OF FIGURES

Figure 3-1: The OCCC with concurrent endometriosis transcriptomic profile is molecularly distinct from benign endometrioma 47
Figure 3-2: OCCC with concurrent endometriosis differentially clusters from benign endometrioma 48
Figure 3-3: Cell cycle and DNA replication/repair pathways are enriched in upregulated genes from OCCC with concurrent endometriosis 52
Figure 3-4: Matrisome and cytokine pathways are enriched in downregulated genes from OCCC with concurrent endometriosis 53
Figure 3-5: Molecular comparison of cell line transcriptomic profiles with clinical samples....64
Figure 4-1: OCCC with concurrent endometriosis is molecularly distinct from benign endometrioma using miRNA expression 72
Figure 4-2: MiR-10a-5p is significantly upregulated in human tissue samples of ovarian clear cell carcinoma 81
Figure 4-3: MiR-10a-5p expression across a panel of ovarian cancer cell lines 83
Figure 4-4: Expression of hsa-miR-10a-5p across OCCC cell lines 84
Figure 5-1: MiR-10a-5p is significantly overexpressed in SMOV-2 and KK cells transfected with a miR-10a-5p mimic....90
Figure 5-2: MiR-10a overexpression resulted in a significant decrease in cellular proliferation in SMOV-2 and KK cells....91
Figure 5-3: Overexpression of hsa-miR-10a-5p shifts cell cycle from S and G2 phase to G1....93
Figure 5-4: MiR-10a-5p potential target genes from MiRNA:mRNA target prediction software....102
Figure 5-5: Putative miR-10a target genes, involved in cellular proliferation and the G1/S checkpoint, are downregulated with miR-10a-5p overexpression 109
Figure 6-1: The working hypothesis for the mechanism of miR-10a-5p overexpression in OCCC G_0 or G_1/S Checkpoint....121

LIST OF ABBREVIATIONS

°C	degrees Celsius
ACTB	Actin Beta, Beta-Actin
ARID1A	AT-rich interaction domain1A
BC^2	Biospecimen Collection and Banking Core at the Indiana University Melvin and Bren Simon Comprehensive Cancer Center
BDNF	brain-derived neurotrophic factor
CA-125	Cancer antigen 125
CCLE	Cancer Cell Line Encyclopedia
CCNA2	Cyclin A2
CCNE1	Cyclin E1
CDK6	Cyclin dependent kinase 6
cDNA	complementary DNA
CDX2	caudal type homeobox 2
CHL1	cell adhesion molecule L1 like
CK7	cytokeratin 7 (keratin 7)
CKS2	CDC28 protein kinase regulatory subunit 2
cm	centimeter
CSRNP3	cysteine and serine-rich nuclear protein3
CW	Cyst wall
DMEM	Dulbecco's modified Eagle's medium
DNA	Deoxyribonucleic acid
EAOC	endometriosis-associated ovarian cancer
EnOC	endometrioid ovarian carcinoma
EOC	Epithelial ovarian cancer
Eoma	endometrioma
EPHA4	Ephrin type A receptor 4
FBS	fetal bovine serum
FDR	false discovery rate
FIGO	Federation Internationale de Gynécologie et d'Obstétrique
GEO	gene expression omnibus
GPCR	G protein-coupled receptors
GSEA	Gene Set Enrichment Analysis
H&E	hematoxylin and eosin
HGSOC	high-grade serous ovarian carcinoma
HNF-1β	HNF1 homeobox B
hr	hours
IC50	half-maximal inhibitory concentration
IHC	immunohistochemistry
IRB	Institutional Review Board
IUSCCC	Indiana University Melvin and Bren Simon Comprehensive Cancer Center
KRAS	Kirsten rat sarcoma virus
KRT20	keratin 20
KRT7	keratin 7

LGSOC	low-grade serous ovarian carcinoma
LIX1L	limb and CNS expressed 1 like
MDS	multidimensional scaling
miRNA	microRNA
mm	millimeter
MOC	mucinous ovarian carcinoma
mRNA	messenger RNA
NAPSA	Napsin A aspartic peptidase
ng	nanogram
NGS	next generation sequencing
nM	nanomolar
NRG BB	NRG Oncology Biospecimen Bank
NRG Oncology	National Surgical Adjuvant Breast and Bowel Project (NSABP), the Radiation Therapy Oncology Group (RTOG), and Gynecologic Oncology Group (GOG)
OCCC	ovarian clear cell carcinoma
PALM2-AKAP2	PALM2 and AKAP2 fusion
PAS	pathway activity scores
PBS	phosphate buffered saline
PCA	principle component analysis
PGR	progesterone receptor
PI	Propidium Iodide
PIK3CA	phosphatidylinositol-4,5-bisphosphate 3-kinase, catalytic subunit alpha
qPCR	quantitative polymerase chain reaction
RAP2A	RAP2A, member of RAS oncogene family
RIN	RNA integrity number
RNA	ribonucleic acid
RNA-seq	RNA sequencing
RORA	RAR related orphan receptor A
RT-PCR	real time polymerase chain reaction
SATB2	SATB homeobox 2
SERPINE1	Serpin Family E Member 1
SEM	Standard error of the mean
SKP2	S-phase kinase-associated protein 2
STR	short tandem repeat
TP53	tumor protein p53
UMAP	Uniform manifold approximation and projection
US	United States of America
USPSTF	United States Preventative Service Task Force
WT1	Wilm's tumor 1

CHAPTER 1: INTRODUCTION

1.1 Ovarian Cancer

Ovarian cancer is one of several gynecologic cancers, the most common gynecologic cancers being uterine, ovarian, cervical, vaginal, and vulvar cancers in the United States [1]. As of 2023, while more than 66,000 persons with a uterus will get uterine cancers and more than 19,710 persons with ovaries will get ovarian cancer in the United States (US), the estimated mortality rate for uterine and ovarian cancers is the same at about 13,000 deaths per year from each cancer, making ovarian cancer the deadliest gynecologic cancer for women in the United States [1].

Unlike other carcinomas, which have seen a decrease in mortality, such as a 43% decrease in breast cancer deaths since 1989 [2], ovarian cancer mortality has not decreased in over 20 years [1]. The difficulty in improving ovarian cancer mortality is multifactorial; however, two of the most clinically significant problems are: 1) late stage of diagnosis due to non-specific patient symptoms and lack of non-invasive screening tools and 2) the histological and molecular heterogeneity of ovarian cancer and the imprecise effectiveness of therapies.

Late-stage diagnosis of ovarian cancer causes and need for improvement

Due to non-specific and non-alarming symptoms in the abdomen and pelvis (*i.e.,* pain and bloating) [3-12], women may wait to seek medical care. Further, ovarian cancer might not be a highly ranked potential diagnosis on the healthcare provider's differential, leading to further delay of diagnosis and treatment and subsequent poorer outcomes [13-15]. In the Goff *et al.* 2000 National Ovarian Cancer Survey (n = 1725), of the women reporting symptoms, 65% reported symptom duration of six months or less before diagnosis, while 35% reported symptoms for seven months or longer before diagnosis [5]. This delay from symptom onset to diagnosis is highlighted in studies from the COVID-19 Pandemic, where delays in diagnosis by one month were attributable to 81 additional ovarian cancer deaths and a delay of six months, 464 additional deaths [16]. Thus, delayed diagnosis results in decreased survival. The lack of consensus on symptoms and screening tests to identify ovarian cancer largely contributes to the deficiencies in diagnosis. Improving screening tests and identification of early markers of disease (biomarkers) are crucial to decreasing mortality.

Non-invasive screening tools for ovarian cancer and need for improvement

Health screening tests can be used in asymptomatic populations to monitor for pre-cancerous results with further follow-up diagnostic testing, resulting in diagnosis at an earlier stage of the disease [17]. While screening tests are available for cervical cancer (pap smear), colon cancer (colonoscopy), and breast cancer (mammogram) [17], for example, screening tests for ovarian cancer have been studied [18-21] and, unfortunately, none so far meet adequate criteria so that they are more beneficial than their risk of harm [22-24]. Previous studies have looked at three main potential screening techniques for early diagnosis of ovarian cancer: 1) gynecologic exam [18, 19], 2) serum cancer antigen 125 (CA-125) [20, 21, 25], and/or 3) ultrasound [21-23, 25]. Unfortunately, while some of these trials report a significant or non-significant increase in epithelial ovarian cancer diagnosis, they have not found a significant decrease in mortality in the women undergoing screening [22, 23, 25].

CA-125 was first described by Bast *et al*., where they found a monoclonal antibody, OC125, that reacted with tumor cells from 6/6 epithelial ovarian cancer cell lines and tumor cells from ascites fluid of 7/11 patients with ovarian cancer [26]. CA-125 is thought to be used as a screening and/or diagnostic tool for ovarian cancer. However, by definition, it is, in fact, a poor screening tool for ovarian cancer, as it is not effective in asymptomatic and early-stage detection of the disease. Rather, CA-125 has more clinical benefit in monitoring the recurrence of disease in women being treated for ovarian cancer [27]. While CA-125 is elevated in 80% of ovarian cancers [27, 28] and 90% of advanced-stage tumors [29], serum CA-125 is only elevated in 23-67% of early-stage tumors [29-31]. Further complicating the use of CA-125 as a biomarker for ovarian cancer is its variable expression in different subtypes of ovarian cancer. High-grade serous and endometrioid ovarian cancers generally have higher CA-125 levels, while the mucinous subtype of ovarian cancer has the lowest levels of CA-125 [27, 32]. Thus, CA-125 is not an ideal screening test alone for early disease.

Since CA-125 biomarker sensitivity and specificity are limited at the early stages of disease and ovarian cancer is a relatively low-occurring cancer, studies of CA-125 as a screening tool in women with average risk for ovarian cancer found a large number of false positives. A study by Moss *et al*. in 751 women and 48 men, found abnormal CA-125 in 29% of the women and 46% of the men [20]. Of the women with abnormal CA-125, only 20% were attributed to ovarian cancer [20]. False positives were attributed to other malignancies and benign gynecological diseases (*i.e.,* endometriosis and pelvic inflammatory disease) [20]. CA-125 levels can also be increased in various other cancers, including breast, endometrial, gastrointestinal, and lung [29]. Benign diseases of the uterus, ovaries, liver, and gastrointestinal tract may also have elevated serum CA-125 [29, 33].

Due to the high risk of harm and low benefit of screening the general population, the United States Preventative Services Task Force (USPSTF) practice guidelines recommend against the use of screening tests for ovarian cancer in the general population [34]. Therefore, there is a need to investigate the molecular landscape of ovarian cancer progression to identify better biomarkers for ovarian cancer screening tools.

1.1.1 The Histological and Molecular Heterogeneity of Ovarian Cancers

Ovarian cancer is surgically staged. Surgical staging means that the stage or extent of disease spread is decided at the time of surgery by evaluation of pathological specimens. The Federation Internationale de Gynécologie et d'Obstétrique (FIGO) criteria are used for staging female reproductive cancers, including ovarian carcinomas [35]. The October 2021 criterion considers the primary site of the malignancy, lymphatic system involvement, and metastatic sites [35].

Histologic Types of Ovarian Cancers

The most common types of ovarian carcinomas are epithelial ovarian carcinomas (EOC), comprising ≥ 90% of all ovarian carcinomas [36]. Less common ovarian malignancies, or non-epithelial ovarian cancers (<10%), consist of germ-cell tumors, sex cord-stromal tumors, metastatic lesions to the ovary, and other rare tumors [37]. Malignant germ-cell tumors are derived from the germ cells of the embryonic gonad and are histologically stratified into primitive germ-cell tumors and teratomas from dermoid cysts. Women with malignant germ-cell tumors are typically younger than 30 years of age at diagnosis and make up 1-2% of ovarian cancers [38]. Malignant sex-cord stromal tumors derive from sex cord and/or stromal cells and account for 3-5% of all ovarian cancers [37]. Sex-cord stromal tumors occur over a more comprehensive age range. Granulosa cell tumors, a subtype of sex-cord stromal tumors, are more common in peri- and postmenopausal women [37]. Non-epithelial ovarian cancers have a favorable prognosis, with a surgical removal of the ovary commonly being curative, with early-stage disease having a 95% 5-year survival [39].

EOC are divided into broad histological subtypes. The prevalence within the US is: high-grade serous ovarian carcinoma (HGSOC; 50-70%) [36, 40], ovarian clear cell carcinoma (OCCC; 5-25%) [41-43], endometrioid ovarian carcinoma (EnOC; 5-10%) [36], mucinous ovarian carcinoma (MOC; 3-10%) [44], and low-grade serous ovarian carcinomas (LGSOC; ~3%) [44]. Historically, EOC histological subtypes are categorized by histologic features of surgical specimens, although the field is moving toward molecular classification [45, 46]. Immunohistochemistry (IHC) staining for specific proteins can be subtype-specific, further aiding pathologists in classifying ovarian cancer subtypes (more below).

Histologic and Pathologic Features of EOC Subtypes

High-grade serous ovarian cancer (HGSOC)

On gross inspection, HGSOC can range in size from <1 cm to 20 cm. They can be purely solid or mixed with cystic components, commonly creating an irregular ovarian surface [47]. Grossly, papillary or finger-like structures can be seen throughout the tumor and can also contain poorly differentiated necrotic and hemorrhagic areas [47].

Microscopic inspection commonly displays a mixture of morphologies, such as “solid, complex glandular with slit-like spaces, cribriform, and papillary” [47]. Nuclei are atypical with eosinophilic nucleoli, and cells are frequently multinucleated with a high mitotic activity [47]. IHC staining that is indicative of HGSOC includes strong staining for tumor protein p53 (TP53) and Wilms’ tumor 1 (WT1) (>80% of tumors) [48, 49].

Low-Grade Serous Ovarian Cancer (LGSOC)

LGSOC were originally thought to be highly similar to HGSOC. However, the two types have distinct histologic and molecular profiling with distinct cells of origin. Women with LGSOC tend to be younger than women with HGSOC [50]. Unlike other non-HGSOC subtypes, LGSOC are commonly found on both ovaries at presentation. Like HGSOC, LGSOC are commonly solid in gross appearance, or they may have cystic masses with papillary structures. However, unlike HGSOC and other EOC, LGSOC typically do not contain grossly necrotic lesions [47].

Microscopically, LGSOC contain irregular, small nests of both microscopic and macroscopic papillae [47]. Invasion into the stroma is destructive, and cells have a low mitotic activity. Unlike other EOC subtypes, LGSOC commonly contain large numbers of psammoma bodies or calcifications [47]. These classifications are typically so abundant that they cause a gritty appearance to the tumor that can be seen on gross observation [47]. Immunohistochemically, LGSOC are largely similar to HGSOC where they positively stain for WT1 and may be negative for Napsin A aspartic peptidase (NAPSA) and progesterone receptor (PGR) stains [49]. However, unlike HGSOC, LGSOC largely do not stain for TP53 [49].

Endometrioid ovarian carcinoma (EnOC)

Grossly, EnOC is often unilateral and solid but may be cystic [47]. Histologically, EnOC tumors have two common growth patterns. The most common growth pattern is “expansile invasion,” where cells are confluent in a “back-to-back glandular proliferation” [47]. The glandular architecture contains a complex mixture of cribriform, villoglandular, or papillary patterns with a loss of intervening stroma [47]. The expansile invasion growth pattern is visually similar to endometrial endometrioid carcinomas. Less commonly, EnOC has a destructive stromal invasion growth pattern containing irregular glands, clusters of cells, or single cells that infiltrate the stroma [47]. Like HGSOC, EnOC cells have significant nuclear atypia. However, EnOC classically resemble endometrial glandular epithelium with pseudostratified, elongated nuclei and non-mucinous cytoplasm [47]. While EnOC and HGSOC can appear similar histologically and have been occasionally misidentified, with some HGSOC being recategorized as having a “pseudoendometrioid” pattern [51, 52], the use of IHC can provide a clear differentiation between the two subtypes. While both EnOC and HGSOC typically have absent staining for NAPSA, WT1, TP53, and PGR can be used to discern EnOC from HGSOC. Whereas HGSOC are typically positive for WT1 and TP53 and have more variable staining with PGR, EnOC typically do not stain with WT1 and TP53. EnOC tumors have a high positive staining for PGR [53]. EnOC can frequently be found in close proximity with endometriosis lesions and, as such, are considered an endometriosis-associated ovarian cancer (more below).

Ovarian clear cell carcinoma (OCCC)

OCCC can reach a similar size as HGSOC with a mean size of 15cm, but grossly, OCCCs are typically more cystic, and when sectioned, solid features may be hemorrhagic and necrotic [47]. Histologically, OCCC have a characteristic clearing of the cytoplasm with hematoxylin and eosin (H&E) stain due to their increased glycogen content. Microscopically, OCCC can contain three architectural patterns: tubulocystic with large cystic glands, papillary, and solid large sheets of tumor cells [47]. In contrast to HGSOC, OCCC tumors have low mitotic activity, but they still contain atypical nuclei and prominent nucleoli. In addition to “clear cells,” OCCC characteristically contains hobnail cells, which are round cells with “apical expansion of the cytoplasm by atypical nuclei.” Cyst walls are composed of cuboidal cells with eosinophilic secretions. The characteristic “clear cells” are surrounded by hyalinized, fibrous stroma in most tumors [47].

Like EnOC, OCCC tumors are negative for WT1 and TP53 staining [49]. While PGR staining is typical of EnOC, OCCC tumors have a more variable staining pattern, making PGR a poor identifier of OCCC. However, NAPSA is a characteristic positive stain for OCCC (>80%) [53]. HNF1 homeobox B (HNF-1β) is another characteristic IHC stain for OCCC, with studies reporting nearly 100% positive staining in OCCC tumors, whereas nearly 100% of non-OCCC tumors studied did not stain for HNF-1β [54]. OCCC are considered an endometriosis-associated ovarian cancer (more below) and frequently found near atypical endometriosis lesions (more below) [55].

Mucinous Ovarian Cancer (MOC)

MOC are often unilateral without metastasis at the time of presentation. MOC can be non-invasive (without a stromal component) or invasive once stromal invasion is measured at greater than 5 mm [47]. Grossly, mucinous tumors are quite large, typically > 10 cm, with their mean size of 18-22 cm [47]. Necrotic and hemorrhagic lesions may be present, but most commonly, the tumors have a multicystic pattern with solids areas. Like other ovarian carcinomas, MOC have two main patterns of invasion or growth. Expansile mucinous ovarian cancer characteristically contains confluent glandular growth without normal ovarian parenchyma [47]. The less common, destructive invasive MOC have irregular and atypical glands, nests, and single cells that infiltrate the stroma. MOC have moderate to marked nuclear atypia with increased nuclear to cytoplasmic ratio and commonly contain profuse goblet cells [47].

More unique to MOC is the potential to be misdiagnosed as gastrointestinal tract metastases [56]. This similarity to gastrointestinal metastases makes IHC classification markers beneficial for both the confirmation of mucinous subtypes of ovarian cancer and distinguishing MOC from metastases to the ovary. The standard clinical panel for distinguishing metastatic gastrointestinal lesions from primary MOC uses stains for keratin 7 (KRT7), keratin 20 (KRT20), and caudal type homeobox 2 (CDX2). However, a 2019 study by Meagher *et al*. found a combination of CK7 (positive in primary MOC) and SATB homeobox 2 (SATB2) (negative in primary MOC) staining could distinguish primary MOC from lower gastrointestinal metastases with 95% accuracy [57]. The algorithm proposed by Köbel *et al*. can be utilized to distinguish MOC from other EOC subtypes [53]. MOC commonly does not stain for WT1, distinguishing them from HGSOC [53]. Unlike OCCC tumors, most MOC tumors do not stain for NAPSA. PGR staining to further distinguish subtypes would be absent in MOC compared to EnOC [53].

Molecular Heterogeneity of Epithelial Ovarian Cancers

Each histologic subtype of epithelial ovarian cancer has distinct gross and microscopic histologic features (see above). However, more recently, multi-platform genomics approaches have been used to further categorize tumors, particularly in their *in vitro* derivatives (*i.e.,* human immortalized ovarian cancer cell lines), creating more distinct molecular subtypes [32, 45, 58-103].

The most studied histological subtype of EOC is HGSOC. HGSOC samples make up a majority of studies for both single subtype analyses and comparisons across multiple histological subtypes. Likely the most well-known of HGSOC molecular analyses is The Cancer Genome Atlas (TCGA) [64], but the other large bioinformatic analyses of ovarian cancer, performed by the Memorial Sloan Kettering Cancer Center (MSK-IMPACT and MSK-SPECTRUM) also include samples from women with HGSOC [104]. From TCGA analysis, four distinct transcriptional subtypes, three microRNA subtypes, four promoter methylation subtypes, and one transcriptional signature associated with survival duration were identified [64]. Transcriptional subtypes were: i) immunoreactive subtype is characterized by C-X-C motif chemokine ligand 11 (*CXCL11*), C-X-C motif chemokine ligand 10 (*CXCL10*), and C-X-C motif chemokine receptor 3 (*CXCR3*), ii) differentiated subtype associated with expression of mucin 1, cell surface associated (*MUC1*), mucin 16, cell surface associated (*MUC16*), and secretory leukocyte peptidase inhibitor (*SLPI*) and a more mature stage of development, iii) proliferative subtype has high expression of minichromosome maintenance complex component 2 (*MCM2*), proliferating cell nuclear antigen (*PCNA*), high mobility group AT-hook 2 (*HMGA2*), and SRY-box transcription factor 11 (*SOX11*) while having a low expression of *MUC1* and *MUC16*, iv) mesenchymal subtype containing high expression of HOX genes, fibroblast activation protein alpha (*FAP*), angiopoietin like 2 (*ANGPTL2*), and angiopoietin like 1 (*ANGPTL1*) [64].

The most common mutation seen in the HGSOC samples from TCGA is tumor protein P53 (*TP53; 96%*) [64]. However, further histological analysis of 14 of the samples not containing *TP53* mutations by five gynecologic pathologists collectively diagnosed 10/14 (71%) as non-HGSOC [105]. An additional two cases were considered not purely HGSOC or "represented a diagnosis other than high-grade serous," leading the authors to conclude that *TP53* mutations are essential to HGSOC and lack of *TP53* mutation is inconsistent with HGSOC diagnosis, and other classifications should be more closely considered [105]. Like in the TCGA HGSOC samples, *TP53* was the most frequently mutated gene and more frequently mutated in HGSOC than in all other cancer types (98%) in the MSK-IMPACT [106]. The second and third most frequent mutations in TCGA HGSOC are breast cancer gene 1 (*BRCA1,* 12%) and breast cancer gene 2 (*BRCA2,* 11%) [64].

While large HGSOC studies have found molecular subtypes within HGSOC, transcriptomic studies have also elucidated the molecular distinctions between the histological subtypes. For instance, transcriptomics has been instrumental in differentiating HGSOC and LGSOC as distinct types of EOC, as LGSOC were historically thought to be precursor lesions to HGSOC [60, 84, 107]. Studies have also used transcriptomic microarray to distinguish HGSOC and OCCC [92, 99, 108-117], with results including distinct immunomarkers (*i.e.,* Cyclin E, estrogen receptor, HNF-1B, Ki-67, p21, p53, and WT1) [109].

While OCCC samples may be included in the analysis, they are commonly not the focus of the study or results. However, transcriptomic studies of OCCC typically do not contain or do not define the endometriosis status of the women from which the samples were derived and/or were performed using *in vitro* models (*i.e.,* human cell lines) [54, 59, 111, 115, 118-126]. At the time of data collection for this dissertation began, only two transcriptomic analyses of concurrent OCCC and endometriosis were available, including plasma samples from 7 women with endometriosis and 3 with OCCC (2 had endometriosis on final pathology) [127]. The pivotal transcriptomic analysis by Wiegand *et al.,* analyzed 18 OCCC tumors, including 2 that were found to have contiguous atypical endometriosis on pathology [128]. Wiegand *et al.* found a crucial relationship in ARID1A expression in endometriosis and OCCC. In the two women with contiguous atypical endometriosis, ARID1A mutations were seen in both the OCCC and contiguous atypical endometriosis but not in the distant endometriosis lesions studied [128]. This supported the hypothesis that endometriosis is a precursor lesion for OCCC [128]. Since then, two more transcriptomic datasets have been published with OCCC and endometriosis [59, 129]. Of these two, Bolton *et al.* was the only one to contain samples of OCCC with concurrent endometriosis: n = 43, 6 of which were confirmed by pathology. While Wiegand *et al.* suggested a precursor relationship between endometriosis and OCCC, the molecular events leading to this transformation remain unknown.

1.1.2 Ovarian Cancer Treatment: Imprecise Effectiveness of Therapies

Ovarian cancer specimens can contain a mixture of histological subtypes or be classified as a single histologic subtype. Each histologic subtype has a unique molecular profile [130-133]. Although each epithelial ovarian cancer is molecularly and histologically heterogeneous, the standard-of-care therapy is largely the same. Overall, this standard of care therapy makes therapy nonspecific, imprecise (*i.e.,* lower precision), and thus, less effective. Thus, the overall heterogeneity of tumor histologic types makes treating a single disease "ovarian cancer" challenging.

A confirmed diagnosis of ovarian cancer is made with invasive testing (i.e., a biopsy of a suspicious mass) or primary surgery. The goal of debulking surgery for ovarian cancer is to remove as much tumor as safely as possible. Surgery for ovarian cancer is considered surgical debulking and/or cytoreduction, where the cervix, uterus, fallopian tubes, and ovaries are commonly removed along with the omentum and any other tissue involved in the disease (*i.e.,* lymph nodes). This may include the rectum, vagina, colon, and/or other abdominal organs [134].

Cisplatin was officially approved by the Food and Drug Administration in 1978 for the treatment of advanced ovarian cancers [135]. The landmark trial for cisplatin as a member of the first-line combination therapy in the treatment of ovarian cancers was a Gynecologic Oncology Group study published in 1986 (GOG #47) [136]. The 1986 trial followed up on the response of cyclophosphamide with doxorubicin compared to melphalan therapy without survival improvement (GOG #22) [137]. Cisplatin was added to cyclophosphamide and doxorubicin to evaluate the clinical response in advanced ovarian cancers. This study found a significant increase in complete response (51.4%

versus 25.8%; $P < 0.0001$) and a significant increase in progression-free survival (13.1 versus 7.7 months; $P < 0.0001$) with the addition of cisplatin [136]. However, they did not observe a significant increase in overall survival (19.3 versus 16.4 months). The authors attributed this to potential differences in the distribution of surgical debulking success, as they had a "wide spectrum of cases from minimally bulky to massive" [136]. The significant improvement in outcomes other than overall survival led to the continued study of cisplatin combination therapies.

The Impact of Chemoresistance in Ovarian Cancer Mortality

The leading cause of death in women with ovarian cancer occurs from chemoresistance (90%) [138]. Chemoresistance occurs when cancer cells do not respond to a drug meant to kill them. Resistance can be intrinsic or acquired after initial treatment [139]. Intrinsic chemoresistance exists prior to treatment, while acquired resistance is observed after treatment when cancers recur [140]. Intrinsic chemoresistance has been attributed to multiple factors: drug metabolism by enzymes, mutations at the site of a drug's target, variations in the membrane transport of the drug into the cancer cell, poor tumor vascularity affecting drug delivery, extracellular matrix interactions, and cellular metabolic processes [140]. Alternatively, acquired resistance is seen after an initial response to therapy. Acquired resistance can be related to increased mutations or selection of cells carrying a mutation decreasing the drug's effectiveness: increased drug efflux, activation of survival signaling pathways, and inactivation of DNA damage repair pathways avoiding cell death [140]. Chemoresistance in ovarian cancer is prominently in relation to platinum. The Gynecologic Oncology Group defined platinum response by a woman's time to disease recurrence after platinum therapy: platinum-free interval [141]. Women with a platinum-free interval of 6 months or more were considered to have platinum-sensitive disease and platinum-resistant disease if their platinum-free interval was less than 6 months [141].

Women with the more common HGSOC typically have a positive response to platinum-based first-line therapy (70-80%) [142, 143]. Unfortunately, chemotherapy resistance in women with HGSOC is more commonly acquired, developing over time (16-18 months) [143-147]. Recurrent HGSOC potentially responds to the reintroduction of platinum-based therapy, with 30-66% having a positive response [148, 149]. However, the positive response declines with each reintroduction of therapy, eventually resulting in these women's deaths [138]. On the other hand, chemotherapy resistance in OCCC is commonly intrinsic and present at initial therapeutic intervention. Up to 89% of women with OCCC do not respond to initial therapy (*i.e.,* progression on therapy) [150-154]. Women with OCCC have been found in multiple studies to have a worse prognosis and outcome than their stage-matched peers with HGSOC. Many of these studies have found this significant disparity most prominent in the later stages of disease (Stages III and IV) [153, 155-158]. However, another study by Ceppi *et al*. showed that while stage I HGSOC and OCCC have similar cancer-specific survival, OCCC has a significantly decreased post-relapse cancer-specific survival than HGSOC [159]. Taken together, the specific platinum-resistant and molecular features of OCCC need to be studied to hone in on new therapeutic options for women with OCCC.

1.2 The Importance of Endometriosis in Ovarian Cancer

Endometriosis

Endometriosis is a benign disease where endometrial-like tissue grows outside the uterus [160, 161], causing considerable morbidity, including pelvic pain, multiple operations, and infertility [160]. Women with endometriosis also have additional negative effects on their quality of life, such as increased incidence of depression, increased risk for chronic disease, and significant economic burden due to lost income and healthcare costs [162-168]. An estimated 10% of reproductive-aged women and girls are affected by endometriosis [160]. However, numbers may be higher as the definitive diagnosis of endometriosis requires pathological confirmation [161]. There are typically 4-11 years between symptom onset and diagnosis [164, 169-173], suggesting a higher rate of women affected by endometriosis that goes undiagnosed [174].

Theories of Endometriosis Development and Spread

While endometriosis was first described symptomatically in the Ebers Papyrus dating to 16th century BCE in Egypt [175], it wasn't until 1690 that it was described in more detail, including gross descriptions of adhesions and endometriomas during autopsies by Daniel Schrön [176]. In 1860 Karl Freiherr von Rokitansky was the first to give a histologic and pathologic description of endometriosis [177]. Although originally described centuries ago, the mechanism(s) of endometriosis development remains unclear. Many theories for developing endometriosis exist, including retrograde menstruation [178-180], coelomic development [181], Müllerian remnant [182-185], and lymphatic metastasis [186]. Though these theories have been around for decades, none have been sufficient to describe endometriosis pathogenesis, leading experts in the field of endometriosis to suggest they are insufficient on their own, and new theories should be proposed in order to improve the study of endometriosis [187].

Anatomic Locations of Endometriosis and Types of Endometriotic Lesions

Endometriosis has been identified in all organs of the human body except the spleen [188]. A simple classification system for endometriosis lesions includes superficial peritoneal lesions, cystic lesions of the ovary, and deep infiltrating endometriotic lesions [183, 189, 190]. The World Endometriosis Research Foundation (WERF) Endometriosis Phenome and Biobanking Harmonisation Project (EPHect) has developed a standard operating procedure tool used to classify lesions [191-194].

Superficial peritoneal lesions are ectopic endometrial-like lesions that extend less than 5 mm into the peritoneum or pelvic viscera [195]. Superficial peritoneal lesions are further characterized by their gross appearance during surgery [183]. Unlike deep infiltrating endometriosis and ovarian endometriomas, superficial peritoneal endometriosis is difficult to identify using non-invasive imaging modalities as they can be millimeters in size compared to centimeters-wide nodules seen in ovarian endometriosis [190]. Their incidence is unknown, but they have been considered the most common type of endometriosis, with some estimates as high as 80% [196]. However, some recent studies rank endometrioma as the most commonly occurring, followed by peritoneal lesions [197, 198].

Endometriosis of the ovary is a unique form of endometriosis called an endometrioma, found in 17-46% of women with endometriosis [198, 199] and 28% are present on both ovaries [199]. They are characteristically epithelial-lined cysts of the ovary containing thick brown and/or blood fluid ("chocolate cysts") [47]. Unlike superficial peritoneal endometriosis, endometriomas can be seen using transvaginal ultrasound and magnetic resonance imaging with high specificity and sensitivity [200] due to their ability to significantly increase the size of the ovary (>10 cm) [47].

Deep-infiltrating endometriosis is categorized by >5 mm extension into the peritoneum or viscera [201]. It is also histologically defined by a pattern of well-differentiated glandular cells, pure stoma, glandular or mixed differentiated cells, and undifferentiated glandular cells [201]. Deep-infiltrating lesions can be visualized in the rectum or rectovaginal septum using transvaginal ultrasound and magnetic resonance imaging [201].

Like ovarian cancers, endometriosis lesions are staged. While the staging systems contain similarities, such as size and location factoring into stage requirements, they differ in other areas. Four standard classification systems for endometriosis exist: the revised American Society for Reproductive Medicine (rASRM) score [202], ENZIAN classification [203], the endometriosis fertility index [204], and the American Association of Gynecological Laparoscopists classification [205].

Molecular Profile of Endometriosis and Similarities to OCCC

While considered a benign disease, endometriosis shares many hallmarks commonly attributed to malignancies [206], such as sustained proliferation, resistance to cell death, induced angiogenesis, invasive and metastatic potential, inflammation, and genetic mutations [207-210]. Cancer-driver mutations are frequently shown in endometriosis. Mutations with the highest reported rate in endometriosis include *ARID1A*

(50-70%) [211-216], *KRAS* (30-50%) [217], and *PIK3CA* (34-%) [215, 217], those commonly mutated in endometriosis-associated ovarian carcinomas, like OCCC [128, 211-215, 218-224]. Additionally, endometriotic lesions have been transcriptomically profiled in a number of studies [212, 217, 219, 225-228]. Endometriosis lesions are molecularly distinct based on their anatomic location and lesion type [216, 217, 229]. Endometriosis is also a significant risk factor for developing endometriosis-associated ovarian carcinomas, with EnOC, OCCC, and LGSOC being the highest risk [230]. With endometriosis at any anatomic location, OCCC risk increases 5.1-fold, and endometrioid ovarian carcinoma is a 3.1-fold increased risk [230-232]. The risk of malignancy is even higher in women with ovarian endometrioma, increasing the risk of ovarian endometrioid carcinomas by 4.7-fold and ovarian clear cell carcinomas by 10.1-fold [231]. Furthermore, endometriosis is reported in up to 50% of OCCC, and commonly, atypical endometriosis is appreciated during surgical debulking of malignant ovarian tumors [215, 225, 233, 234]. Atypical endometriosis is endometriotic lesions that contain cytologic atypia and/or hyperplasia. There have been multiple findings of a continuous transition of benign epithelial cells to atypical endometriosis to carcinoma in a single surgical specimen [128, 235-237]. When the molecular, pathological, and epidemiologic data are taken together, endometriosis, particularly atypical endometriosis and ovarian endometriomas, is a precursor lesion to OCCC [128, 218, 225, 230, 231, 235, 236, 238-245].

Studies have shown a unique transcriptional profile of EnOC with concurrent endometriosis [246]. While several studies have compared endometriosis-associated ovarian cancers to endometriosis [129, 247-252], none have included large bioinformatics analysis of human tissue samples of ovarian cancer with concurrent endometriosis or endometriosis lesions from women with concurrent ovarian cancer, particularly in OCCC.

1.3 MicroRNAs in endometriosis and ovarian carcinomas

MicroRNAs (miRNA) are small, ~22 nucleotides, single-stranded non-coding RNAs [253, 254]. MiRNAs can regulate large gene networks, with one miRNA capable of targeting multiple mRNAs. Some estimates suggest that all mRNA contain a target binding site for at least one miRNA [254, 255]. Recognition of miRNAs and their mRNA target occurs through the unique, miRNA-specific, 8-nucleotide seed sequence [256]. Traditionally understood, miRNA targeting occurs through binding the seed sequence to the 3'UTR of the target mRNA, repressing translation, transcript destabilization leading to transcript degradation, or both [257]. Due to their potential ability to regulate large gene networks, miRNAs are essential to development and normal physiology [258] and dysregulation or dysfunction of miRNAs has been implicated in disease states, including endometriosis and ovarian cancer [259].

MiRNA's role as master regulators of large gene networks makes them critical molecules in the study of disease initiation and progression. Their expression has been found in noninvasive fluid samples, including urine [260] and saliva [261], and minimally invasive sample collections (*i.e.,* serum or plasma) [262], suggesting their potential as disease biomarkers [263].

In endometriosis, several miRNAs have been found to be dysregulated [127, 264-281]. In these studies, miRNA expression in endometriotic lesions, or ectopic endometrium, is compared to eutopic endometrium [268, 282]. Comparison of studies and expression are complicated by the samples, including the ratio of epithelial and stromal cells, and the detection methods used [283].

Additionally, over the last several decades, numerous miRNAs have been found to be dysregulated in ovarian carcinomas [120, 284{Laios, 2008 #11824, 285-291]. Many miRNAs are functionally implicated in cellular processes, including proliferation, apoptosis, migration, cell cycle, invasion, angiogenesis, and chemotherapy sensitivity [284]. But like non-small RNA studies, miRNA expression has been mostly studied in HGSOC with fewer studies including and focusing on non-HGSOC EOC, such as OCCC or EnOC. Like endometriosis studies, the control or comparison tissue differs across studies as well as the platform used, complicating the comparison of expression across multiple studies.

MiR-10a as a tumor suppressor and oncogene in cancer

Hsa-miR-10a-5p (miR-10a) is part of the larger microRNA family, miR-10, that also contains miR-99a, miR-100, miR-10b, miR-125b(-1 and -2), miR-125a, and miR-99b [292-294]. MiR-10a is encoded on chromosome 17, notably associated with homeobox genes and embryogenesis as one of its normal functions [295]. In the ovary, miR-10a expression regulates the proliferation and apoptosis of granulosa cells [296]. Other non-diseased state functions of miR-10a are the regulation of angiogenesis [297], the transcription of actin cytoskeleton [298], and ephrin receptor signaling [298]. It has varied expression in normal tissues [299] and is dysregulated in multiple cancers [300]. MiR-10a has potential oncogenic and tumor suppressor effects, depending on tissue type.

MiR-10a has been implicated as a tumor suppressor in prostate cancer [301], breast carcinomas [302-304], and osteosarcoma [305]. In other cases, miR-10a has oncogenic properties in cutaneous squamous cell carcinoma [306], squamous cell cervical carcinomas [307-311], non-small cell lung carcinomas [312-314], acute myeloid leukemias [315], granulosa cell tumors [316], and pancreatic ductal adenocarcinomas [317-321]. Interestingly, while miR-10a is overexpressed (oncogenic) in these carcinomas, its direct functional effects are inconsistent across diseases, nor are the critical target genes studies. For example, in cervical carcinomas, miR-10a-5p overexpression has been shown to be involved in tumorigenesis, hyper-proliferation, metastasis, and invasion [307, 311, 322], while another study found overexpression of miR-10a decreased cellular proliferation [309]. For example, in breast cancer [302] and kidney cancer cells [323], miR-10a overexpression inhibited proliferation.

Along with regulating cellular functions, miR-10a expression has been implicated in chemotherapy response. In acute myeloid leukemia, miR-10a overexpression was found to be a strong predictor of insensitivity to the MDM2 inhibitor and cytarabine therapy [324]. Similarly, overexpression of miR-10a has been seen in platinum-resistant lung cancers [325, 326] and gemcitabine-resistant pancreatic ductal adenocarcinomas [319]. MiR-10a has also been found to be overexpressed in an isogenic platinum-resistant MCF-7, a breast cancer cell line [327]. Critical to ovarian cancer, Benson *et al*. analyzed plasma miRNAs as a potential, minimally invasive biomarker in 14 women undergoing treatment for recurrent, platinum-resistant ovarian cancer [328]. They detected 10 significantly altered miRNAs following one treatment cycle with decitabine and carboplatin [328]. MiR-10a was one of the miRNAs that were significantly altered in women considered responsive to treatment (*P* = 0.024), showing that miR-10a can be detected in minimally invasive blood draws and suggesting expression changes in serum could serve as a biomarker for treatment response [328]. The wide array of functions and resistance pathways involving miR-10a suggest its potential as a molecule of interest in the platinum-resistance disease of OCCC. Particularly, miR-10a expression changes to therapy make it a potential biomarker for predicting OCCC response to chemotherapy.

1.4 Summary and Overall Aims of this Study

The aim of this project is to investigate the effects of concurrent endometriosis on ovarian clear cell carcinoma, with particular interest in miR-10a expression and its effects on cellular functions involved in platinum-based therapy response. Ovarian cancer is known to be the deadliest gynecologic malignancy in the US. Most women with ovarian cancer will die from acquired or intrinsic chemoresistance. OCCC shows high rates of intrinsic resistance (≥80%) to traditional platinum and taxane-based chemotherapy, compared to <30% intrinsic resistance seen in the more common HGSOC. Women with OCCC have poorer clinical outcomes (*i.e.,* cancer-specific survival) at all stages of disease compared to HGSOC but are still treated the same. Endometriosis has been shown to significantly increase the risk of EOC, particularly OCCC, and endometriosis frequently contains cancer driver mutations (*i.e., ARID1A, KRAS, PIK3CA*), suggesting endometriosis may be a precursor lesion for OCCC and influence the molecular profile of the disease.

Chapter 2 describes the methods utilized to 1) transcriptomically profile OCCC from women with pathologically-confirmed endometriosis and bioinformatic analyses to determine the significant miR-10a overexpression, 2) analyze the baseline relationship between miR-10a expression and platinum response (IC50) in human OCCC cell lines and 3) determine miR-10a's effect on cellular proliferation and cell cycle in OCCC cell lines.

Chapter 3 details the 1) analyses of 2449 upregulated and 3131 downregulated protein-coding genes in OCCC with concurrent endometriosis compared to endometriomas, 2) enrichment of pathways involved in cell cycle regulation, DNA replication, cytokine receptor signaling, and matrisome, and 3) molecular similarities of OCCC with concurrent endometriosis, using pathway activation scores from the clinical samples and publicly-available datasets to OCCC cell lines.

Chapter 4 details the 1) analyses of 64 upregulated and 61 downregulated mature miRNA molecules, 2) selection of miR-10a-5p as significantly upregulated in OCCC and abundantly expressed as it represented over 21% of the miRNA molecules in OCCC with endometriosis, 3) positive correlation ($R^2 > 0.93$) of miR-10a expression level in OCCC cell lines with carboplatin IC50 (50% inhibitory concentration).

Chapter 5 details that 1) MiR-10a overexpression *in vitro* resulted in a significant decrease in proliferation and a significant shift in cells from S and G_2 to G_1; 2) the bioinformatic analysis predicted that miR-10a-5p target genes downregulated in OCCC with endometriosis were involved in receptor signaling pathways, proliferation, and cell cycle progression; 3) MiR-10a overexpression *in vitro* was correlated with decreased expression of predicted miR-10a target genes critical for proliferation, cell-cycle regulation, and cell survival, including [*SERPINE1* (3-fold downregulated; $P < 0.05$), *CDK6* (2.4-fold downregulated; $P < 0.05$), and *RAP2A* (2-3-fold downregulated; $P < 0.05$)].

Overall, these studies focused on the role of miR-10a in OCCC and suggest that miR-10a-5p is an impactful, potentially oncogenic molecule. These studies offer insight into the potential to detect miR-10a in plasma and serve as a biomarker for OCCC and chemotherapy resistance.

CHAPTER 2: MATERIAL AND METHODS

Institutional review board approval for collection of human tissues and metadata:

The expedited protocol to obtain and use tissues for this study was reviewed and approved by the Institutional Review Board (IRB) at Indiana University (#1812764043). The participants provided written informed consent to participate in this study. De-identified flash-frozen specimens, surgical pathology reports, and demographic data were obtained from tissue banks or previous studies [264]. Tissue banks included the NRG Oncology Biospecimen Bank (NRG BB) and the Biospecimen Collection and Banking Core (BC^2) at the Indiana University Melvin and Bren Simon Comprehensive Cancer Center (IUSCCC). Table 2-1 summarizes the metadata and associated experiments for each de-identified human tissue sample.

OCCC with concurrent endometriosis and OCCC without endometriosis were pure clear cell histology samples collected from adnexal masses. These studies did not include tumors with mixed histology (*i.e.,* clear cell with endometrioid or clear cell with serous). Inclusion criteria for OCCC with concurrent endometriosis samples were defined as the explicit mention of endometriosis on the surgical pathology report. Per banking protocols, ovarian cancer samples were removed from obvious pathologies such as necrotic tissue or endometriosis. The malignant samples were 50-90% malignant cells (Supplementary Table 1) [329]. Endometrioma cyst wall tissues were collected from women undergoing surgery for endometriomas, suspected endometriosis, and other non-malignant gynecologic indications. Endometrioma cyst walls were directly placed into RNALater (Ambion, Austin, TX) and frozen at -80°C until RNA extraction [264].

Table 2-1. Clinical characteristics of patient samples.

	Benign ($n = 16$)	Malignant ($n = 19$)		P-value
Median age, y (range)	30.5 (21-48)	53 (39-79)		$^{*}P < 0.0001$
		With Endometriosis ($n = 9$)	Without Endometriosis ($n = 10$)	
Median age, y (range)		51 (45-72)	56.5 (39-79)	$^{*}P = 0.15$
Stage				^P >0.10
I		4 (44%)	5 (50%)	
II		3 (33%)	2 (20%)	
III		2 (22%)	1 (10%)	
IV		0	2 (20%)	

*Student's t-test, one-sided, unpaired; ^Fisher's exact test, comparing stage I to stage II+.

Next-generation sequencing studies:

Total RNA was isolated from 50-100 mg of fresh frozen tissue using the *mir*Vana miRNA Isolation Kit with phenol (Thermo Fisher Scientific, Waltham, MA). RNA was treated with the Turbo DNA-*free* Kit (Thermo Fisher Scientific). RNA quality control was assessed with RNA electrophoresis using a 2100 Bioanalyzer (Agilent Technologies, Palo Alto, CA) at the Center for Medical Genomics at Indiana University School of Medicine (Indianapolis, IN). Sample quality was determined by RNA integrity levels of sample degradation using RIN scoring. High-quality RNA samples, RIN $\geq$ 6, were sent to the Center for Genomics and Bioinformatics at Indiana University (Bloomington, IN).

Library preparation for sequencing is platform specific, with the Illumina platform used here offering two main methods of tagmentation and adapter ligation. Tagmentation T Poly-A RNA libraries were constructed using mRNA Stranded TruSeq protocol (Illumina, San Diego, CA). Small RNA library construction was performed using the TruSeq Small RNA kit (Illumina). Purified libraries were visualized and quantified using a TapeStation HSD1000 (Agilent Technologies).

For poly-A bulk RNA sequencing analysis, NextSeq reads were trimmed using fastp (version 0.23.2) with parameters "-l 17 -g -p" [330]. The resulting reads were mapped against GRCh38 using HISAT2 version 2.2.1 with default parameters [331]. HISAT uses Bowtie2, based on the Burrows-Wheeler transform algorithm, for sequence alignment and allows for mapping across exon junctions [332]. Read counts for each gene were created using featureCounts from the Subread package version 2.0.3 with the parameters "-O -M --primary --largestOverlap -s 2" and Gencode v42 as the annotation [333-335]. For small RNA sequencing analysis, NextSeq reads were trimmed using fastp (version 0.23.2) with parameters "-l 17 -g -p" [330]. MiRDeep2 version 2.0.0.8 was used to map the resulting reads against GRCh38 and miRBase version 22 as a reference to detect known, mature miRNA sequences [292, 293, 336]. MiRDeep2 uses Bowtie to perform mapping of the reads and includes tools for the identification and quantification of miRNAs [337]. Bowtie version 1.3.0 was the version of Bowtie installed. Differential expression analysis for bulk RNA and miRNA was performed using the DESeq2 package (version 1.36.0) in R/Bioconductor (R version 4.2.0) [338]. Transcriptomic data have been deposited into the Gene Expression Omnibus (GSE230956). Figures from poly-A bulk RNA and small RNA sequencing analysis were created using R (version 4.2.0) and R libraries: ggplot2, complex heatmap, and ggrepel.

Quantitative RT-PCR for mRNA and miRNA expression:

Total RNA was extracted from 50-100 mg of fresh frozen tissue or cultured cells using the miRNeasy Mini Kit (Qiagen, Hilden Germany) following the manufacturer's protocol with on-column RNase-Free DNase Set (Qiagen) or previously extracted DNase-treated RNA using the *mir*Vana kit described above. A NanoDrop ND-1000 (Thermo Fisher Scientific) was used for the determination of RNA quantity and purity. For mRNA expression experiments, 1000 ng of DNase-treated RNA was reverse transcribed in a 20 µL reaction using 50 units MultiScribe Reverse Transcriptase (Thermo Fisher Scientific), 1X reverse transcriptase Buffer (Thermo Fisher Scientific), 0.5 mM deoxynucleotide triphosphate (Thermo Fisher Scientific), 6 units RNase Inhibitor (Thermo Fisher Scientific), and 2.5 µM random hexamers (Thermo Fisher Scientific) on a 2720 Thermo Cycler (Thermo Fisher Scientific): 10 minutes at 25°C, 30 minutes at 48°C, and 5 minutes at 95°C. Samples were diluted 1:5 for qPCR. QPCR was performed using 2 mL of diluted cDNA using either SYBR Green PCR Master Mix (Thermo Fisher Scientific) with previously published primers [339] or custom-designed primers (Table 2-2) in a reaction volume of 10 ml. Only custom-designed primer pairs specific for the gene of interest, intron-spanning, with a primer efficiency of 80-110%, lacking primer dimers, and $R^2 > 0.95$ were used [340, 341]. mRNA experiments were normalized to the human β-actin (*ACTB*) [339]. For miRNA expression experiments, total RNA (25 ng) was reverse transcribed using the TaqMan MicroRNA Reverse Transcription Kit (Thermo Fisher Scientific) in a reaction volume of 15 ml. Mature miRNA expression was performed using TaqMan mature microRNA assays on undiluted cDNA. U6 snRNA was used for normalization [264, 342]. Table 2-2 lists the TaqMan assays used. Both mRNA and miRNA assays were run on a QuantStudio 3 Real-Time PCR Instrument (Thermo Fisher Scientific) with reaction conditions as follows: 2 minutes at 50°C, 10 minutes at 95°C, followed by 40 cycles of 15 seconds at 95°C (denaturation), and 1 minute at 60°C (annealing/extension). All SYBR Green assays ran dissociation curves to detect primer dimers. Each sample was analyzed in duplicate. Expression fold change calculations utilized the $2^{-\Delta\Delta CT}$ method [343]. Data were plotted as mean ± SEM and statistical analyses were performed with GraphPad Prism (Dotmatics, Boston, MA). $P < 0.05$ was considered statistically significant. Power analyses were performed using G*Power (version 3.1.9.7) [344, 345]. Post-hoc analysis of A2780 and A2780CR5 miR-10a expression, with a type I error set at 0.05, found that we had greater than 95% power to detect a three-fold change with effect size d= 9.6 with a sample size of two in each group using a two-tailed t-test. For tissue miR-10a expression, due to greater variability, a total sample size of 24 was calculated to achieve greater than 80% power to detect a 0.7 effect size f and a type I error set at 0.05 using a one-way ANOVA.

Table 2-2. Primer Sequences used for qPCR expression.

Custom primers	**Forward Primer**	**Reverse Primer**
ACTB	AGAGAGGCATCCTCACCCTGAAGTACC	GACGTAGCACAGCTTCTCCTTAATGTC
CDK6	TGCAGTCCTTCTACCTGGTG	GAAATAAGCACAGCCTGGGG
RAP2A	ATTAAAACCCCAAACCCGCC	TCTGCAAACGGGAACATGTG
SERPINE1	GAAGCCCCTAGAGAACCTGG	ATCTTCACTTTCTGCAGCGC
PALM2-AKAP2	CTGGGCGATGAAGGACAATG	GGCTGCTGGAGAAAATGGAG
EPHA4	GAGTGGCTGCCTTGCTTATC	AGAACACAATGCCACACACC
TaqMan	**Assay ID**	
hsa-miR-10a-5p	000387	
U6 snRNA	001973	

Pathway and Cell Line Bioinformatic Analyses:

To compare tissue and cell lines collected from different studies, we computed the pathway activity scores (PAS) of an extensive collection of canonical biological pathways for each sample. We utilized the PAS to assess the similarity between samples. We assume that the cell lines and tissue samples of high similarity should have a similar profile in more similarly activated cellular pathways. Noting that cell line samples do not have the biological characteristics of tumor microenvironments, we excluded stromal genes and related pathways from the PAS analysis. Specifically, canonical gene sets were downloaded from MSigDB version 6 c2, containing 1329 gene sets [346-348]. Cancer Cell Line Encyclopedia (CCLE) cell line RNA-seq gene expression data were downloaded from the Broad Institute [349]. The housekeeping genes and immune and stromal cell marker genes derived from our previous analysis were excluded [350, 351]. Pathway activity scores (PAS) were assigned using the following function for each sample and pathway. For a given gene expression profile $x^{1\times N}$ of N genes and a pathway P as a set of genes, denote $y^{1\times N}$ as the sorted $x^{1\times N}$ in the decreasing order and i_g as the rank of gene g in y, the pathway activity score of P on x, denoted as $PAS(x, P, K)$ is computed by

$$PAS(x, P, K) = \frac{\sum_{g\in P} \max\left(\frac{K - i_g}{|P|}, 0\right)}{K}$$

, where K is the hyperparameter in this study. Here, K is set as 3000. Here, the PAS can be viewed as a normalized and weighted sum of the rank of the pathway genes whose expression is within the top K=3000 rank. PAS is computed for each pathway and each sample. Then Pearson Correlation Coefficients of the PAS of all pathways were computed between samples and used as their molecular similarity measure.

Ovarian cancer cell lines:

ES-2 [352, 353], TOV-21G [354], and IGROV-1 [355] were obtained from the American Type Culture Collection (ATCC, Manassas, VA). SKOV3ip1 [356] was obtained from the Cytogenetics and Cell Authentication Core at the University of Texas M.D. Anderson Cancer Center (Houston, TX, USA). OVISE [357], OVAS [358], and OVTOKO [357] were generously obtained from Dr. Hiroshi Minaguchi (Yokohama City University, Yokohama, Japan). KK [359] was generously obtained from Dr. Yoshihiro Kikuchi (National Defense Medical College, Tokorozawa, Japan). SMOV-2 [360] was generously obtained from Dr. Tomohiro Iida (St. Marianna University, Kawasaki, Japan). A2780 [361] and A2780CR5 [362] were provided by Dr. Kenneth P. Nephew (Indiana University, Bloomington, IN, USA). SKOV3 [363] was generously obtained from Dr. Salvatore Condello (Indiana University School of Medicine, Indianapolis, IN, USA). RMG-I [364] was generously obtained from Dr. Samuel C. Mok (The University of Texas MD Anderson Cancer Center, Houston, TX, USA). Cell line authentication was confirmed using a short tandem repeat (STR) marker profile (IDEXX BioAnalytics, Westbrook, ME) within six months of experiments and tested for mycoplasma contamination monthly (MycoAlert Plus Mycoplasma Detection Kit, Lonza, Switzerland).

KK, OVISE, OVTOKO, IGROV-1, RMG-I, A2780, A2780CR5, and SKOV3 were maintained in RPMI 1640 (Thermo Fisher Scientific). OVAS was maintained in DMEM/F12 (Thermo Fisher Scientific). TOV-21G was maintained in a 1:1 ratio of Medium 199 to MCBD 105 (Sigma-Aldrich, St. Louis, MO). ES-2 was grown in McCoy's (Thermo Fisher Scientific). All cell lines were supplemented with 1% penicillin and streptomycin (Thermo Fisher Scientific) and 10% fetal bovine serum (Atlanta Biologicals, Minneapolis, MN) except for TOV-21G, which was supplemented with 15%. All cells were cultured in a humidified incubator at 37°C with 5% carbon dioxide. Table 2-3 lists the ovarian carcinoma subtype, growth medium, acquisition source, and experimental use for the cell lines used in this text.

Table 2-3. Growth medium and source for ovarian carcinoma cell lines used in experiments.

Cell Line	Original Tissue Derivation	Putative Histotype by Molecular Studies	Growth Medium	Acquired From	Use in studies
A2780	Ovarian adenocarcinoma	Endometrioid	RPMI 1640 + 10% Fetal Bovine Serum + 1% Pen-Strep	Dr. Kenneth Nephew (Indiana University, Bloomington, IN, USA)	CCLE miR-10a qPCR
ES-2	Ovarian adenocarcinoma – clear cell (primary tumor, poorly differentiated)	Clear cell	McCoy's + 10% Fetal Bovine Serum + 1% Pen-Strep	American Type Culture Collection (ATCC, Manassas, VA)	CCLE miR-10a qPCR
IGROV-1	Ovarian adenocarcinoma - endometrioid with serous and clear cell features	Endometrioid / Clear cell	RPMI 1640 + 10% Fetal Bovine Serum + 1% Pen-Strep	American Type Culture Collection (ATCC, Manassas, VA)	CCLE miR-10a qPCR
KK	Ovarian adenocarcinoma – clear cell	Clear cell	RPMI 1640 + 10% Fetal Bovine Serum + 1% Pen-Strep	Dr. Yoshihiro Kikiuchi (National Defense Medical College, Tokorozawa, Japan)	Carboplatin IC50 miR-10a qPCR
OVAS	Ovarian adenocarcinoma – clear cell	Clear cell	DMEM/F12 + 10% Fetal Bovine Serum + 1% Pen-Strep	Dr. Hiroshi Minaguchi (Yokohama City University, Yokohama, Japan)	Carboplatin IC50 miR-10a qPCR
OVISE	Ovarian adenocarcinoma – clear cell (pelvic metastasis)	Clear cell	RPMI 1640 + 10% Fetal Bovine Serum + 1% Pen-Strep	Dr. Hiroshi Minaguchi (Yokohama City University, Yokohama, Japan)	Carboplatin IC50 CCLE
OVTOKO	Ovarian adenocarcinoma – clear cell (spleen metastasis)	Clear cell	RPMI 1640 + 10% Fetal Bovine Serum + 1% Pen-Strep	Dr. Hiroshi Minaguchi (Yokohama City University, Yokohama, Japan)	Carboplatin IC50 CCLE miR-10a qPCR
RMG-I	Ovarian adenocarcinoma – clear cell (ascites)	p53-mutant clear cell type	RPMI 1640 + 10% Fetal Bovine Serum + 1% Pen-Strep	Dr. Samuel C. Mok (The University of Texas MD Anderson Cancer Center, Houston, TX, USA)	Carboplatin IC50 miR-10a qPCR CCLE
SKOV3	Ovarian adenocarcinoma (ascites)	Endometrioid / Clear cell	RPMI 1640 + 10% Fetal Bovine Serum + 1% Pen-Strep	Dr. Salvatore Condello (Indiana University School of Medicine, Indianapolis, IN, USA)	CCLE miR-10a qPCR Carboplatin IC50
SMOV-2	Ovarian adenocarcinoma – clear cell	Clear cell	RPMI 1640 + 10% Fetal Bovine Serum + 1% Pen-Strep	Dr. Tomohiro Iida (St. Marianna University, Kawasaki, Japan)	Carboplatin IC50 miR-10a qPCR
TOV-21G	Ovarian adenocarcinoma – clear cell	Clear cell	Medium 199/MCDB105 1:1 + 15% Fetal Bovine Serum + 1% Pen-Strep	American Type Culture Collection (ATCC, Manassas, VA)	Carboplatin IC50 CCLE miR-10a qPCR

Carboplatin Cytotoxicity Assays

Carboplatin cytotoxicity assays were performed using the CellTiter 96 AQueous One Solution Cell Proliferation Assay (MTS) (Promega, Madison, WI). Cells were plated $1x10^3$ cells per 96-well. After 24 hours, cells were treated with ten increasing (5-200 µM) doses of carboplatin [cis-diammine (1,1-cyclobutane-dicarboxylate) platinum(II), (C2358, Sigma)] diluted in tissue culture grade water (Thermo Fisher Scientific) in triplicate. Following 72 hours of carboplatin treatment, absorbance was read on a Synergy H1 Hybrid Reader (BioTek, Winooski, VT), background absorbance was subtracted, and data were presented as normalized to vehicle control. GraphPad Prism version 9.3.0 (Dotmatics) was used to calculate an IC50 (50% inhibitory concentration). GraphPad Prism (Dotmatics) was used to calculate the correlation between IC50 and miR-10a-5p expression. With a type I error set at 0.05, we will have 90% power to detect a correlation of 0.85 with a total sample size of 8. Figures were created using GraphPad Prism (Dotmatics).

miRNA target prediction:

Putative miRNA:mRNA pairs were facilitated using SigTerms [365] with input from TargetScan [256, 366, 367], miRDB [368, 369], and miRTarBase [370]. Using manual annotation, putative target genes were further curated for potential as impactful miR-10a-5p targets.

MiR-10a-5p mimic transfection of human OCCC cell lines.

Each cell line underwent optimization of transfection conditions using the siGLO Red Transfection Indicator (Horizon Discovery, Cambridge, United Kingdom) to determine the optimum amount of lipid transfection reagent, miRNA mimic concentration, and initial cell density. Cells were seeded at a density of 2-3x10^5 cells per well of a 6-well plate. After 24 hours, cells were transfected using Lipofectamine RNAiMAX Transfection Reagent (Thermo Fisher Scientific) with 100 nM hsa-miR-10a-5p mimic (*mir*Vana miRNA mimic, Assay ID MC10787) or 100 nM negative control (*mir*Vana miRNA mimic, Negative Control #1, catalog #4464058).

Transfected cells were used simultaneously for four different endpoints: confirmation of miR-10a overexpression, cellular proliferation, cell cycle analysis, and associated putative target gene expression by qPCR. To confirm miR-10a overexpression and associated putative target gene expression, cells were lysed at 24 hours after transfection for RNA isolation. To evaluate the effects of miR-10a overexpression on proliferation, 24 hours after transfection, cells were seeded into a 96-well plate at a density of 1000 cells/well. Cellular proliferation was measured using CellTiter 96 AQueous One Solution Cell Proliferation Assay (MTS) (Promega) in triplicate at 24-hour intervals. Absorbance was read with the Synergy H1 Hybrid Reader (BioTek). Proliferation was plotted as the percent of viable cells as a function of time using GraphPad Prism (Dotmatics). To assess the effects of miR-10a overexpression on the cell cycle, 24 hours post-transfection cells were fixed using 66% ethanol (Decon Laboratories Inc., King of Prussia, PA) and stained with Propidium Iodide (PI) according to the manufacturer's protocol (Thermo Fisher Scientific, F#10797). Stained cells were analyzed using BD LSRFortessa (BD Biosciences, Franklin Lakes, NJ), and cell cycle analysis was performed with ModFit LT4.1 (Verity Software House, Topsham, ME). A two-tailed Student's t-test was performed using GraphPad Prism (Dotmatics). Figures were created using GraphPad Prism (Dotmatics).

CHAPTER 3: BIOINFORMATIC ANALYSIS OF POLY-A TRANSCRIPTOMIC PROFILING OF OCCC WITH CONCURRENT ENDOMETRIOSIS COMPARED TO ENDOMETRIOMA

3.1 Background

Previous studies have shown that each histotype of EOC, including HGSOC, EnOC, and OCCC, are transcriptomically distinct [32, 45, 58-103, 371]. Large-scale molecular analyses of HGSOC showed unique classifications of tumors based on integrating multi-platform profiling [64]. Molecular profiling of endometriosis-associated ovarian cancer, including EnOC and OCCC, showed frequent loss-of-function mutations in *ARID1A* [128, 224, 372]. Previous work showed a unique transcriptomic profile in EnOC from women with concurrent endometriosis compared to those without concurrent endometriosis, supporting the role of the endometriotic microenvironment in ovarian cancer development [246, 373].

Endometriosis, a benign, chronic inflammatory condition where endometrial-like tissue grows outside the uterus, is a significant and potentially modifiable risk factor for ovarian cancer development [160, 161]. Women with any amount or anatomical location of endometriosis have an increased risk of developing ovarian endometrioid (3.1-fold) or clear cell (5.1-fold) carcinoma [230, 231]. Specifically, women with ovarian endometriomas or deep infiltrating endometriotic lesions of the ovary are at even higher risk for developing ovarian endometrioid (4.7-fold) or clear cell (10.1-fold) carcinoma [231]. OCCC is a rare histological subtype composing 5-25% of ovarian malignancies, with the wide variation thought to be due to the subjective evaluation of histologic features and country-specific differences in prevalence [41-43].

Unlike the large sample size HGSOC transcriptomic profiling studies focusing only on HGSOC histology, transcriptomic profiling of OCCC is more limited in sample size or primarily used to show differences between transcriptomic profiles of different histological types of EOC [54, 59, 64, 111, 115, 118-126, 129, 247, 250, 374, 375]. Significantly, up to 50% of OCCC are associated with endometriosis [225, 376]. However, most transcriptomic studies of primary tumors classified as OCCC do not characterize samples as coming from women with concurrent endometriosis, pathology-proven endometriosis, or even a history of endometriosis (Supplementary Table 2-3). Only recently was a large sample size, OCCC-focused, multi-platform study performed that characterized samples as from women with a history of endometriosis [59]. In this study, samples from women with a history of endometriosis were more likely to have loss-of-function mutations in *ARID1A.* In contrast, those with p53 mutations were likely to have poorer outcomes [59]. While the tumors transcriptomically clustered into two groups – a traditional OCCC group and an aggressive p53-mutant high-grade serous-like group [59], the study did not discern particular transcriptomic contributions in samples from women with a history of endometriosis. To fill this gap, we focused our transcriptomic profiles on OCCC with pathology-proven concurrent endometriosis using bulk RNA and miRNA sequencing.

3.2 Results

OCCC samples with concurrent endometriosis had unique molecular characteristics.

While nearly half of all women with OCCC have endometriosis [225, 376], transcriptomic profiling studies have not examined OCCC samples from women with pathology-proven endometriosis. Only one transcriptomic study contained OCCC samples from women with a history of endometriosis [59], but the samples were not defined as pathology-proven, nor were their transcriptomic profiles analyzed independently. Here, we focused on OCCC samples from women with pathologically confirmed endometriosis. Supplementary Table 1 summarizes the clinical and pathological characteristics. OCCC with concurrent endometriosis was defined as having endometriosis at the time of staging surgery, listed on the pathology report. Women with OCCC were significantly older (median 53 years; range 39-79 years, $P < 0.0001$) than women with benign endometriomas (median 30.5 years; range 21-48 years). Women with OCCC and concurrent endometriosis did not differ in age (median 51 years; range 45-72 years, $P = 0.15$) from those without concurrent endometriosis (median 56.5 years; range 39-79). Using the Federation Internationale de Gynécologie et d'Obstétrique (FIGO) ovarian cancer staging system implemented in 2014 [377], there was no difference in the stage between the women with and without concurrent endometriosis (Fisher's exact test = 1, $P > 0.1$). Thus, the OCCC samples were clinically similar except for concurrent endometriosis.

Poly-A bulk RNA and small RNA sequencing were performed on RNA isolated from specimens ($n = 8$), including endometrioma ($n = 4$) and OCCC with concurrent endometriosis ($n = 4$). Endometrioma samples were full cyst wall thickness samples taken from areas without gross pathology such as necrosis or abscess, with pathology-proven endometriosis without atypia and no evidence of ovarian cancer. OCCC samples were taken from adnexal masses and areas free from gross endometriosis, necrosis, or abscess.

Poly-A bulk sequencing revealed over 437 million mapped reads (mean: 54,646,311 ± 6,117,236 mapped reads per clinical sample). There was no difference between endometrioma and OCCC with concurrent endometriosis samples regarding overall alignment rate, as all eight bulk RNA samples had greater than 97% of mapped reads aligned. HISAT analysis was used to categorize mapped reads into RNA categories or feature counts (Table 3-1). More reads were assigned in endometrioma (145,847,035 reads) than OCCC with concurrent endometriosis (124,361,541 reads, Student's *t*-test, $P < 0.01$). OCCC with concurrent endometriosis had more reads assigned to mitochondrial RNA species (33,929,857 to 22,296,699; endometrioma, Student's *t*-test, $P < 0.01$). More reads were assigned to protein-coding genes in benign endometrioma (98,430,773 reads) than OCCC with concurrent endometriosis (70,984,332 reads, Student's *t*-test, $P < 0.01$).

Table 3-1. RNA Sequencing Reads Summary.

Sample Label	Eoma_1	Eoma_3	Eoma_4	Eoma_5	OCCC_1	OCCC_2	OCCC_4	OCCC_5
Sample	CW44	CW9	LCW62	CW195	G618	G506	G741	G002
TRIMMING: Read1 before filtering total reads	49,857,191	47,141,979	58,131,893	49,050,586	62,319,046	58,419,713	61,131,464	56,196,155
TRIMMING: Read1 after filtering total reads	48,988,096	46,112,714	57,178,608	47,989,788	62,028,447	58,154,385	60,809,794	55,908,654
TRIMMING: Percent after filtering total reads	98.26%	97.82%	98.36%	97.84%	99.53%	99.55%	99.47%	99.49%
TRIMMING: Filtering result reads failed due to low quality	228,004	201,369	297,888	216,606	278,193	254,369	310,183	275,248
TRIMMING: Filtering result reads failed due to too many N	3,759	3,562	4,546	3,708	4,815	4,547	4,713	4,450
TRIMMING: Filtering result reads failed due to too short	637,332	824,334	650,851	840,484	7,591	6,412	6,774	7,803
TRIMMING: Filtering result reads with adapter trimmed	1,820,233	2,401,811	1,864,903	2,379,166	0	0	0	0
TRIMMING: Duplication rate (may be overestimated since this is SE data)	96.12	106.78	95.81	107.44	83.39	81.01	81.38	86.12
MAPPING: Overall alignment rate	98.06%	98.05%	97.84%	97.61%	97.92%	97.29%	97.63%	97.39%
MAPPING: Total reads	48,988,096	46,112,714	57,178,608	47,989,788	62,028,447	58,154,385	60,809,794	55,908,654
MAPPING: Aligned 0 time	948,190	901,158	1,237,036	1,148,053	1,289,440	1,574,221	1,441,942	1,461,600
MAPPING: Aligned 0 time%	1.94%	1.95%	2.16%	2.39%	2.08%	2.71%	2.37%	2.61%
MAPPING: Aligned 1 time	42,838,029	40,307,285	50,254,446	41,021,070	56,109,942	52,512,707	54,076,844	49,436,194
MAPPING: Aligned 1 time%	87.45%	87.41%	87.89%	85.48%	90.46%	90.30%	88.93%	88.42%

MAPPING: Aligned >1 times	5,201,877	4,904,271	5,687,126	5,820,665	4,629,065	4,067,457	5,291,008	5,010,860
MAPPING: Aligned >1 times%	10.62%	10.64%	9.95%	12.13%	7.46%	6.99%	8.70%	8.96%
MAPPING: reads mapped:	48,039,906	45,211,556	55,941,572	46,841,735	60,739,007	56,580,164	59,367,852	54,447,054
MAPPING: reads unmapped:	948,190	901,158	1,237,036	1,148,053	1,289,440	1,574,221	1,441,942	1,461,600
MAPPING: reads MQ0:	296,529	221,738	256,669	240,226	198,910	177,076	287,927	281,520
MAPPING: reads QC failed:	0	0	0	0	0	0	0	0
MAPPING: non-primary alignments:	14,589,813	13,307,450	15,810,773	16,478,801	13,450,095	11,724,172	15,105,593	15,255,895
MAPPING: mismatches:	6,240,026	6,033,746	7,211,699	6,550,673	8,171,680	7,720,676	8,040,589	8,375,850
MAPPING: error rate:	0	0	0	0	0	0	0	0
MAPPING: average length:	79	79	79	79	79	79	79	79
MAPPING: average quality:	34.8	34.7	34.8	34.8	34.8	34.8	34.8	34.8
FeatureCount: Assigned	34,978,792	35,333,682	39,507,297	36,027,264	34,792,336	29,699,270	30,502,524	29,367,411
FeatureCount: Assigned%	71.40%	76.62%	69.09%	75.07%	56.09%	51.07%	50.16%	52.53%
FeatureCount: Unassigned_Unmapped	948,190	901,158	1,237,036	1,148,053	1,289,440	1,574,221	1,441,942	1,461,600
FeatureCount: Unassigned_Secondary	14,589,813	13,307,450	15,810,773	16,478,801	13,450,095	11,724,172	15,105,593	15,255,895
FeatureCount: Unassigned_NoFeatures	13,061,114	9,877,874	16,434,275	10,814,471	25,946,671	26,880,894	28,865,328	25,079,643
FeatureCount: IG_C_gene	70,926	44,805	30,571	111,999	123	81	20	16,162

Transcriptomic profiles of the endometrioma and OCCC with concurrent endometriosis samples were first evaluated using multidimensional scaling (MDS) analysis [378]. The MDS plot shows a significant differential clustering of the OCCC samples with concurrent endometriosis from endometriomas (Figure 3-1A). This difference is most apparent at the MDS1 level. Similar clustering was noted on uniform manifold approximation and projection (UMAP) and principal component analysis (PCA) for dimension reduction plots (Figure 3-2A-B). At a global level, malignant OCCC with concurrent endometriosis is molecularly distinct from benign endometriomas.

We directly compared transcriptomic profiles of OCCC with concurrent endometriosis (n = 4) to endometriomas (n = 4). Endometrioma was used as a comparison tissue due to its significant increase in risk for the development of OCCC, studies supporting increased molecular mutations in atypical endometriosis and concurrent OCCC, strong genomic correlation and causal relationship between endometriosis and OCCC, and the high incidence of concurrent endometriosis seen in women with OCCC [128, 129, 225, 231, 250, 376]. Differential gene expression analysis was conducted with DESeq2. Significant differential expression was determined using a false discovery rate <0.05, giving 6865 protein-coding transcripts significantly differentially expressed. Limiting to log2 fold-change >|1| identified 2449 upregulated and 3131 downregulated unique protein-coding genes (Figure 3-1B-C). Hierarchical clustering shows that endometriomas cluster separately from OCCC with concurrent endometriosis (Figure 3-1C).

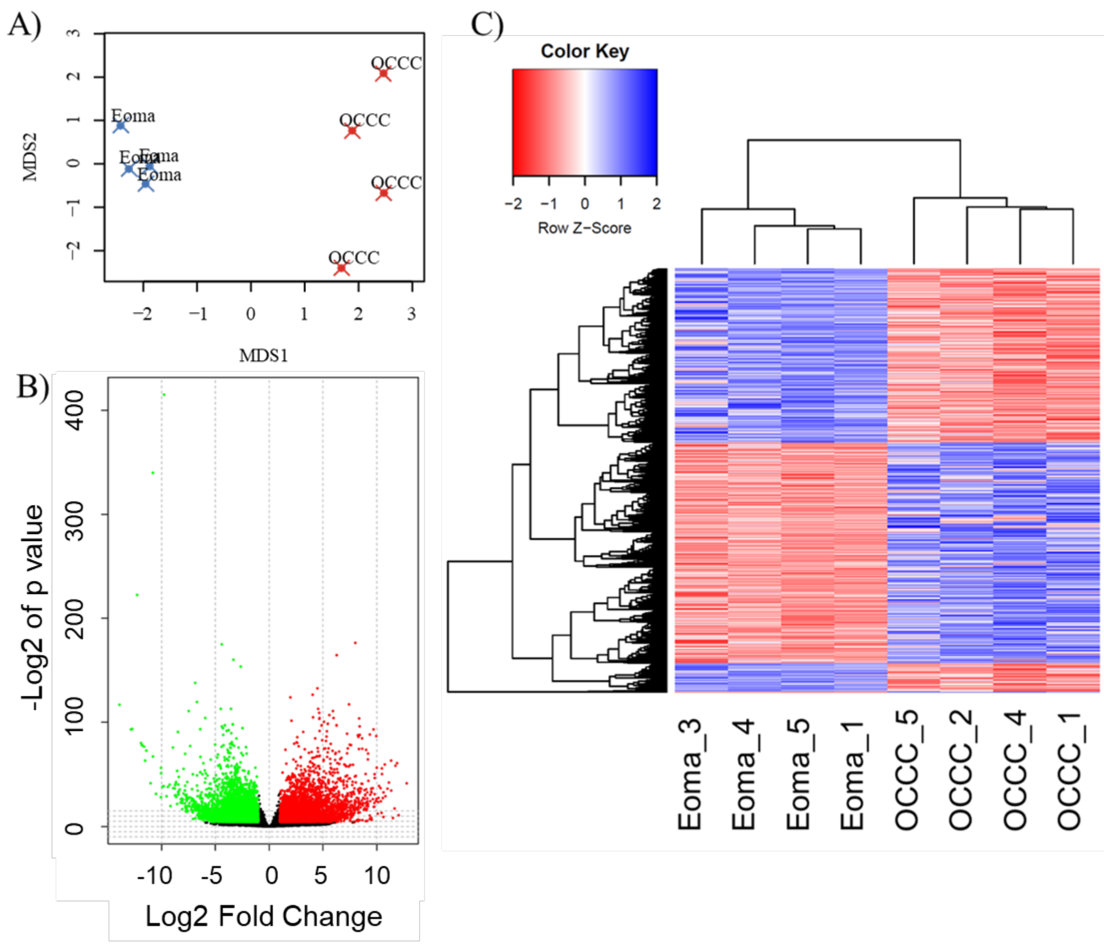

Figure 3-1. **The OCCC with concurrent endometriosis transcriptomic profile is molecularly distinct from benign endometrioma**. **A)** Multidimensional scaling (MDS) plot of transcriptomic profiles for endometrioma (Eoma, blue X's) and ovarian clear cell carcinoma (OCCC, red X's) with concurrent endometriosis. **B)** Volcano plot representation of protein-coding transcripts overexpressed (red dots), similarly expressed (black dots), and under-expressed (green dots) in OCCC with concurrent endometriosis versus endometriomas ($P_{adj} < 0.05$; Log2-Fold change < |1|. **C)** Heat map representation of 5575 differentially expressed unique protein-coding gene transcripts overexpressed (red) and under-expressed (blue). Dendrogram of hierarchical clustering. Rows, protein-coding gene transcripts; columns, profiled samples.

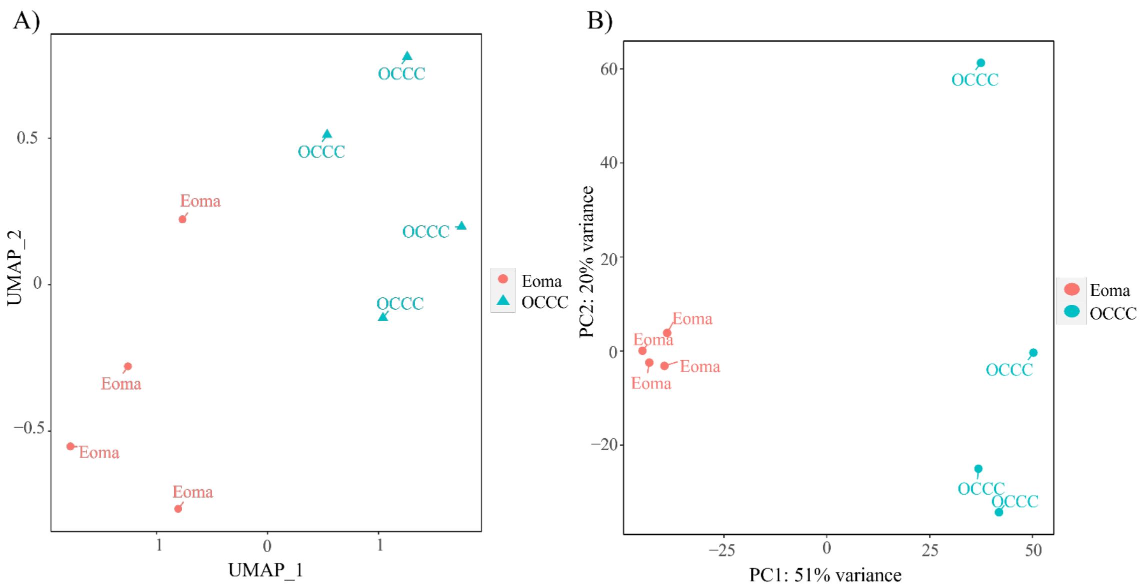

Figure 3-2. OCCC with concurrent endometriosis differentially clusters from benign endometrioma. A) Uniform manifold approximation and projection (UMAP) plot of malignant OCCC with concurrent endometriosis (blue triangles) clusters separately from benign endometrioma (red circles) using UMAP1 and UMAP2. **B)** Similarly, principal component (PC) analysis of malignant OCCC with concurrent endometriosis (blue circles) clusters separately from benign endometrioma samples (red circles), using PC1 and PC2.

Matrisome, secreted factors, cell cycle, and DNA replication pathways are dysregulated in OCCC with concurrent endometriosis.

To explore potentially impactful molecular processes, we performed pathway enrichment analysis of the upregulated and downregulated genes using a hypergeometric test and Gene Set Enrichment Analysis (GSEA) against MSigDB v6 canonical pathway set, with a significant cutoff determined by $P < 0.005$ [346-348]. Complete lists of the pathways significantly enriched by upregulated and downregulated genes can be found at https://www.ncbi.nlm.nih.gov/geo/query/acc.cgi?acc=GSE230956. We observed a limited list of pathways from upregulated genes in OCCC with concurrent endometriosis (Table 3-2). The upregulated genes showed significant enrichment in cell cycle and DNA replication pathways, including cyclin A B1-mediated G2-M transition, G1-S transcription, and E2F-mediated DNA replication (Figures 3-3A-C). Previous work has shown that OCCC exhibited dysregulation of p27-related cell cycle effects [379]. Important drivers of p27-related cell cycle dysregulation that were upregulated in OCCC with concurrent endometriosis include *SKP2* (S-phase kinase-associated protein 2, log2 fold-change = 1.3, P = 1.1e-2), *CKS2* (CDC28 protein kinase regulatory subunit 2, log2 fold-change = 2.2, P = 6.6e-9), *CCNA2* (Cyclin A2, log2 fold-change = 1.7, P = 2.9e-3), and *CCNE1* (Cyclin E1, log2 fold-change = 5.2, P = 8.5e-10). GSEA plots of the cyclin A-mediated G2-M transition (P = 8.95e-6) and E2F-mediated DNA replication (P = 8.61e-4) top enriched pathways from upregulated genes are shown in Figure 3-3B-C. Table 3-3 lists the upregulated genes involved in the cell cycle with their fold change.

There were many more significantly enriched pathways in OCCC with concurrent endometriosis (Table 3-4). Significantly downregulated genes in OCCC with concurrent endometriosis showed significant enrichment in the pathways of matrisome, secreted factors, GPCR signaling, and cytokine-cytokine-receptor interaction (Figure 3-4A). GSEA plots of matrisome (P = 2.64e-69) and cytokine-cytokine receptor interaction (P = 2.43e-20) pathways from downregulated genes are shown in Figure 3-4B-C. Essential genes involved in the cytokine-cytokine receptor interaction pathway are predominantly upregulated in endometriomas [246, 264, 380-383]. Table 3-5 shows the downregulated genes in OCCC with concurrent endometriosis compared to endometrioma in the cytokine-cytokine receptor interaction pathway.

Table 3-2. Gene Set Enrichment Analysis of upregulated genes.

	hits	pathway_size	p.value
REACTOME_CYCLIN_A_B1_ASSOCIATED_EVENTS_DURING_G2_M_TRANSITION	10	15	8.95E-06
REACTOME_G1_S_SPECIFIC_TRANSCRIPTION	10	18	8.41E-05
REACTOME_E2F_MEDIATED_REGULATION_OF_DNA_REPLICATION	13	34	8.61E-04
KEGG_TASTE_TRANSDUCTION	14	39	1.14E-03
PID_FOXM1_PATHWAY	14	39	1.14E-03
REACTOME_TIGHT_JUNCTION_INTERACTIONS	10	24	1.58E-03
PID_AURORA_B_PATHWAY	13	37	2.12E-03
KEGG_CELL_CYCLE	32	124	2.27E-03
REACTOME_CELL_CYCLE	74	350	2.60E-03
BIOCARTA_SRCRPTP_PATHWAY	6	11	2.77E-03
REACTOME_TRANSPORT_OF_INORGANIC_CATIONS_ANIONS_AND_AMINO_ACIDS_OLIGOPEPTIDES	23	82	2.82E-03
REACTOME_G2_M_CHECKPOINTS	14	41	3.18E-03
REACTOME_AMINO_ACID_AND_OLIGOPEPTIDE_SLC_TRANSPORTERS	14	42	3.58E-03
REACTOME_CELL_CYCLE_MITOTIC	64	303	4.73E-03

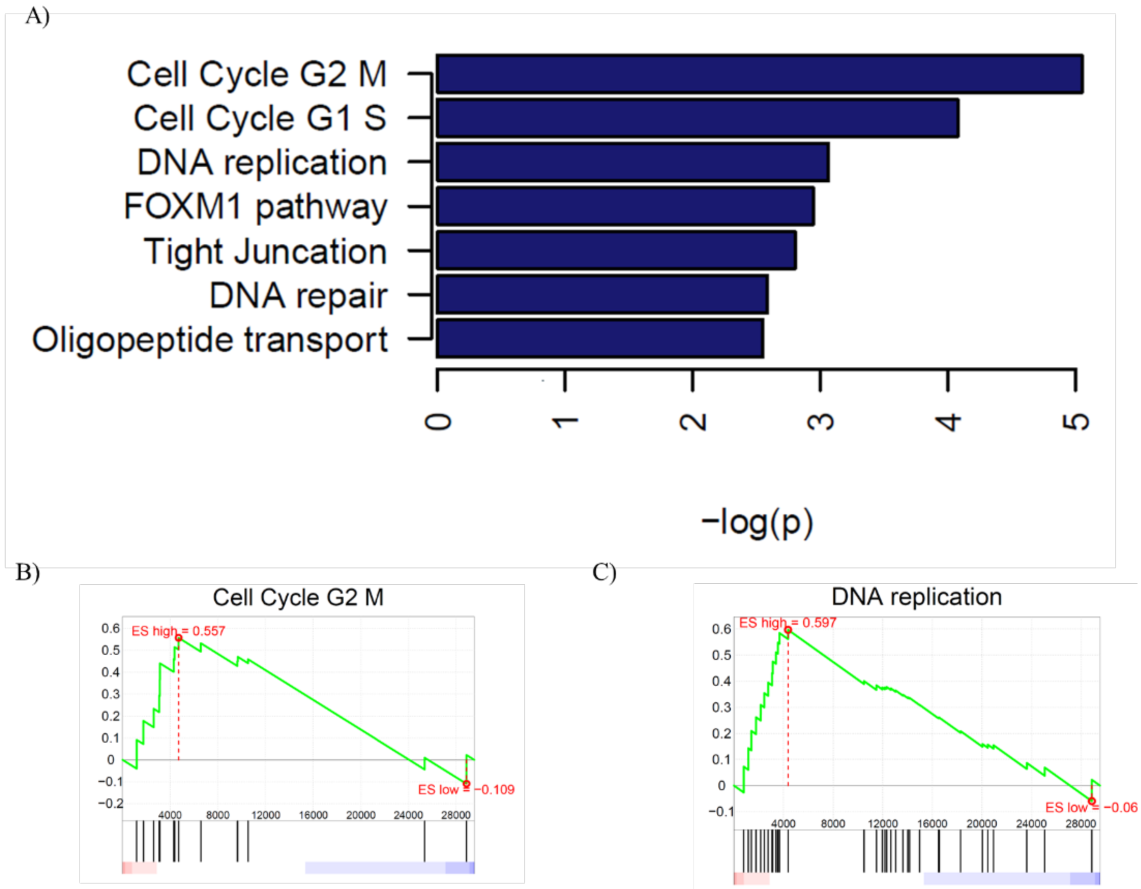

Figure 3-3. Cell cycle and DNA replication/repair pathways are enriched in upregulated genes from OCCC with concurrent endometriosis. **A)** Waterfall plot of significantly upregulated pathways in OCCC with concurrent endometriosis. Gene set enrichment plots for **B)** REACTOME_CYCLIN_A_B1_ASSOCIATED_EVENTS_DURING_G2_M_TRANSITION and **C)** REACTOME_E2F_MEDIATED_REGULATION_OF_DNA_REPLICATION.

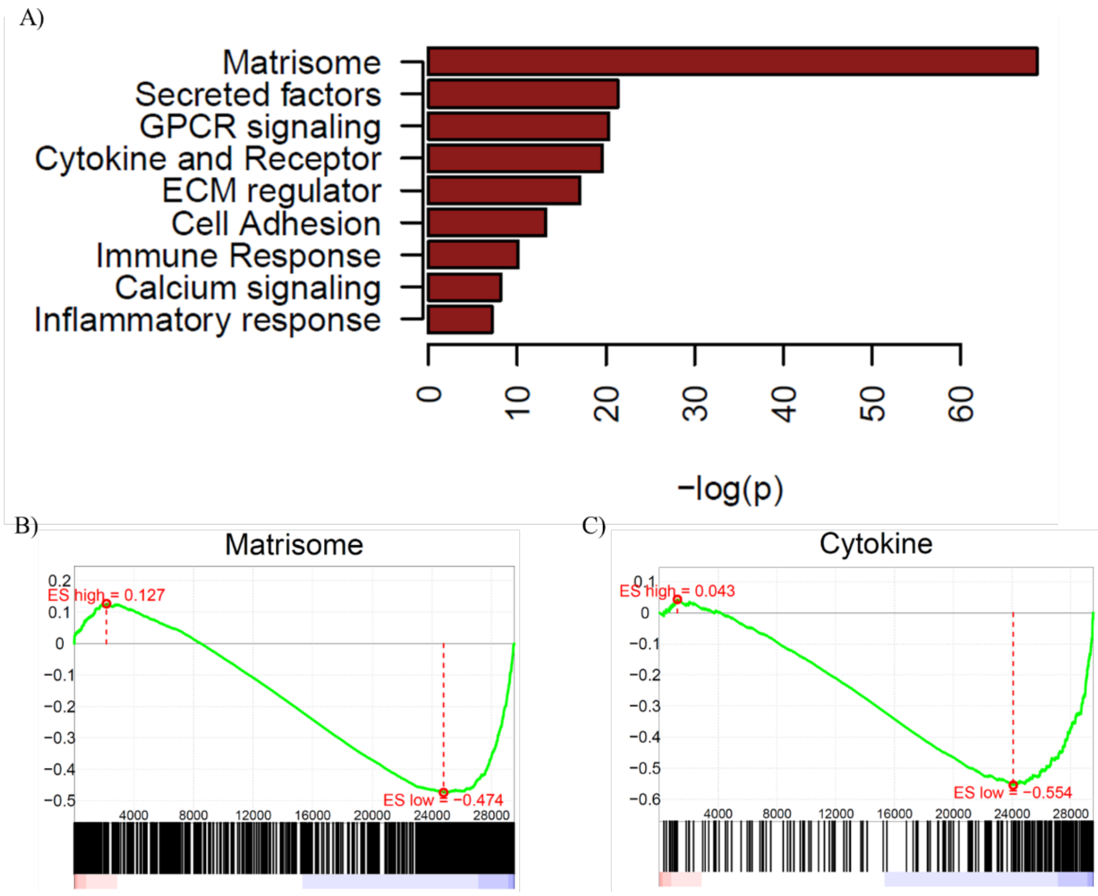

Figure 3-4. Matrisome and cytokine pathways are enriched in downregulated genes from OCCC with concurrent endometriosis. **A)** Waterfall plot of significantly downregulated pathways in OCCC with concurrent endometriosis. Gene set enrichment plots for **B)** NABA_MATRISOME and **C)** KEGG_CYTOKINE_CYTOKINE_RECEPTOR_INTERACTION.

Table 3-3. Genes dysregulated in OCCC and involved in cell cycle.

Gene Symbol	Gene Name	log2FoldChange	padj
SMC1B	structural maintenance of chromosomes 1B	6.0	1.98E-08
TERT	telomerase reverse transcriptase	5.3	1.18E-02
CCNE1	cyclin E1	5.1	8.49E-10
RRM2	ribonucleotide reductase regulatory subunit M2	4.2	6.04E-08
PKMYT1	protein kinase, membrane associated tyrosine/threonine 1	4.2	4.85E-08
ESPL1	extra spindle pole bodies like 1, separase	3.9	4.53E-07
NEK2	NIMA related kinase 2	3.9	1.84E-11
CDT1	chromatin licensing and DNA replication factor 1	3.8	1.86E-06
UBE2C	ubiquitin conjugating enzyme E2 C	3.8	1.94E-05
AURKB	aurora kinase B	3.7	4.07E-05
CDC20	cell division cycle 20	3.4	1.47E-06
CDC25C	cell division cycle 25C	3.4	2.76E-05
ORC6	origin recognition complex subunit 6	3.3	3.91E-07
CDCA8	cell division cycle associated 8	3.2	1.46E-08
MYBL2	MYB proto-oncogene like 2	3.1	6.74E-04
FOXM1	forkhead box M1	3.1	7.97E-05
CDC45	cell division cycle 45	3.1	1.51E-07
CENPF	centromere protein F	3.0	1.14E-07
MCM10	minichromosome maintenance 10 replication initiation factor	2.9	1.17E-04
TYMS	thymidylate synthetase	2.8	2.15E-05
E2F2	E2F transcription factor 2	2.8	3.85E-04
NUF2	NUF2 component of NDC80 kinetochore complex	2.7	8.94E-06
KNTC1	kinetochore associated 1	2.7	6.80E-06
HJURP	Holliday junction recognition protein	2.7	6.74E-04
KIF2C	kinesin family member 2C	2.7	2.16E-04
PLK1	polo like kinase 1	2.7	1.79E-05
CENPM	centromere protein M	2.6	2.20E-07
KIF20A	kinesin family member 20A	2.6	1.06E-03
ERCC6L	ERCC excision repair 6 like, spindle assembly checkpoint helicase	2.6	9.54E-05
SYNE2	spectrin repeat containing nuclear envelope protein 2	2.6	6.40E-13
ORC1	origin recognition complex subunit 1	2.6	2.50E-07
GINS1	GINS complex subunit 1	2.5	9.82E-06
NCAPH	non-SMC condensin I complex subunit H	2.5	5.56E-04
TTK	TTK protein kinase	2.5	4.91E-04

DNA2	DNA replication helicase/nuclease 2	2.5	2.60E-12
CCNB1	cyclin B1	2.4	2.59E-09
CDC25B	cell division cycle 25B	2.4	2.71E-03
CDK1	cyclin dependent kinase 1	2.4	1.11E-04
NCAPG	non-SMC condensin I complex subunit G	2.4	2.40E-03
BUB1B	BUB1 mitotic checkpoint serine/threonine kinase B	2.3	4.91E-05
MCM8	minichromosome maintenance 8 homologous recombination repair factor	2.2	1.99E-06
PTTG1	PTTG1 regulator of sister chromatid separation, securin	2.2	4.76E-03
SKA1	spindle and kinetochore associated complex subunit 1	2.2	5.45E-03
SPC25	SPC25 component of NDC80 kinetochore complex	2.2	1.10E-03
E2F1	E2F transcription factor 1	2.1	8.94E-04
BUB1	BUB1 mitotic checkpoint serine/threonine kinase	2.1	9.31E-04
CDC6	cell division cycle 6	2.1	2.38E-05
ZWINT	ZW10 interacting kinetochore protein	2.0	3.87E-05
KIF18A	kinesin family member 18A	2.0	3.72E-03
NDC80	NDC80 kinetochore complex component	2.0	4.81E-03
BRCA1	BRCA1 DNA repair associated	2.0	3.40E-08
E2F5	E2F transcription factor 5	1.9	8.95E-08
CCNB2	cyclin B2	1.8	2.81E-03
CDC25A	cell division cycle 25A	1.8	3.50E-03
OFD1	OFD1 centriole and centriolar satellite protein	1.8	6.84E-08
GINS2	GINS complex subunit 2	1.8	2.48E-03
CENPK	centromere protein K	1.8	2.77E-03
CCNA2	cyclin A2	1.7	2.88E-03
KIF23	kinesin family member 23	1.7	6.41E-03
SMC4	structural maintenance of chromosomes 4	1.5	5.80E-03
NINL	ninein like	1.5	9.34E-05
SRC	SRC proto-oncogene, non-receptor tyrosine kinase	1.5	2.96E-09
MCM4	minichromosome maintenance complex component 4	1.5	2.63E-04
CEP72	centrosomal protein 72	1.5	1.06E-03
CENPO	centromere protein O	1.5	6.55E-03
LMNB1	lamin B1	1.4	2.93E-02
PLK4	polo like kinase 4	1.4	2.71E-03

POLE	DNA polymerase epsilon, catalytic subunit	1.4	6.00E-04
EP300	E1A binding protein p300	1.3	1.92E-06
CHEK1	checkpoint kinase 1	1.3	3.22E-02
RANGAP1	Ran GTPase activating protein 1	1.3	1.94E-05
SKP2	S-phase kinase associated protein 2	1.3	1.09E-02
MCM2	minichromosome maintenance complex component 2	1.2	3.85E-04
CDK7	cyclin dependent kinase 7	1.2	7.26E-03
HSP90AA1	heat shock protein 90 alpha family class A member 1	1.2	7.89E-06
TERF1	telomeric repeat binding factor 1	1.2	1.12E-03
TUBG1	tubulin gamma 1	1.2	4.06E-03
SDCCAG8	SHH signaling and ciliogenesis regulator SDCCAG8	1.1	5.07E-03
INCENP	inner centromere protein	1.1	4.67E-03
CSNK1D	casein kinase 1 delta	1.1	2.57E-03
CREBBP	CREB binding protein	1.1	1.28E-03
OIP5	Opa interacting protein 5	1.1	3.11E-02
NCAPD2	non-SMC condensin I complex subunit D2	1.0	3.57E-03

Table 3-4. Gene Set Enrichment Analysis of downregulated genes.

	hits	pathway_size	p.value
NABA_MATRISOME	325	881	2.64E-69
NABA_MATRISOME_ASSOCIATED	230	632	6.53E-48
NABA_CORE_MATRISOME	95	249	3.28E-22
NABA_SECRETED_FACTORS	102	279	4.23E-22
REACTOME_SIGNALING_BY_GPCR	157	540	4.46E-21
KEGG_CYTOKINE_CYTOKINE_RECEPTOR_INTERACTION	88	233	2.43E-20
REACTOME_GPCR_LIGAND_BINDING	102	311	4.12E-18
REACTOME_GPCR_DOWNSTREAM_SIGNALING	131	448	6.54E-18
NABA_ECM_REGULATORS	77	205	8.00E-18
REACTOME_PEPTIDE_CHAIN_ELONGATION	54	116	9.99E-18
NABA_ECM_GLYCOPROTEINS	68	173	4.18E-17
KEGG_HEMATOPOIETIC_CELL_LINEAGE	42	78	5.11E-17
REACTOME_CLASS_A1_RHODOPSIN_LIKE_RECEPTORS	81	231	1.27E-16
REACTOME_3_UTR_MEDIATED_TRANSLATIONAL_REGULATION	56	137	3.18E-15
KEGG_CHEMOKINE_SIGNALING_PATHWAY	66	178	3.61E-15
REACTOME_INFLUENZA_VIRAL_RNA_TRANSCRIPTION_AND_REPLICATION	54	132	9.46E-15
KEGG_SYSTEMIC_LUPUS_ERYTHEMATOSUS	32	55	1.36E-14
REACTOME_SRP_DEPENDENT_COTRANSLATIONAL_PROTEIN_TARGETING_TO_MEMBRANE	55	139	2.91E-14
KEGG_RIBOSOME	41	86	2.97E-14
KEGG_CELL_ADHESION_MOLECULES_CAMS	51	125	5.87E-14
REACTOME_NONSENSE_MEDIATED_DECAY_ENHANCED_BY_THE_EXON_JUNCTION_COMPLEX	54	137	5.99E-14
REACTOME_HEMOSTASIS	112	410	2.40E-13
KEGG_COMPLEMENT_AND_COAGULATION_CASCADES	34	66	2.63E-13
REACTOME_IMMUNOREGULATORY_INTERACTIONS_BETWEEN_A_LYMPHOID_AND_A_NON_LYMPHOID_CELL	29	57	2.21E-11
KEGG_LEISHMANIA_INFECTION	32	69	4.84E-11
REACTOME_IMMUNE_SYSTEM	181	829	7.56E-11

REACTOME_TRANSLATION	58	178	7.90E-11
NABA_ECM_AFFILIATED	51	148	1.06E-10
REACTOME_INFLUENZA_LIFE_CYCLE	54	164	2.47E-10
REACTOME_CHEMOKINE_RECEPTORS_BIND_CHEMOKINES	25	49	4.89E-10
REACTOME_G_ALPHA_I_SIGNALLING_EVENTS	51	155	8.16E-10
REACTOME_G_ALPHA_Q_SIGNALLING_EVENTS	50	154	1.83E-09
KEGG_FOCAL_ADHESION	58	192	2.24E-09
REACTOME_GASTRIN_CREB_SIGNALLING_PATHWAY_VIA_PKC_AND_MAPK	54	175	3.22E-09
REACTOME_PLATELET_ACTIVATION_SIGNALING_AND_AGGREGATION	58	194	3.23E-09
KEGG_VIRAL_MYOCARDITIS	28	64	3.99E-09
REACTOME_EXTRACELLULAR_MATRIX_ORGANIZATION	32	80	4.81E-09
PID_IL4_2PATHWAY	27	61	5.53E-09
KEGG_CALCIUM_SIGNALING_PATHWAY	51	164	7.03E-09
REACTOME_PEPTIDE_LIGAND_BINDING_RECEPTORS	45	139	1.32E-08
REACTOME_SMOOTH_MUSCLE_CONTRACTION	15	23	1.70E-08
BIOCARTA_COMP_PATHWAY	13	18	2.42E-08
KEGG_VASCULAR_SMOOTH_MUSCLE_CONTRACTION	37	106	2.48E-08
KEGG_NEUROACTIVE_LIGAND_RECEPTOR_INTERACTION	62	224	3.86E-08
PID_INTEGRIN2_PATHWAY	16	27	4.06E-08
PID_INTEGRIN1_PATHWAY	27	66	4.28E-08
REACTOME_NEURONAL_SYSTEM	66	247	6.27E-08
BIOCARTA_CLASSIC_PATHWAY	11	14	7.32E-08
REACTOME_COMPLEMENT_CASCADE	16	28	8.26E-08
KEGG_ARRHYTHMOGENIC_RIGHT_VENTRICULAR_CARDIOMYOPATHY_ARVC	26	67	2.66E-07
KEGG_DILATED_CARDIOMYOPATHY	29	80	3.10E-07
REACTOME_GLYCOSAMINOGLYCAN_METABOLISM	35	107	5.10E-07
REACTOME_INNATE_IMMUNE_SYSTEM	58	222	6.43E-07
BIOCARTA_BLYMPHOCYTE_PATHWAY	9	11	6.86E-07

Table 3-5. Cytokine genes that are dysregulated in OCCC.

Gene	Gene Name	log2FoldChange	padj
CXCL12	C-X-C motif chemokine ligand 12	-4.5	1.08E-34
PDGFRA	platelet derived growth factor receptor alpha	-3.6	1.21E-24
TGFBR1	transforming growth factor beta receptor 1	-2.1	7.71E-22
CCL21	C-C motif chemokine ligand 21	-7.8	8.63E-22
TGFB3	transforming growth factor beta 3	-3.1	2.05E-12
IL11RA	interleukin 11 receptor subunit alpha	-1.9	5.56E-12
IFNGR1	interferon gamma receptor 1	-2.3	1.32E-11
IL7R	interleukin 7 receptor	-4.4	1.00E-10
TNFSF12	TNF superfamily member 12	-2.4	1.04E-10
CCL11	C-C motif chemokine ligand 11	-7.8	8.74E-10
IL10	interleukin 10	-4.8	1.25E-09
IL18R1	interleukin 18 receptor 1	-4.4	1.52E-09
CCL2	C-C motif chemokine ligand 2	-5.5	1.57E-09
CSF1	colony stimulating factor 1	-2.2	3.02E-09
CCL26	C-C motif chemokine ligand 26	-6.4	7.53E-09
PLEKHO2	pleckstrin homology domain containing O2	-2.7	1.59E-08
IL13RA1	interleukin 13 receptor subunit alpha 1	-1.6	1.60E-08
TNFSF8	TNF superfamily member 8	-4.0	2.57E-08
IFNGR2	interferon gamma receptor 2	-1.7	5.52E-08
IL6ST	interleukin 6 cytokine family signal transducer	-2.1	9.59E-08
CSF3	colony stimulating factor 3	-8.2	1.23E-07
IL5RA	interleukin 5 receptor subunit alpha	-4.8	2.98E-07
CCR6	C-C motif chemokine receptor 6	-2.7	4.73E-07
FLT3LG	fms related receptor tyrosine kinase 3 ligand	-2.3	6.65E-07
IL20	interleukin 20	-6.9	7.26E-07
CCR2	C-C motif chemokine receptor 2	-3.9	1.50E-06
VEGFC	vascular endothelial growth factor C	-2.6	5.74E-06
INHBA	inhibin subunit beta A	-4.6	6.25E-06
CCL23	C-C motif chemokine ligand 23	-8.1	9.18E-06
IL18RAP	interleukin 18 receptor accessory protein	-3.1	1.42E-05
LIF	LIF interleukin 6 family cytokine	-4.0	1.73E-05
HGF	hepatocyte growth factor	-2.5	2.69E-05
CCL13	C-C motif chemokine ligand 13	-6.3	4.80E-05
ACVR2A	activin A receptor type 2A	-1.5	5.14E-05
CCL18	C-C motif chemokine ligand 18	-5.7	7.17E-05
CCL14	C-C motif chemokine ligand 14	-4.1	7.54E-05
TNFSF13B	TNF superfamily member 13b	-2.1	1.03E-04
CXCL6	C-X-C motif chemokine ligand 6	-5.2	1.43E-04
NGFR	nerve growth factor receptor	-3.9	1.62E-04

PDGFRB	platelet derived growth factor receptor beta	-2.5	2.64E-04
BMPR1B	bone morphogenetic protein receptor type 1B	-3.3	2.78E-04
AMHR2	anti-Mullerian hormone receptor type 2	-3.0	2.84E-04
IL10RA	interleukin 10 receptor subunit alpha	-2.7	3.26E-04
IL10RB	interleukin 10 receptor subunit beta	-1.3	4.54E-04
CCL4	C-C motif chemokine ligand 4	-3.2	7.54E-04
BMPR2	bone morphogenetic protein receptor type 2	-1.3	8.40E-04
CXCL5	C-X-C motif chemokine ligand 5	-4.8	9.81E-04
CCR7	C-C motif chemokine receptor 7	-2.9	1.19E-03
CD40	CD40 molecule	-2.0	1.30E-03
CCL8	C-C motif chemokine ligand 8	-3.8	1.71E-03
CXCR2	C-X-C motif chemokine receptor 2	-2.1	1.73E-03
CCL24	C-C motif chemokine ligand 24	-4.7	1.92E-03
XCR1	X-C motif chemokine receptor 1	-3.2	1.96E-03
TNFSF4	TNF superfamily member 4	-3.4	2.05E-03
IL1B	interleukin 1 beta	-3.4	2.37E-03
CXCR5	C-X-C motif chemokine receptor 5	-5.3	2.48E-03
CCR1	C-C motif chemokine receptor 1	-2.9	2.57E-03
LEPR	leptin receptor	-1.9	2.73E-03
IL3RA	NA	-2.2	3.42E-03
TNFRSF8	TNF receptor superfamily member 8	-2.9	4.28E-03
CCR10	C-C motif chemokine receptor 10	-2.2	5.25E-03
RELT	RELT TNF receptor	-1.9	6.53E-03
IL1RAP	interleukin 1 receptor accessory protein	-1.9	8.86E-03
IL15RA	interleukin 15 receptor subunit alpha	-1.1	1.03E-02
IL19	interleukin 19	-2.9	1.10E-02
TNFSF18	TNF superfamily member 18	-2.8	1.14E-02
CCR4	C-C motif chemokine receptor 4	-4.3	1.17E-02
KIT	KIT proto-oncogene, receptor tyrosine kinase	-1.7	1.22E-02
CCL17	C-C motif chemokine ligand 17	-5.0	1.27E-02
PDGFC	platelet derived growth factor C	-1.7	1.42E-02
IL3RA	interleukin 3 receptor subunit alpha	-2.0	1.59E-02
TNFSF14	TNF superfamily member 14	-3.0	1.61E-02
CCL3	C-C motif chemokine ligand 3	-2.8	1.72E-02
CSF1R	colony stimulating factor 1 receptor	-1.9	2.69E-02
BMPR1A	bone morphogenetic protein receptor type 1A	-1.0	3.13E-02
CXCR4	C-X-C motif chemokine receptor 4	-1.7	3.41E-02
IL1R1	interleukin 1 receptor type 1	-1.9	3.58E-02
CCL19	C-C motif chemokine ligand 19	-4.0	3.83E-02
CCL15	C-C motif chemokine ligand 15	-4.2	3.87E-02
CXCR6	C-X-C motif chemokine receptor 6	-3.4	3.87E-02

CCL3L3	C-C motif chemokine ligand 3 like 3	-3.5	4.00E-02
CCL4L2	C-C motif chemokine ligand 4 like 2	-3.1	4.14E-02
KITLG	KIT ligand	-1.8	4.43E-02
CCL22	C-C motif chemokine ligand 22	-2.7	4.50E-02
CXCR1	C-X-C motif chemokine receptor 1	-2.2	4.57E-02
IL12A	interleukin 12A	-1.8	4.61E-02
CCR5	C-C motif chemokine receptor 5	-2.4	4.98E-02

Determining a model cell line of OCCC with concurrent endometriosis based on human gene expression by RNA sequencing.

Genomically, OCCC cell lines frequently classify as OCCC rather than other histological subtypes of epithelial ovarian cancer [60, 80, 116, 384-386]. However, none of the widely shared or commercially available OCCC cell lines are characterized as being derived from OCCC with concurrent endometriosis. To determine which available cell lines most closely recapitulate our transcriptomic profiling data from OCCC with concurrent endometriosis, we used bioinformatic analysis of datasets from the Cancer Cell Line Encyclopedia (CCLE) [349]. Gene expression datasets for ovarian carcinoma cell lines [endometrioid/clear cell (IGROV-1, SKOV3, A2780), clear cell (TOV-21G, OVTOKO, OVISE, OVMANA, JHOC_5), p53-altered clear cell (RMG-I, ES-2), endometrioid (TOV112D), high-grade serous (OVCAR8), and low-grade serous (HEYA8)], endometrial cancer cell lines (AN3CA, HEC1A, ISHIKAWA, HEC1B), and a leukemia cell line (JURKAT) were downloaded and used. For the RNA-seq gene expression data from the OCCC with concurrent endometriosis tissue samples and endometrioma samples, we utilized multiclass logistic regression with variable selection by L1 penalty. We selected pathways whose pathway activity scores (PAS) are most predictive of cancer types. PAS of the 394 cancer-types predictive pathways were computed for OCCC with concurrent endometriosis tissue, endometrioma, and the selected cell line samples. In order to measure the similarity, we computed a Pearson correlation between the PAS of 394 pathways in tissue and cell line data.

Examination of the PAS results (Figure 3-5) showed that endometrioma samples (Eoma1, Eoma4, Eoma5) clustered most closely to endometrioma sample 3 (Eoma3), ES2, and HEYA8. ES-2 is considered a p53-altered OCCC cell line [84, 385], and HEYA8 is considered a KRAS-mutant low-grade serous line [84]. Studies suggest that both HEYA8 and ES-2 most closely represent low-grade serous [386]. The dendrogram suggests that ES2 and HEYA8 cluster more closely to each other than Eoma3. OCCC samples with concurrent endometriosis (OCCC4, OCCC2) clustered together with OCCC5, OVTOKO, OVISE, RMG-I, and OVMANA. OVTOKO, OVISE, and OVMANA are considered clear cell ovarian cancer cell lines as they were derived from metastatic lesions of OCCC and contain a mutant ARID1A [357, 384, 386]. RMG-I may be a p53-mutant clear cell type rather than a mutant ARID1A type [59, 116, 386]. OCCC sample with concurrent endometriosis 1 (OCCC1) clustered with IGROV-1, JHOC5, SKOV3, and TOV-21G. IGROV-1 is derived from a mixed histology tumor and contains mutant ARID1A and PIK3CA and could be considered a clear cell-like line [60, 84, 385, 386]. SKOV3 was derived from ascites of ovarian adenocarcinoma and contains mutant ARID1A and PIK3CA and is frequently more closely associated with clear cell tumors [60, 84, 363, 385, 386]. TOV-21G is considered a clear cell line as it was derived from OCCC and contains mutations in ARID1A and PIK3CA [60, 84, 354, 385, 386] (Table 3-6).

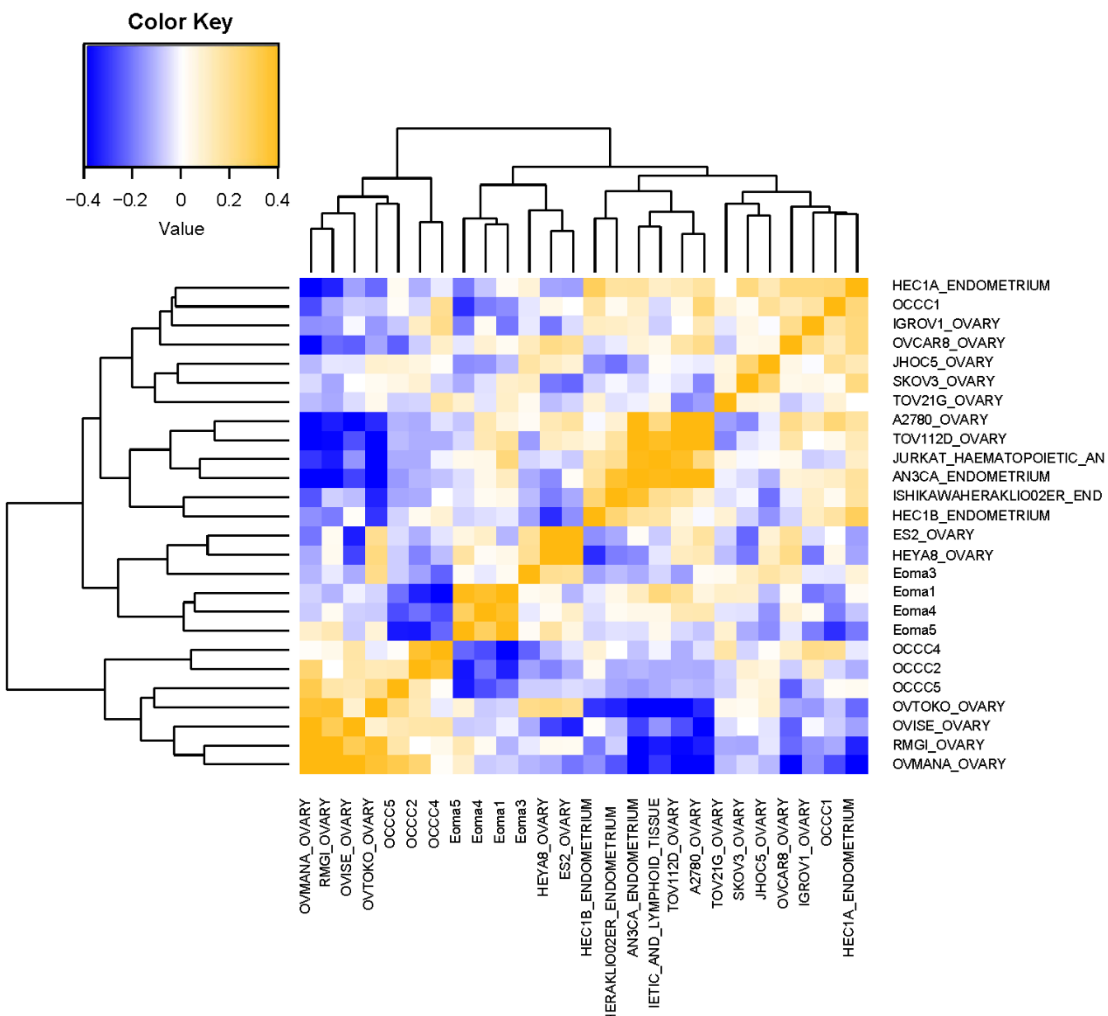

Figure 3-5. Molecular comparison of cell line transcriptomic profiles with clinical samples. Pathway activation score (PAS) analysis of molecular features from clinical samples (Eoma, benign endometrioma or OCCC, OCCC with concurrent endometriosis) or cell lines from CCLE. Cell line nomenclature is the CCLE name of the line_tissue type. A yellow color represents a higher PAS; blue, a lower PAS.

Table 3-6. Common characteristics of ovarian carcinoma cell lines used in experiments.

Cell Line	**Original Tissue Derivation**	**Putative Histotype by Molecular Studies**	**Genetic Mutations**	**Drug Response**	**References**
A2780	Ovarian adenocarcinoma	Endometrioid	ARID1A - nonsense & frameshift deletion PTEN - in frame deletion PICK3CA – missense mutation	Cisplatin – sensitive Doxorubicin – sensitive Paclitaxel – sensitive	[60, 80, 84, 349, 361, 384, 387-389]
ES-2	Ovarian adenocarcinoma – clear cell (primary tumor, poorly differentiated)	Clear cell	TP53 – missense mutation	Cisplatin – sensitive Oxaliplatin – sensitive Carboplatin – sensitive Docetaxel – sensitive Paclitaxel – intermediate response	[60, 80, 84, 349, 352, 384, 387-389]
IGROV-1	Ovarian adenocarcinoma - endometrioid with serous and clear cell features	Endometrioid / Clear cell	ARID1A – frameshift deletion & frameshift insertion TP53 – splice site & frameshift insertion PTEN – missense & frameshift insertion PIK3CA – missense & nonstop mutation	Cisplatin – sensitive Cyclophosphamide – resistant	[60, 80, 84, 384, 389, 390]
KK	Ovarian adenocarcinoma – clear cell	Clear cell	ARID1A – truncating mutation PIK3CA- missense mutation BRCA2- deletion	Cisplatin – resistant	[359, 385, 391, 392]
OVAS	Ovarian adenocarcinoma – clear cell	Clear cell	ARID1A – truncating mutation PIK3CA – missense mutation	Cisplatin – resistant	[151, 391, 392]
OVISE	Ovarian adenocarcinoma	Clear cell	ARID1A – insertion and truncating deletion	Cisplatin – intermediate response	[60, 84, 151, 349,

	– clear cell (pelvic metastasis)		PIK3CA – missense mutation	Cyclophosphamide – resistant	357, 384, 389]
OVTOKO	Ovarian adenocarcinoma – clear cell (spleen metastasis)	Clear cell	ARID1A –frameshift deletion	Cisplatin- sensitive Cyclophosphamide – resistant	[60, 84, 349, 357, 391, 393]
RMG-I	Ovarian adenocarcinoma – clear cell (ascites)	p53-mutant clear cell type	TP53 - homozygous deletion	Cisplatin – resistant	[60, 84, 151, 364, 384, 389, 391]
SKOV3	Ovarian adenocarcinoma (ascites)	Endometrioid / Clear cell	ARID1A – nonsense, truncating mutation PIK3CA - missense mutation P53 - frameshift deletion	Cisplatin – resistant	[60, 80, 84, 151, 363, 384, 388, 389, 394]
SMOV-2	Ovarian adenocarcinoma – clear cell	Clear cell	ARID1A – truncating mutation PIK3CA – missense mutation	Cisplatin – sensitive Paclitaxel – sensitive	[151, 360, 391]
TOV-21G	Ovarian adenocarcinoma – clear cell	Clear cell	ARID1A – frameshift insertion KRAS – missense mutation PTEN – frameshift deletion PIK3CA – missense mutation TP53 – missense mutation	Carboplatin – resistant	[60, 80, 84, 354, 384, 389, 391]

3.3 Discussion

Given that the current analysis was performed to compare a malignant disease to a non-malignant disease, it was expected that the finding that OCCC with concurrent endometriosis would be molecularly distinct from benign endometriomas. However, the large number of significantly differentially expressed genes was unexpected. Because endometriosis and ovarian cancers are commonly considered inflammatory and proliferative diseases, we were not expecting some of the highest dysregulations to occur in related pathways. Surprisingly, the greatest dysregulated pathways found with GSEA were proliferation (cell cycle G2 M, cell cycle G1 S, and DNA replication) and inflammatory signaling (matrisome, cytokine, and inflammatory response). As the OCCC and EOMA samples clustered distinctly in MDS, UMAP, and PCA analyses, it was expected that they would cluster more closely when using their transcriptomic profiles to determine the best *in vitro* models for OCCC with concurrent endometriosis. From the first bifurcation of the hierarchical clustering, 3 of the 4 OCCC samples are most closely modeled by RMG-I, OVISE, OVMANA, and OVTOKO. The other OCCC sample was distinctly clustered but was most closely related to other OCCC cell lines SKOV3, IGROV-1, and JHOC5. In MDS and PCA analysis, the EOMA samples were more tightly clustered, which translated to close clustering by PAS analysis. Though one sample, EOMA3, was separated by an additional node with hierarchical clustering and similarity to ES-2 and HEYA8, the EOMA samples were more similar to each other rather than any of the cell lines analyzed. Unfortunately, due to the lower number of OCCC transcriptomic studies available at the time of analysis, OCCC cell lines such as

SMOV-2 and KK did not have comparable transcriptomic profiles available to include in the analysis.

CHAPTER 4: SMALL RNA TRANSCRIPTOMIC PROFILING IDENTIFYING MIR-10A OVEREXPRESSION AND ITS RELATIONSHIP TO CHEMORESISTANCE IN OCCC

4.1 Background

MiRNAs are single-stranded, 22-24 nucleotide RNA molecules that function through an eight-nucleotide seed sequence to modulate gene networks [284]. MiRNAs are dysregulated in malignant and benign gynecological diseases and play impactful, functional roles in endometriomas and OCCC cell lines [120, 264, 284, 395]. For example, previous work has shown that endometriomas have distinct miRNA profiles and specific miRNAs, including miR-29c, play critical roles in uterine dysfunction [264]. As another example, next-generation sequencing of OCCC cell lines showed that miR-100 played a critical role in rapamycin resistance *in vitro* [120]. These limited studies suggest that miRNA molecules play essential roles. However, miRNA profiles in OCCC with concurrent endometriosis have not been examined. As a multi-platform approach, we integrated small RNA sequencing for miRNAs on matched samples of OCCC from women with pathology-confirmed concurrent endometriosis. From our list of dysregulated miRNAs, miR-10a was chosen to explore potential cellular and molecular associations in OCCC cell lines.

4.2 Results

OCCC with concurrent endometriosis have dysregulated miRNA expressions

MiRNAs are impactful for their potential as disease biomarkers and role as upstream regulators of multiple signaling pathways in diseases of the female reproductive tract [284, 395]. However, large-scale profiling of miRNAs has focused broadly on epithelial ovarian cancers without a direct analysis of OCCC, included only a small number of OCCC samples, or did not describe any samples with a history of or pathology-proven endometriosis [114, 396-399]. To complement our protein-coding transcriptomic studies, we profiled miRNAs on RNA isolated from clinical samples (n = 8), including endometrioma (n = 4) and OCCC with concurrent endometriosis (n = 4).

Small RNA sequencing gave over 43 million reads (mean: 5,382,728 ± 644,063 mapped reads per clinical sample). There were no significant differences in the mirDeep2 total mapped count percentage between endometrioma and OCCC with concurrent endometriosis (Table 4-1). Of the 2588 human mature miRNA molecules, 446 were expressed in at least one clinical sample. Principal component analysis (Figure 4-1A) with miRNA expression profiles showed PC1 and PC2 differential clustering of the OCCC with concurrent endometriosis from the benign endometrioma. Differential miRNA expression analysis was conducted with DESeq2. A comparison of dysregulated miRNAs between endometrioma and OCCC with endometriosis is shown on the volcano plot (Figure 4-1B). Significant differential expression was determined using a false discovery rate < 0.05, giving 128 significantly differentially expressed mature miRNA molecules. Limiting to log2 fold change > |1| identified 64 upregulated and 61 downregulated mature miRNA molecules (Table 4-2 – 4-3).

Table 4-1. Small RNA Sequencing Summary.

Sample Label	Eoma_1	Eoma_3	Eoma_4	Eoma_5	OCCC_1	OCCC_2	OCCC_4	OCCC_5
Sample	CW44	CW9	LCW62	CW195	G618	G506	G741	G002
TRIMMING: Read1 before filtering total reads	5,077,288	5,398,895	5,634,161	5,325,907	4,306,222	4,911,428	6,287,257	6,120,669
TRIMMING: Read1 after filtering total reads	4,856,700	4,998,221	5,322,652	5,140,647	4,075,055	4,553,826	5,941,947	5,290,756
TRIMMING: Percent after filtering total reads	95.66%	92.58%	94.47%	96.52%	94.63%	92.72%	94.51%	86.44%
TRIMMING: Filtering result reads failed due to low quality	13,377	18,142	13,581	12,305	10,500	12,451	14,005	16,371
TRIMMING: Filtering result reads failed due to too many N	36	34	44	43	33	29	38	28
TRIMMING: Filtering result reads failed due to too short	207,175	382,498	297,884	172,912	220,634	345,122	331,267	813,514
TRIMMING: Filtering result reads with adapter trimmed	4,351,674	4,865,939	4,887,023	4,728,035	3,757,745	4,248,171	5,651,876	5,428,215
TRIMMING: Duplication rate (may be overestimated since this is SE data)	95.77	94.46	84.68	87.81	87.33	86.03	95.16	90.6
MAPPING: mirDeep2TotalMappedCount	4,012,351	2,930,562	4,639,874	4,670,822	3,507,601	3,935,907	4,349,815	3,850,478
MAPPING: mirDeep2TotalMappedCount%	82.61%	58.63%	87.17%	90.86%	86.07%	86.43%	73.21%	72.78%

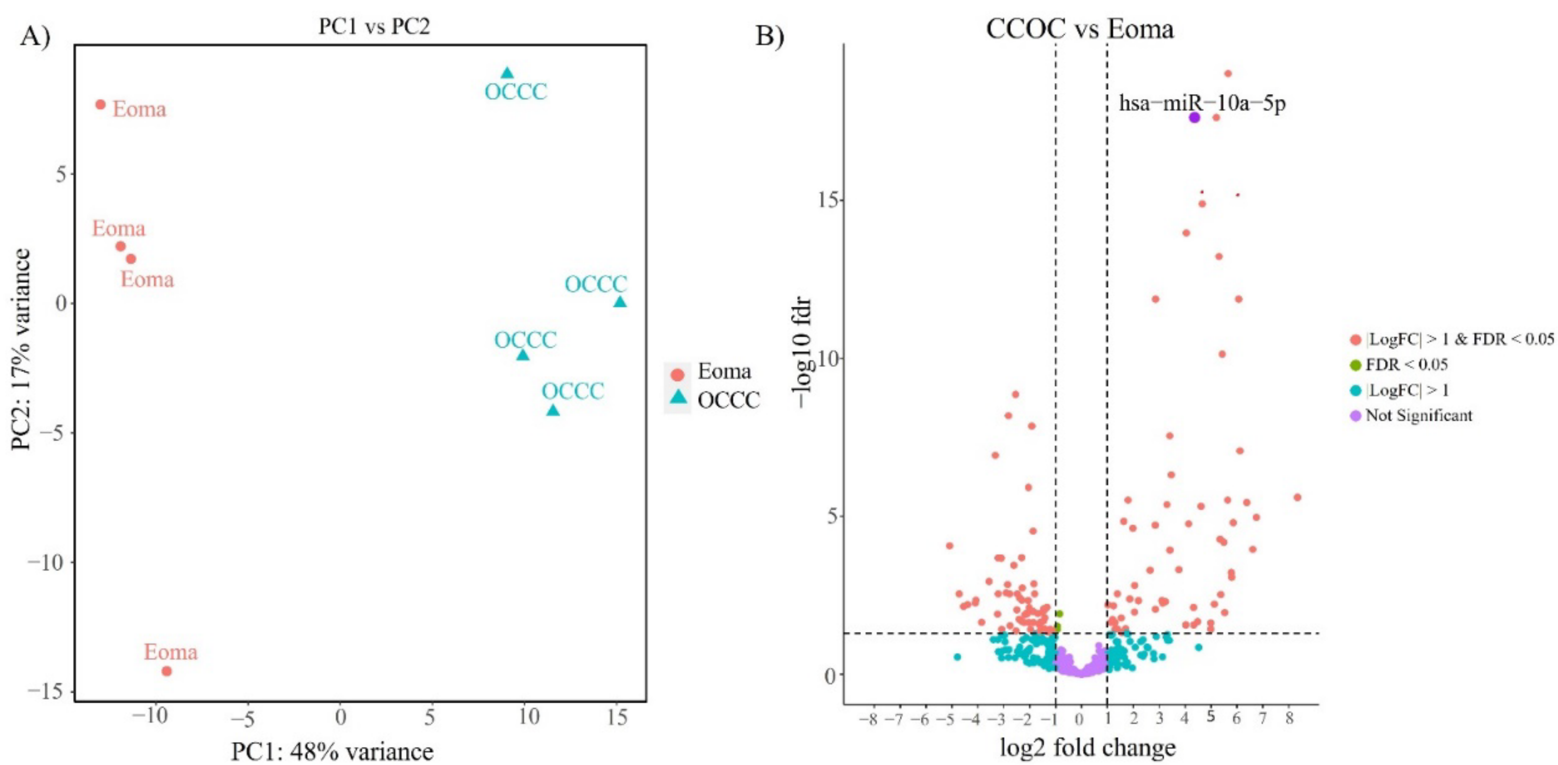

Figure 4-1. OCCC with concurrent endometriosis is molecularly distinct from benign endometrioma using miRNA expression. A) Principal component (PC) analysis of malignant OCCC with concurrent endometriosis (triangles, OCCC) clusters separately from benign endometrioma samples (circles, Eoma), using PC1 and PC2. B) Volcano plot of the significantly dysregulated miRNAs. Red represents miRNAs with $P < 0.05$, log2 fold-change > |1|. Blue dots represent miRNAs log2 fold-change > |1|. Green represents miRNAs with $P < 0.05$. Purple dots represent non-statistically significant miRNAs. The labeled dot represents hsa-miR-10a-5p.

Table 4-2. Upregulated miRNA in OCCC compared to endometrioma.

miRNA	baseMean	log2FoldChange	padj
hsa-miR-200c-3p	607.094365	5.66916129	9.91E-20
hsa-miR-203a-3p	186.221097	5.21648412	2.43E-18
hsa-miR-10a-5p	126649.249	4.3691492	2.43E-18
hsa-miR-141-3p	7868.77882	4.66647942	1.31E-15
hsa-miR-30a-3p	587.469956	4.05525273	1.09E-14
hsa-miR-200a-3p	256.501802	5.32072348	6.07E-14
hsa-miR-429	43.5327066	6.07738512	1.37E-12
hsa-miR-30a-5p	38986.2312	2.8669583	1.37E-12
hsa-miR-200b-3p	256.305643	5.44184353	7.45E-11
hsa-miR-345-5p	120.308225	3.41784325	2.88E-08
hsa-miR-335-3p	546.624927	6.13062781	8.61E-08
hsa-miR-1307-3p	60.7449127	3.47336228	4.94E-07
hsa-miR-3180	25.9012757	8.34819059	2.55E-06
hsa-miR-3180-3p	25.9012757	8.34819059	2.55E-06
hsa-miR-224-5p	33.587884	5.65089325	3.10E-06
hsa-miR-30b-5p	589.504625	1.80726541	3.10E-06
hsa-miR-200b-5p	6.64581117	6.38936842	3.68E-06
hsa-miR-30c-2-3p	15.3707792	3.30585684	4.28E-06
hsa-miR-183-5p	1436.86507	4.61713257	4.90E-06
hsa-miR-885-5p	23.3474239	6.75712666	1.10E-05
hsa-miR-30d-5p	5252.0051	1.63180778	1.44E-05
hsa-miR-10a-3p	7.67353569	5.87071805	1.61E-05
hsa-miR-96-5p	34.6772153	4.14401135	1.74E-05
hsa-miR-7706	21.8222699	2.85297709	1.93E-05
hsa-miR-30c-5p	822.021349	1.98239083	2.39E-05
hsa-miR-200a-5p	8.96933632	5.35742255	5.30E-05
hsa-miR-141-5p	6.02167	5.49753096	6.67E-05
hsa-miR-516a-5p	7.84286492	6.62466231	0.00011195
hsa-miR-335-5p	108.927108	3.41962003	0.00011946
hsa-miR-182-5p	2152.39576	3.76812169	0.00049358
hsa-miR-1301-3p	10.9583202	2.65369595	0.0005142
hsa-miR-1910-5p	7.41755196	5.78262093	0.00059763
hsa-miR-205-5p	24.5787964	5.79884224	0.0008466
hsa-miR-324-5p	12.7866504	2.05751494	0.00155912
hsa-miR-98-5p	2918.31403	1.38801617	0.00286713
hsa-miR-522-3p	3.39424874	5.38283151	0.00303948
hsa-miR-365a-3p	35.7462187	1.86973503	0.00416146

hsa-miR-365b-3p	35.7462187	1.86973503	0.00416146
hsa-miR-210-3p	55.7405817	3.10850748	0.00466097
hsa-miR-148b-5p	9.16377202	2.20628312	0.00466097
hsa-miR-7-5p	78.2019354	2.20069596	0.00475872
hsa-miR-452-5p	15.8614538	3.24623185	0.00504673
hsa-miR-135b-5p	16.0806609	3.13936716	0.00561583
hsa-miR-519a-3p	2.86157732	5.138562	0.00607174
hsa-miR-148b-3p	924.656332	1.0227384	0.00637582
hsa-miR-191-5p	4315.6881	1.24056735	0.00686553
hsa-miR-375-3p	10.8626465	4.33884577	0.00772848
hsa-miR-330-5p	6.31691425	2.85939164	0.00881403
hsa-miR-10399-3p	14.7421068	2.05182976	0.01076066
hsa-miR-525-5p	3.74112188	5.53452011	0.01112687
hsa-miR-941	128.068855	1.53830603	0.01653753
hsa-miR-744-5p	21.9039333	1.20439591	0.01849868
hsa-miR-10527-5p	1.76623046	4.48588164	0.02130695
hsa-miR-425-3p	20.5839853	1.29746952	0.02294365
hsa-miR-769-5p	120.965676	1.12987461	0.02294365
hsa-miR-3180-5p	2.54415861	4.98812893	0.02364663
hsa-miR-203b-3p	1.57010818	4.33386598	0.02722978
hsa-miR-1268a	2.29029029	4.02826544	0.02722978
hsa-miR-1268b	2.29029029	4.02826544	0.02722978
hsa-miR-362-5p	244.14105	1.70774603	0.03612069
hsa-miR-512-3p	2.53853575	4.98764301	0.03696841
hsa-miR-1307-5p	111.894291	1.3950378	0.03696867
hsa-miR-378a-3p	472.049095	1.29710684	0.0375021
hsa-miR-378c	12.7153093	1.56330515	0.04796444

Table 4-3. Downregulated miRNA in OCCC compared to endometrioma.

miRNA	baseMean	log2FoldChange	Padj
hsa-let-7b-3p	32.4896153	-2.0157326	0.00785447
hsa-let-7c-5p	2414.63619	-3.093993	0.00021081
hsa-miR-1-3p	23.5847964	-5.088709	8.66E-05
hsa-miR-101-3p	505.726498	-1.5123444	0.01122919
hsa-miR-1247-5p	4.37790957	-4.7194631	0.00286713
hsa-miR-125b-1-3p	48.740264	-2.0526296	0.00466097
hsa-miR-125b-2-3p	407.96742	-3.2131467	0.00020762
hsa-miR-125b-5p	579.521942	-2.7671218	0.00286713
hsa-miR-126-3p	691.629998	-2.2178797	0.02294365
hsa-miR-127-3p	1458.27972	-1.9120607	1.41E-08
hsa-miR-127-5p	9.04878054	-1.6171368	0.02724738
hsa-miR-133a-3p	21.9803772	-4.0716559	0.00455933
hsa-miR-134-5p	52.0566278	-1.330546	0.007579
hsa-miR-136-3p	86.0574124	-1.8328965	0.00138271
hsa-miR-136-5p	14.6595972	-2.6072189	0.00035358
hsa-miR-142-5p	613.240826	-2.4894117	0.00921626
hsa-miR-143-3p	113163.691	-2.8134704	6.61E-09
hsa-miR-144-5p	64.0081074	-4.0921469	0.00555847
hsa-miR-145-3p	206.343578	-3.3210702	1.18E-07
hsa-miR-145-5p	287.789302	-2.3095195	0.00020333
hsa-miR-146b-3p	25.5629326	-1.9599174	0.03826396
hsa-miR-146b-5p	37585.2789	-2.1174841	0.01181794
hsa-miR-150-5p	41.0884577	-2.4750721	0.00286713
hsa-miR-195-3p	6.14414576	-2.7524025	0.02913558
hsa-miR-195-5p	685.395789	-2.2944599	0.00455933
hsa-miR-199a-3p	2580.62568	-2.3797924	0.0038595
hsa-miR-199a-5p	1498.43626	-2.18183	0.01311134
hsa-miR-199b-3p	2580.62568	-2.3797924	0.0038595
hsa-miR-202-5p	112.379418	-2.4050144	0.01817374
hsa-miR-204-5p	239.20754	-2.8994667	0.00266256
hsa-miR-214-3p	185.33253	-2.0947345	0.0122558
hsa-miR-214-5p	16.30874	-2.8467732	0.00146092
hsa-miR-221-3p	430.247562	-1.2710857	0.04593454
hsa-miR-221-5p	18.6868814	-1.5794003	0.02256096
hsa-miR-222-3p	99.9990384	-1.460045	0.00849902
hsa-miR-2355-5p	2.31666026	-4.5496881	0.00716545
hsa-miR-23b-3p	761.958015	-1.5991522	0.04234259

hsa-miR-27a-5p	8.10349774	-3.0748754	0.03793
hsa-miR-27b-3p	5508.38467	-1.803258	0.00286713
hsa-miR-299-3p	7.78091779	-1.8577889	0.02294365
hsa-miR-299-5p	3.49295461	-4.3923757	0.00627837
hsa-miR-376c-3p	18.947238	-1.2019421	0.0375021
hsa-miR-379-5p	137.783592	-2.0420822	1.24E-06
hsa-miR-381-3p	252.060633	-2.5341455	1.40E-09
hsa-miR-382-3p	2.48812893	-3.8492218	0.02271921
hsa-miR-409-3p	64.4641897	-1.4271159	0.03609127
hsa-miR-410-3p	44.5513533	-1.4554711	0.02026921
hsa-miR-411-5p	34.2605388	-1.8588757	2.97E-05
hsa-miR-432-5p	17.8369712	-1.2865298	0.0451098
hsa-miR-450b-5p	14.077348	-2.3182739	0.02072044
hsa-miR-493-3p	13.3677405	-2.282124	0.00186347
hsa-miR-493-5p	34.8427075	-1.1308913	0.04130029
hsa-miR-539-3p	7.61920918	-3.2099923	0.00286713
hsa-miR-654-3p	71.3993942	-1.4071681	0.01637212
hsa-miR-708-3p	12.2810205	-2.5205111	0.04252431
hsa-miR-708-5p	56.3109887	-2.0355844	0.02294365
hsa-miR-874-3p	42.1341068	-1.414821	0.00921626
hsa-miR-887-3p	17.7180029	-1.6865918	0.01200672
hsa-miR-889-3p	36.7902618	-1.8571781	0.0103908
hsa-miR-99a-3p	5.59574996	-3.2332694	0.01250923
hsa-miR-99a-5p	1391.84917	-3.5652137	0.00116158

Because fold change up- or downregulated is a relative number, we examined the most abundant miRNA molecules in endometriomas with statistically significant lower expression in OCCC with concurrent endometriosis. The most abundant miRNA in endometriomas was hsa-miR-143-3p, representing 14.5%. Hsa-miR-146b-5p represented nearly 5% (or 4.47%) of endometrioma miRNAs. Table 4-4 shows the top ten downregulated mature miRNA molecules in OCCC with concurrent endometriosis. Table 4-5 shows the top ten upregulated mature miRNA molecules in OCCC with concurrent endometriosis. MiR-10a-5p was the most abundant miRNA in OCCC with concurrent endometriosis, representing nearly a quarter of all miRNAs (21.5%). Other significantly abundant and upregulated miRNAs included hsa-miR-30a-5p (6.1%), two other miR-30 family members [hsa-miR30d-5p (0.71%) and hsa-miR-30c-5p (0.12%)], and hsa-miR-141-3p (1.35%). Three mature miRNA molecules had a log2 fold change >4 and were in the top ten in terms of abundance in OCCC with concurrent endometriosis: hsa-miR-10a-5p (log2 fold change = 4.37, $P = 2.43e-18$), hsa-miR-141-3p (log2 fold change = 4.67, $P = 1.31e-15$), and hsa-miR-183-5p (log2 fold change = 4.62, $P = 4.90e-6$).

Overexpression of miR-10a has been found in breast, cervical, acute myeloid leukemia, and pancreatic ductal adenocarcinomas [311, 314, 319, 322, 327, 400-402]. Further, miR-10a overexpression was correlated with increased risk of recurrent breast cancer and decreased response to platinum agents *in vitro* [327, 400, 401, 403]. Disease progression on first-line platinum therapy is a hallmark of OCCC, with response rates to chemotherapy ranging as low as 11% [152, 153, 155, 404-406]. While platinum resistance is the most common reason for death from recurrence across all ovarian cancers, progression on platinum therapy is more prevalent in OCCC [153, 405, 407].

Thus, we explored the cellular and molecular effects of miR-10a in OCCC. QPCR expression showed that benign endometrioma exhibited a significantly lower expression of miR-10a-5p than OCCC with or without endometriosis (one-way ANOVA, $P < 0.05$, Figure 4-2). OCCC with concurrent endometriosis exhibited an 8-fold overexpression of miR-10a-5p compared to benign endometrioma (Student's t-test, $P = 0.01$). However, there was no statistically significant difference in miR-10a-5p expression between OCCC with concurrent endometriosis and OCCC without endometriosis (Student's t-test, $P = 0.90$).

Table 4-4: Top ten downregulated mature miRNAs in OCCC with concurrent endometriosis

Mature miRNA	**log2FoldChange**	P_{adj}
hsa-miR-143-3p	-2.81	6.61E-09
hsa-miR-127-3p	-1.91	1.41E-08
hsa-let-7c-5p	-3.09	2.11E-04
hsa-miR-99a-5p	-3.57	1.16E-03
hsa-miR-27b-3p	-1.80	2.87E-03
hsa-miR-199a-3p	-2.38	3.86E-03
hsa-miR-199b-3p	-2.38	3.86E-03
hsa-miR-146b-5p	-2.12	1.18E-02
hsa-miR-199a-5p	-2.18	1.31E-02
hsa-miR-23b-3p	-1.60	4.23E-02

Table 4-5: Top ten upregulated mature miRNA in OCCC with concurrent endometriosis

Mature miRNA	**log2FoldChange**	P_{adj}
hsa-miR-10a-5p	4.37	2.43E-18
hsa-miR-141-3p	4.67	1.31E-15
hsa-miR-30a-5p	2.87	1.37E-12
hsa-miR-183-5p	4.62	4.90E-06
hsa-miR-30d-5p	1.63	1.44E-05
hsa-miR-30c-5p	1.98	2.39E-05
hsa-miR-182-5p	3.77	4.94E-04
hsa-miR-98-5p	1.39	2.87E-03
hsa-miR-148b-3p	1.02	6.38E-03
hsa-miR-191-5p	1.24	6.87E-03

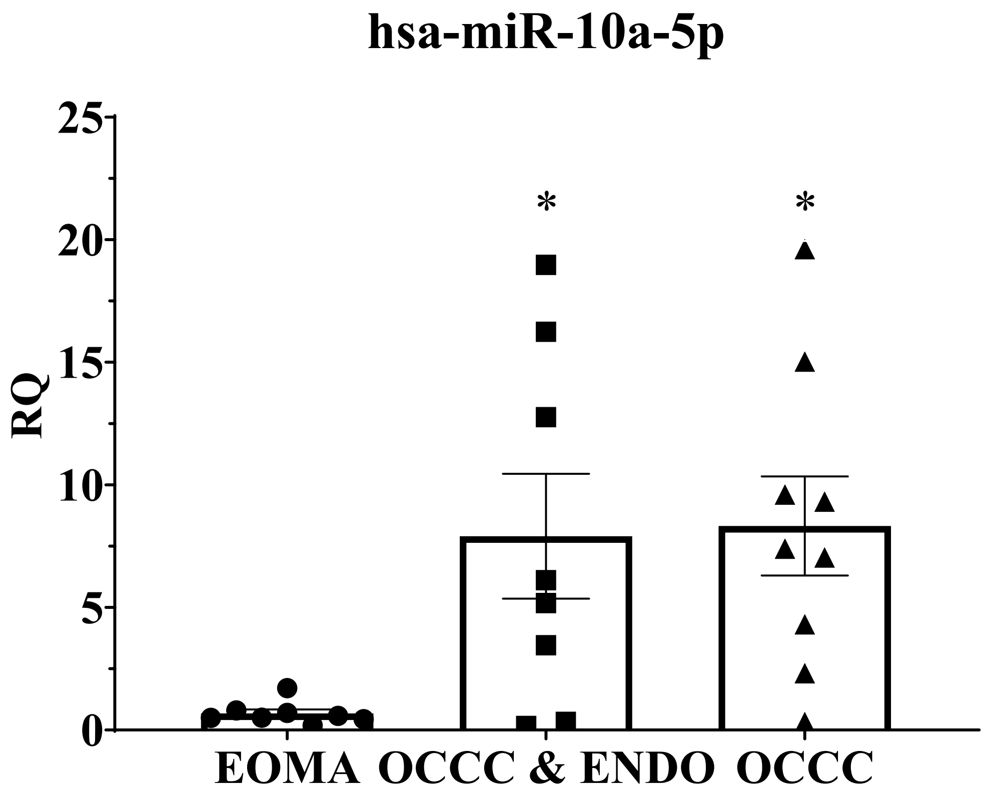

Figure 4-2. MiR-10a-5p is significantly upregulated in human tissue samples of ovarian clear cell carcinoma. Examination of miR-10a-5p expression in endometrioma (EOMA, $n = 8$), ovarian clear cell carcinoma from women with concurrent endometriosis (OCCC & ENDO, $n = 8$), and ovarian clear cell carcinoma from women without pathologically confirmed endometriosis (OCCC, $n = 9$). RQ, the relative quantity of hsa-miR-10a-5p to U6 snRNA, normalized to EOMA. Error bars represent ± SEM. *$P < 0.05$, one-way ANOVA.

MiR-10a-5p expression in human OCCC cell lines correlates with carboplatin IC50.

To explore the role of miR-10a in OCCC, the expression of miR-10a-5p was examined in a panel of human ovarian cancer cell lines (Figure 4-3A). There appeared to be two groups of cell lines – those with low miR-10a expression (A2780, OVISE, TOV-21G, OVTOKO, KK, and SMOV-2) and those with high miR-10a expression (A2780CR5, SKOV3ip1, RMG-I, SKOV3, OVAS, ES-2). To confirm similar results, we analyzed the next-generation small RNA sequencing data from Nagaraja *et al*. [120]. The relative expression of miR-10a in each cell line was similar to our expression. There was low miR-10a expression in OVISE, TOV-21G, SMOV-2, and KK, and those with high relative miR-10a expression included RMG-I, ES-2, and OVAS (Figure 4-4).

A2780CR5 cells are an isogenic line of A2780 that is resistant to platinum [362]. Interestingly, the miR-10a-5p expression was 3.3-fold higher in the platinum-resistant line, A2780CR5 (Mann-Whitney, $P < 0.01$) than in A2780. Increased miR-10a expression has previously been correlated with platinum resistance in lung cancer [326, 403]. As a result of this increased miR-10a-5p expression in the platinum-resistant line, carboplatin response was compared across OCCC cell lines. Carboplatin response was expressed as the half maximum inhibitory capacity (IC50) and correlated with miR-10a-5p expression. A positive correlation ($R^2 = 0.93$) was found between miR-10a expression and carboplatin IC50 (Figure 4-3B).

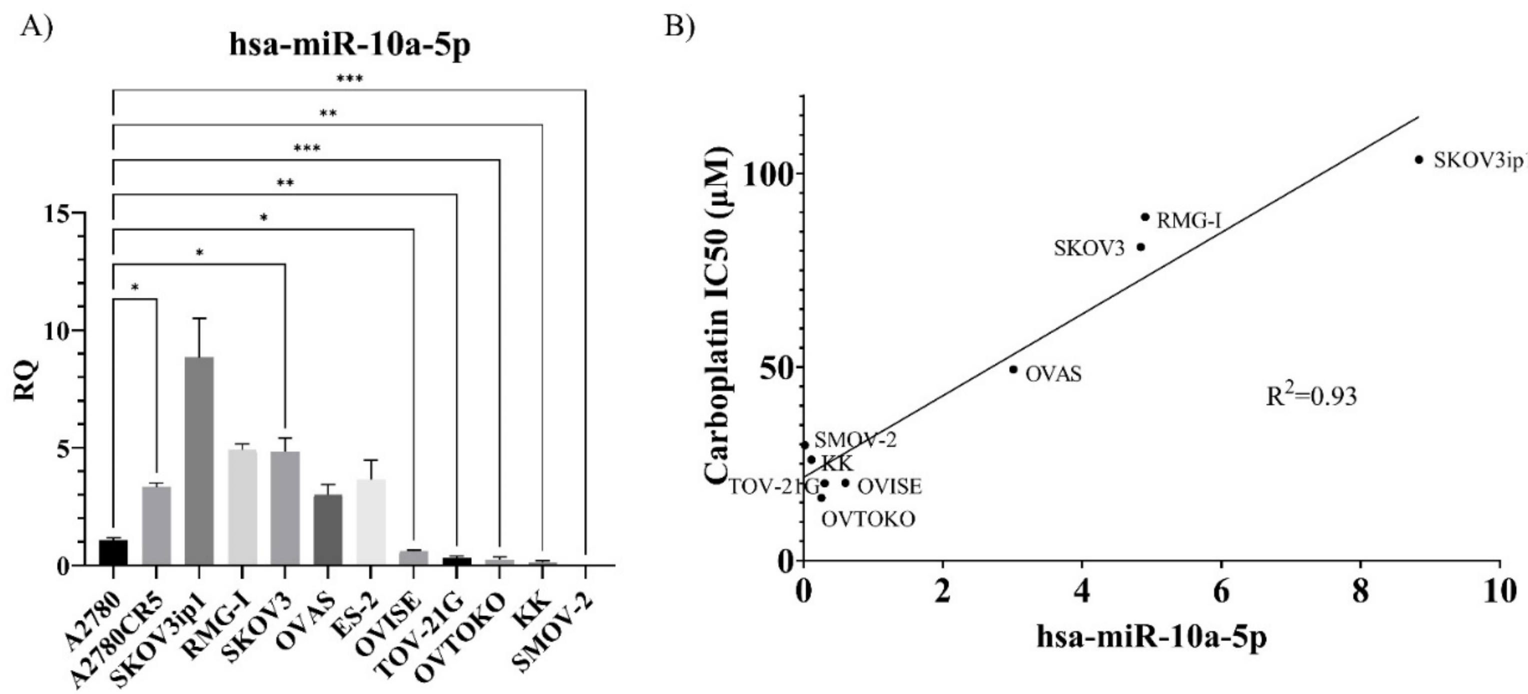

Figure 4-3. MiR-10a-5p expression across a panel of ovarian cancer cell lines. A) RQ, the relative quantity of hsa-miR-10a-5p to U6 snRNA, normalized to A2780. ***P<0.001, **P<0.001, *P < 0.05, Brown-Forsythe and Welch ANOVA. A2780 (n = 6), A2780CR5 (n = 2), SKOV3ip1 (n = 3), RMG-I (n = 2), SKOV3 (n = 4), OVAS (n = 4), ES-2 (n = 4), OVISE (n = 9), TOV-21G (n = 4), OVTOKO (n = 7), KK (n = 3), and SMOV-2 (n = 6). B) Correlation of miR-10a-5p expression to carboplatin IC50 in OCCC cell lines. RMG-I (n = 2), OVAS (n = 4), ES-2 OVISE (n = 9), TOV-21G (n = 2), OVTOKO (n = 7), KK (n = 2), and SMOV-2 (n = 6). Carboplatin IC50 is $n \geq 5$ for each cell line.

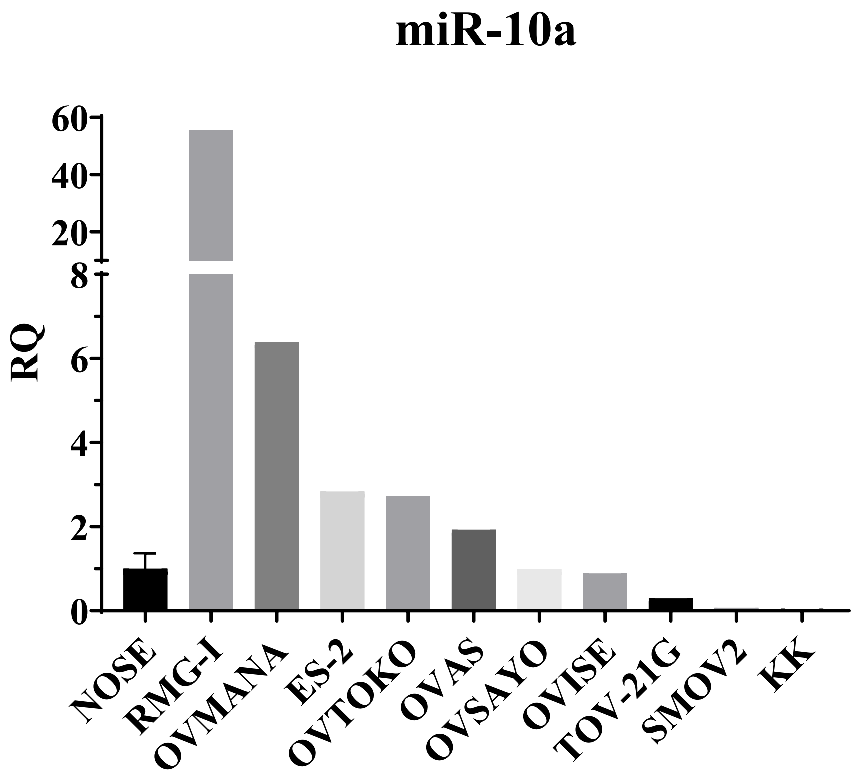

Figure 4-4. Expression of hsa-miR-10a-5p across OCCC cell lines. A plot of read counts from Nagaraja *et al*., 2010. RQ, the relative quantity of hsa-miR-10a-5p normalized read counts in each cell line normalized to primary cultures of normal ovarian surface epithelium (NOSE). Error bars represent ± SEM. Each cell line $n = 1$; NOSE, $n = 4$.

4.3 Discussion

Given the large number of significantly differentially expressed genes in OCCC with concurrent endometriosis compared to endometrioma, it was not surprising to find 128 dysregulated miRNAs in OCCC with concurrent endometriosis compared to endometrioma. However, the finding that hsa-miR-10a-5p (miR-10a) represented nearly a quarter (21.5%) of miRNA sequencing reads in OCCC with concurrent endometriosis was unexpected, particularly given the next most abundant miRNA, hsa-miR-30a-5p, accounted for 6.1% of reads in OCCC with concurrent endometriosis. Not only was miR-10a a large portion of miRNA molecules in OCCC with concurrent endometriosis, but it was also one of the most significantly upregulated (log2 fold change = 4.37, P = 2.43e-18) miRNAs in OCCC with concurrent endometriosis compared to endometriomas. Interestingly, this overexpression of miR-10a in OCCC with concurrent endometriosis, compared to endometrioma, was replicated in OCCC human tissue samples where pathology did not note any endometriosis. These results suggest that miR-10a is upregulated in OCCC independent of endometriosis status thus broadening its potential as a disease biomarker.

MiR-10a has been found to be overexpressed in a variety of other cancers and [306-321] correlated with decreased response to platinum-based agents [325, 326] [327, 328]. Since miR-10a, a molecule correlated with platinum-resistance was found to be overexpressed in OCCC, a commonly platinum-resistance disease, we were interested in exploring the relationship between miR-10a expression in human OCCC cell lines and their response to platinum therapy *in vitro*. Interestingly, the A2780CR5 cell line, known to be platinum-resistant [362], had a significantly increased (3.3 fold, $P < 0.01$) basal expression of miR-10a compared to the platinum-sensitive A2780, from which A2780CR5 was derived. OCCC cell lines with the highest miR-10a expression also required higher carboplatin concentrations to reach their IC50 ($R^2 = 0.93$). Overall, these results suggest that miR-10a plays a role in the *in vitro* platinum response of OCCC cell lines.

CHAPTER 5: MIR-10A OVEREXPRESSION EFFECTS ON OCCC PROLIFERATION AND CELL CYCLE

5.1 Background

MiR-10a as a tumor suppressor and oncogene in cancer

Hsa-miR-10a-5p (miR-10a) is part of the larger miR-10 family containing miR-99a, miR-100, miR-10b, miR-125b(-1 and -2), miR-125a, and miR-99b [292-294]. In the ovary, miR-10a expression regulates the proliferation and apoptosis of granulosa cells [296]. Other non-diseased state functions of miR-10a are the regulation of angiogenesis [297], the transcription of actin cytoskeleton [298], and ephrin receptor signaling [298]. It has varied expression in normal tissues [299] and is dysregulated in multiple cancers [300]. MiR-10a has potential oncogenic and tumor suppressor effects, depending on tissue type. MiR-10a has been implicated as a tumor suppressor in prostate cancer [301], breast carcinomas [302-304], and osteosarcoma [305]. In other cases, miR-10a has oncogenic properties in cutaneous squamous cell carcinoma [306], squamous cell cervical carcinomas [307-311], non-small cell lung carcinomas [312-314], acute myeloid leukemias [315], granulosa cell tumors [316], and pancreatic ductal adenocarcinomas [317-321]. Interestingly, while miR-10a is overexpressed (oncogenic) in these carcinomas, its direct functional effects are inconsistent across diseases, nor are the critical target genes studies. For example, in cervical carcinomas, miR-10a-5p overexpression has been shown to be involved in tumorigenesis, hyper-proliferation, metastasis, and invasion [307, 311, 322], while another study found overexpression of miR-10a decreased cellular proliferation [309]. For example, in breast cancer [302] and kidney cancer cells [323], miR-10a overexpression was found to inhibit proliferation.

Along with regulating cellular functions, miR-10a expression has been implicated in chemotherapy response. In acute myeloid leukemia, miR-10a overexpression was found to be a strong predictor of insensitivity to the MDM2 inhibitor and cytarabine therapy [324]. Similarly, overexpression of miR-10a has been seen in platinum-resistant lung cancers [325, 326] and gemcitabine-resistant pancreatic ductal adenocarcinomas [319]. MiR-10a has also been found to be overexpressed in an isogenic platinum-resistant MCF-7, a breast cancer cell line [327]. In Benson *et al.,* miR-10a was one of the miRNAs that were significantly altered in women considered responsive to treatment ($P = 0.024$), showing that miR-10a can be detected in minimally invasive blood draws and suggesting expression changes in serum could serve as a biomarker for treatment response [328]. The wide array of functions and resistance pathways involving miR-10a suggest its potential as a molecule of interest in the platinum-resistance disease of OCCC. Particularly, miR-10a expression changes to therapy make it a potential biomarker for predicting OCCC response to chemotherapy. Here we explored the effects of miR-10a overexpression *in vitro* on OCCC cell lines.

5.2 Results

MiR-10a-5p overexpression decreases cellular proliferation

SKOV3ip1cells are a xenograft-derived line of the SKOV3 ovarian cancer cell line. Previous work showed increased cellular proliferation of SKOV3ip1 cells compared to SKOV3 [356]. The miR-10a-5p expression was almost 2-fold higher in SKOV3ip1 (un-paired t-test, $P < 0.05$) than in SKOV3. *In vitro* studies overexpressing miR-10a-5p showed potentially cancer-type specific effects on cellular proliferation. For example, overexpression of miR-10a in melanoma, acute myeloid leukemia, and laryngeal squamous cell carcinoma cells decreased cellular proliferation in these cancers [408-410].

To study the effects of miR-10a overexpression on proliferation in OCCC cell lines, SMOV-2 and KK were transiently transfected with a mature miR-10a-5p mimic. After optimization of transfection conditions (data not shown), overexpression of miR-10a was confirmed (Figure 5-1). SMOV-2 and KK miR-10a overexpressing cells (SMOV2-10a and KK-10a) had a statistically significant and sustained decrease in cellular proliferation compared to the non-targeting control transfected cells (SMOV2-10actl and KK-10actl) (Figure 5-2). For SMOV-2 cells, there was a statistically significant decrease in proliferation beginning at 96 hours. Overexpression of miR-10a in SMOV-2 cells showed an almost 2-fold increase in doubling time, from 42.8 hours to 84.9 hours. A statistically significant decrease in cell density was noted beginning at 72 hours in KK cells overexpressing miR-10a compared to a non-targeting control, and continuing through 120 hours, there was a statistically significant decrease in proliferation. Overexpression of miR-10a in KK cells lengthened the double time from 40.9 hours to 47.2 hours.

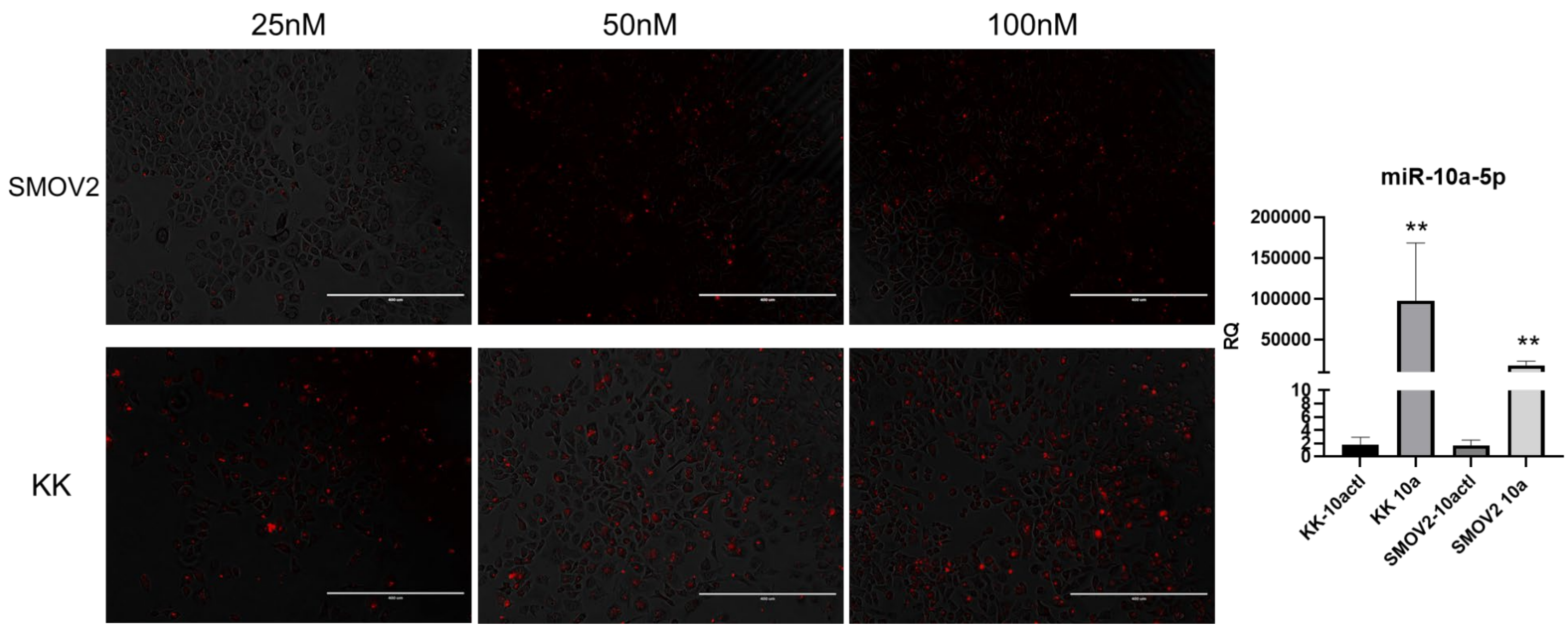

Figure 5-1. MiR-10a-5p is significantly overexpressed in SMOV-2 and KK cells transfected with a miR-10a-5p mimic. SMOV-2 and KK cells were transfected with 25nM, 50nM, and 100nM of siGlo Red Transfection agent (Horizon Discovery) and imaged using an RFP cube on EVOS FL (ThermoFisher). RQ, the relative quantity of hsa-miR-10a-5p to U6 snRNA, normalized to each negative control transfected line. Cells transfected with 100nM mature miRNA mimics for miR-10a (SMOV2-10a and KK-10a) were compared to cells transfected with 100nM Negative Control #1 (SMOV2-10actl and KK-10actl). Error bars represent ± SEM. KK transfection, $n = 6$; SMOV2-10a, $n = 5$. $^{**}P < 0.05$, using Mann-Whitney two-tailed test.

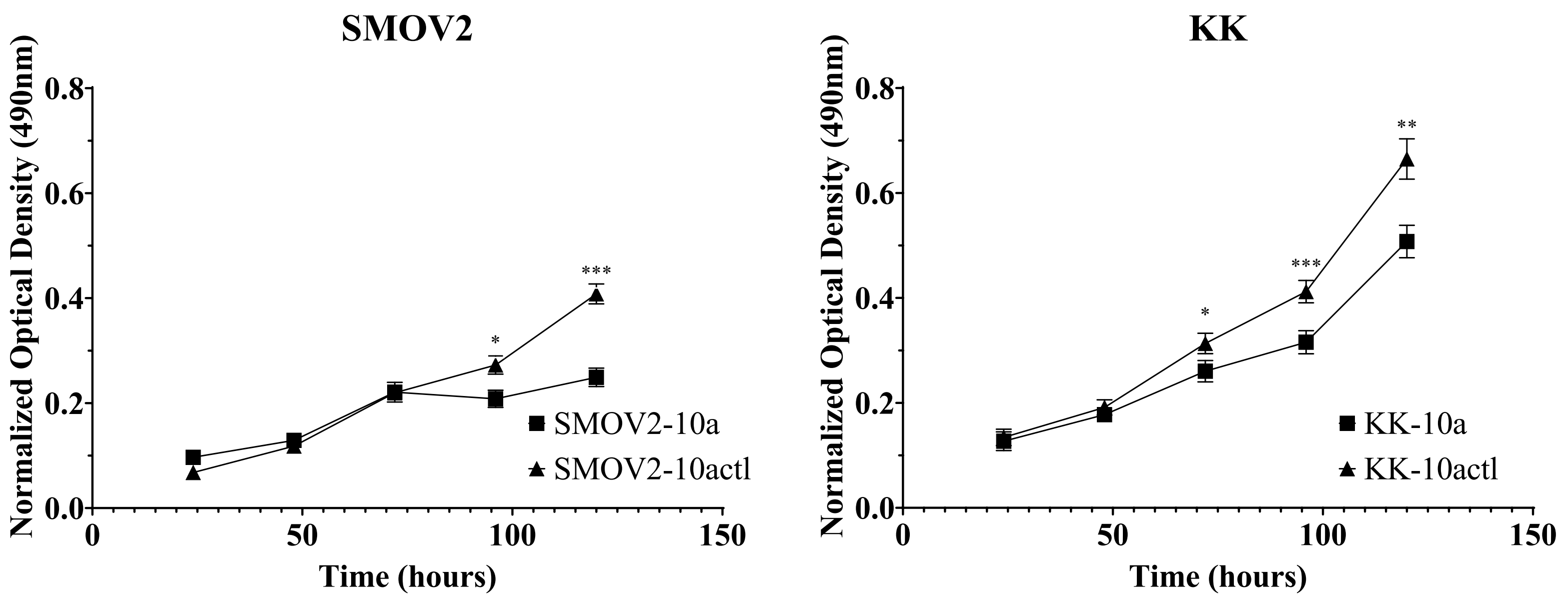

Figure 5-2. MiR-10a overexpression resulted in a significant decrease in cellular proliferation in SMOV-2 and KK cells. MTS was normalized to the growth medium for each measurement. Cells transfected with mature miRNA mimic for miR-10a (SMOV2-10a and KK-10a) were compared to cells transfected with negative control #1 (SMOV2-10actl and KK-10actl) for each cell line and each time point. ***$P < 0.0001$, ** $P < 0.001$, * $P < 0.05$, Student's two-tailed t-test at each time point. $n = 6$ for each cell line, timepoint, and transfection condition.

MiR-10a-5p overexpression shifts cells from S and G_2 to G1 phase

Cell cycle distribution was analyzed in SMOV-2 and KK cells overexpressing miR-10a-5p compared to non-targeting control transfected cells. SMOV-2 and KK cells overexpressing miR-10a-5p had a statistically significant increase in the G_1 population and a decrease in S and G_2 populations ($P < 0.001$) (Figure 5-3). SMOV2-10a had more than a 6% increase in the G_1 population with a 4.5% decrease percent in the S phase ($P < 0.0001$). KK-10a had a similar 7% increase in cells in the G_1 phase, but KK-10a cells had a more distributed decrease in S phase (4%, $P = 0.01$) and G_2 (3%, $P = 0.002$). The amount of cellular debris was not significantly changed in either SMOV-2 or KK samples (Figure 5-3).

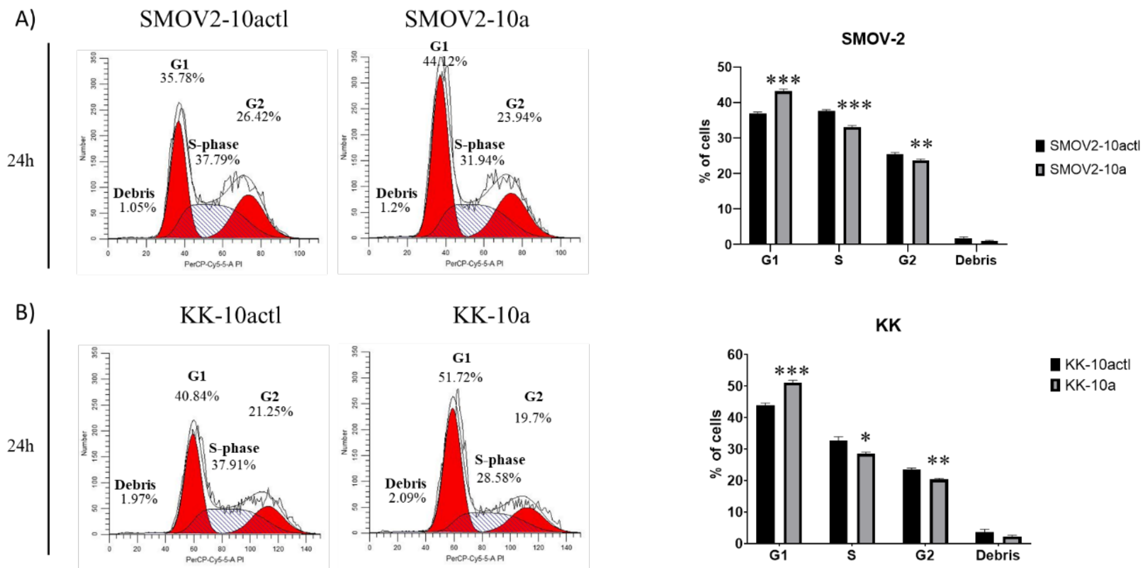

Figure 5-3. Overexpression of hsa-miR-10a-5p shifts cell cycle from S and G2 phase to G1. Cells transfected with mature miRNA mimic for miR-10a (SMOV2-10a and KK-10a) were compared to cells transfected with negative control #1 (SMOV2-10actl and KK-10actl) for each cell line. The flow histograms depict a representative biological replicate for A) SMOV-2 and B) KK. Graphical depictions represent $n = 6$ for each cell line and transfection condition. Statistical analysis was conducted using a 2-tailed Student's *t*-test: *** $P < 0.0001$, ** $P < 0.001$, * $P < 0.05$.

<u>Predicted miR-10a-5p target genes dysregulated in OCCC with endometriosis play a role in signaling receptor binding</u>

MiRNA molecules are considered epigenetic regulators of gene expression [411]. Overexpression of miRNA molecules leads to downregulation largely by destabilization of mRNA transcripts. Importantly, most mRNA molecules are targets of miRNAs [255]. Each miRNA molecule has relative specificity of gene targets based on nucleotide sequence in the 3'UTR of the target gene. *In silico* prediction of genes that could be targeted by individual miRNA families is available in several databases. Target Scan predicts miRNA binding through complementary binding of the seed region of the mature miRNA molecule to the mRNA molecule, typically within the 3'UTR [256, 366, 367]. As a slightly different algorithm for miRNA target gene predictions, miRDB uses *in silico* predicted miRNA binding to mRNA targets and downregulation of target gene expression from high-throughput sequencing data to identify putative targets. Additional predictions are added to miRDB from computational modeling and literature curation [368, 369]. As another resource, miRTarBase uses natural language processing (NLP) to extract miRNA-predicted target gene data across the literature, to give miRNA-target interactions (MTIs). Examples of MTIs from miRTarBase include direct interaction studies of miRNA and target genes from CLIP-seq data, *in silico* seed sequence binding to mRNA from miRanda and miRBase, and experimental validation through reporter assays, western blots, or qPCR [370]. To determine which dysregulated genes in OCCC with concurrent endometriosis were predicted targets of miR-10a-5p, miRNA:mRNA functional interaction prediction was undertaken using datasets from Target Scan v7.2, miRDB, and miRTarBase 2022 [365]. Target Scan predicted 59 (Table 5-1), miRDB predicted 62 (Table 5-2), and miRTarBase predicted 67 (Table 5-3) unique protein-coding genes downregulated in OCCC with concurrent endometriosis to be putative miR-10a-5p targets.

While 151 unique protein-coding genes were predicted to be miR-10a-5p target genes in at least one of the three algorithms, BDNF (brain-derived neurotrophic factor, log2 fold-change -2.42, *P* = 6.8e-5), *RORA* (RAR related orphan receptor A, log2 fold-change -1.98, *P* = 1.48e-7), *CSRNP3* (cysteine and serine-rich nuclear protein3, log2 fold-change -1.93, *P* = 1.57e-3), *CHL1* (cell adhesion molecule L1 like, log2 fold-change -3.08, *P* = 2.09e-5), *LIX1L* (limb and CNS expressed 1 like, log2 fold-change -1.13, *P* = 7.11e-5), and *RAP2A* (RAP2A, member of RAS oncogene family, log2 fold-change -1.52, *P* = 2.63e-5) were genes predicted to be miR-10a-5p targets in each of the three datasets (Figure 5-4). Using the 151 genes as input, the WEB-based Gene SeT AnaLysis Toolkit [WebGestalt [412]] revealed that the top network for miRNA targeting was the miR-10 family as expected (enrichment ratio = 13.67, Table 5-4). Gene ontology molecular function analysis (Table 5-5) showed enrichment in signaling receptor binding genes (enrichment ratio = 1.97, *P* = 1.5e-3). Pathway analysis (Table 5-6) showed enrichment in cellular senescence genes (enrichment ratio = 4.71, *P* = 4.24e-3) and TGFb signaling pathway (enrichment ratio = 7.17, *P* = 2.34e-3). A listing of the downregulated predicted miR-10a-5p target genes from the signaling receptor binding molecular function is listed in Table 5-7. Signaling receptor binding, cellular senescence, and TGFβ-signaling all involve the cell cycle.

Table 5-1. MiR-10a Target Genes Identified by TargetScan.

miRNA	**Symbol**	**Gene Name**
hsa-miR-10a-5p	*ARRDC3*	Arrestin domain containing 3
hsa-miR-10a-5p	*ARSJ*	Arylsulfatase family member J
hsa-miR-10a-5p	*ATCAY*	ATCAY kinesin light chain interacting caytaxin
hsa-miR-10a-5p	*BACH2*	BTB domain and CNC homolog 2
hsa-miR-10a-5p	*BCL6*	BCL6 transcription repressor
hsa-miR-10a-5p	*BDNF*	Brain derived neurotrophic factor
hsa-miR-10a-5p	*BMP2K*	BMP2 inducible kinase
hsa-miR-10a-5p	*C14orf28*	Chromosome 14 open reading frame 28
hsa-miR-10a-5p	*CEP15*	Centrosomal protein 15
hsa-miR-10a-5p	*CCDC71L*	Coiled-coil domain containing 71 like
hsa-miR-10a-5p	*CCDC88A*	Coiled-coil domain containing 88A
hsa-miR-10a-5p	*CDK6*	Cyclin dependent kinase 6
hsa-miR-10a-5p	*CELF2*	CUGBP Elav-like family member 2
hsa-miR-10a-5p	*CHL1*	Cell adhesion molecule L1 like
hsa-miR-10a-5p	*CSRNP3*	Cysteine and serine rich nuclear protein 3
hsa-miR-10a-5p	*DOCK11*	Dedicator of cytokinesis 11
hsa-miR-10a-5p	*ELAVL2*	ELAV like RNA binding protein 2
hsa-miR-10a-5p	*EPHA4*	EPH receptor A4
hsa-miR-10a-5p	*INSYN2A*	Inhibitory synaptic factor 2A
hsa-miR-10a-5p	*FBXO30*	F-box protein 30
hsa-miR-10a-5p	*FLRT2*	Fibronectin leucine rich transmembrane protein 2
hsa-miR-10a-5p	*GATA6*	GATA binding protein 6
hsa-miR-10a-5p	*IRS1*	Insulin receptor substrate 1
hsa-miR-10a-5p	*ITSN1*	Intersectin 1
hsa-miR-10a-5p	*KCNA6*	Potassium voltage-grated channel subfamily A member 6
hsa-miR-10a-5p	*JCAD*	Junctional cadherin 5 associated
hsa-miR-10a-5p	*KLF11*	KLF transcription factor 11
hsa-miR-10a-5p	*KLF7*	KLF transcription factor 7
hsa-miR-10a-5p	*KPNA5*	Karyopherin subunit alpha 5
hsa-miR-10a-5p	*LIX1L*	Limb and CNS expressed 1 like
hsa-miR-10a-5p	*LYVE1*	Lymphatic vessel endothelial hyaluronan receptor 1
hsa-miR-10a-5p	*NEDD4*	NEDD4 E3 ubiquitin protein lipase
hsa-miR-10a-5p	*NFASC*	Neurofascin
hsa-miR-10a-5p	*NFIX*	Nuclear factor I X
hsa-miR-10a-5p	*NPAS3*	Neuronal PAS domain protein 3
hsa-miR-10a-5p	*PALM2-AKAP2*	PALM2 and AKAP2 fusion
hsa-miR-10a-5p	*PCDH10*	Protocadherin 10
hsa-miR-10a-5p	*PEA15*	Proliferation and apoptosis adaptor protein 15
hsa-miR-10a-5p	*RAP2A*	RAP2A, member of RAS oncogene family

hsa-miR-10a-5p	*RASL10B*	RAS like family 10 member B
hsa-miR-10a-5p	*RBMS3*	RNA binding motif single stranded interacting protein 3
hsa-miR-10a-5p	*RORA*	RAR related orphan receptor A
hsa-miR-10a-5p	*RORB*	RAR related orphan receptor B
hsa-miR-10a-5p	*SAMD14*	Sterile alpha motif domain containing 14
hsa-miR-10a-5p	*SCARB2*	Scavenger receptor class B member 2
hsa-miR-10a-5p	*SERPINE1*	Serpin family E member 1
hsa-miR-10a-5p	*SESN3*	Sestrin 3
hsa-miR-10a-5p	*SH3D19*	SH3 domain containing 19
hsa-miR-10a-5p	*SLC38A2*	Solute carrier family 38 member 2
hsa-miR-10a-5p	*SNX12*	Sorting nexin 12
hsa-miR-10a-5p	*SNX18*	Sorting nexin 18
hsa-miR-10a-5p	*SOBP*	Sine oculis binding protein homolog
hsa-miR-10a-5p	*ST6GALNAC6*	ST6 N-acetylgalactosamide alpha-2,6-sialytranferase 6
hsa-miR-10a-5p	*THRA*	Thyroid hormone receptor alpha
hsa-miR-10a-5p	*TMEM167B*	Transmembrane protein 167B
hsa-miR-10a-5p	*TMEM170B*	Transmembrane protein 170B
hsa-miR-10a-5p	*TRPC1*	Transient receptor potential cation channel subfamily C member 1
hsa-miR-10a-5p	*TSPAN9*	Tetraspanin 9
hsa-miR-10a-5p	*ZBTB16*	Zinc finger and BTB domain containing 16

Table 5-2. MiR-10a Target Genes Identified by miRDB.

miRNA	Symbol	Gene Name
hsa-miR-10a-5p	*ACVR2A*	Activin A receptor type 2A
hsa-miR-10a-5p	*ARSJ*	Arylsulfatase family member J
hsa-miR-10a-5p	*ATCAY*	ATCAY kinesin light chain interactin caytaxin
hsa-miR-10a-5p	*BACH2*	BTB domain and CNC homolog 2
hsa-miR-10a-5p	*BDNF*	Brain derived neurotrophic factor
hsa-miR-10a-5p	*CAVIN2*	Caveolae associated protein 2
hsa-miR-10a-5p	*CCDC88A*	Coiled-coil domain containing 88A
hsa-miR-10a-5p	*CDK6*	Cyclin dependent kinase 6
hsa-miR-10a-5p	*CHL1*	Cell adhesion molecule L1 like
hsa-miR-10a-5p	*CHST4*	Carbohydrate sulfotransferase 4
hsa-miR-10a-5p	*CNN1*	Calponin 1
hsa-miR-10a-5p	*CSRNP3*	Cysteine and serine rich nuclear protein 3
hsa-miR-10a-5p	*DOCK11*	Dedicator of cytokinesis 11
hsa-miR-10a-5p	*EIF5A2*	Eukaryotic translation initiation factor 5A2
hsa-miR-10a-5p	*GATA6*	GATA binding protein 6
hsa-miR-10a-5p	*GIMAP8*	GTPase, IMAP family member 8
hsa-miR-10a-5p	*GRIK1*	Glutamate ionotropic receptor kainate type subunit 1
hsa-miR-10a-5p	*IL5RA*	Interleukin 5 receptor subunit alpha
hsa-miR-10a-5p	*INSYN2A*	Inhibitory synaptic factor 2A
hsa-miR-10a-5p	*ITSN1*	Intersectin 1
hsa-miR-10a-5p	*KLF11*	KLF transcription factor 11
hsa-miR-10a-5p	*KLF4*	KLF transcription factor 4
hsa-miR-10a-5p	*LCA5*	Lebercilin LCA5
hsa-miR-10a-5p	*LIX1L*	Limb and CNS expressed 1 like
hsa-miR-10a-5p	*LRRC8C*	Leucine rich repeat containing 8 VRAC subunit C
hsa-miR-10a-5p	*NDUFA4*	NDUFA4 mitochondrial complex associated
hsa-miR-10a-5p	*OTULINL*	OUT deubiquitinase with linear linkage specificity like
hsa-miR-10a-5p	*RBMS3*	RNA binding motif single stranded interacting protein 3
hsa-miR-10a-5p	*RGS8*	Regulator of G protein signaling 8
hsa-miR-10a-5p	*RORA*	RAR related orphan receptor A
hsa-miR-10a-5p	*SERTM1*	Serine rich and transmembrane domain containing 1
hsa-miR-10a-5p	*SH3D19*	SH3 domaining containing 19
hsa-miR-10a-5p	*SIGLEC11*	Sialic acid binding Ig like lectin 11
hsa-miR-10a-5p	*SLC38A2*	Solute carrier family 38 member 2
hsa-miR-10a-5p	*SNX18*	Sorting nexin 18
hsa-miR-10a-5p	*SSPN*	Sarcospan
hsa-miR-10a-5p	*TMEM119*	Transmembrane protein 119
hsa-miR-10a-5p	*TNFSF8*	TNF superfamily member 8
hsa-miR-10a-5p	*TPM4*	Tropomyosin 4
hsa-miR-10a-5p	*TXLNB*	Taxilin beta
hsa-miR-10a-5p	*UNC5D*	unc-5 netrin receptor D
hsa-miR-10a-5p	*VDR*	Vitamin D receptor

hsa-miR-10a-5p	*XYLT1*	Xylosyltransferase 1
hsa-miR-10a-5p	*ZBTB6*	Zinc finger and BTB domain containing 6
hsa-miR-10a-5p	*ZNF154*	Zinc finger protein 154
hsa-miR-10a-5p	*ZNF660*	Zinc finger protein 660

Table 5-3. MiR-10a Target Genes Identifies with miRTarBase.

miRNA	Symbol	Gene Name
hsa-miR-10a-5p	*ABCG2*	ATP binding cassette subfamily G member 2
hsa-miR-10a-5p	*ACVR2A*	Activin A receptor type 2A
hsa-miR-10a-5p	*AGBL2*	AGBL carboxypeptidase 2
hsa-miR-10a-5p	*AMPD1*	Adenosine monophosphate deaminase 1
hsa-miR-10a-5p	*ANO6*	Anoctamin 6
hsa-miR-10a-5p	*ARHGAP18*	Rho GTPase activating protein 18
hsa-miR-10a-5p	*AXL*	AXL receptor tyrosine kinase
hsa-miR-10a-5p	*BAMBI*	BMP and activin membrane bound inhibitor
hsa-miR-10a-5p	*BCL6*	BCL6 transcription repressor
hsa-miR-10a-5p	*BDNF*	Brain derived neurotrophic factor
hsa-miR-10a-5p	*C6orf89*	Chromosome 6 open reading frame 89
hsa-miR-10a-5p	*CAB39L*	Calcium binding protein 39 like
hsa-miR-10a-5p	*CD3D*	CD3 delta subunit T-cell receptor complex
hsa-miR-10a-5p	*CD59*	CD59 molecule
hsa-miR-10a-5p	*CHL1*	Cell adhesion molecule L1 like
hsa-miR-10a-5p	*CHMP1B*	Charged mulivesicular body protein 1B
hsa-miR-10a-5p	*CNTLN*	Centlein
hsa-miR-10a-5p	*COL6A2*	Collagen type VI alpha 2 chain
hsa-miR-10a-5p	*CPED1*	Cadherin like and PC-esterase domain containing 1
hsa-miR-10a-5p	*CRY2*	Cryptochrome circadian regulator 2
hsa-miR-10a-5p	*CSRNP3*	Cysteine and serine rich nuclear protein 3
hsa-miR-10a-5p	*DLG4*	Discs large MAGUK scaffold protein 4
hsa-miR-10a-5p	*DPYSL2*	Dihydropyrimidinase like 2
hsa-miR-10a-5p	*EMB*	Embigin
hsa-miR-10a-5p	*EPHA4*	EPH receptor A4
hsa-miR-10a-5p	*ETS1*	ETS proto-oncogene 1, transcription factor
hsa-miR-10a-5p	*FAM168A*	Faily with sequence similarity 168 member A
hsa-miR-10a-5p	*FAT2*	FAT atypical cadherin 2
hsa-miR-10a-5p	*FEM1B*	Fem-1 homolog B
hsa-miR-10a-5p	*FHL2*	Four and a half LIM domains 2
hsa-miR-10a-5p	*GNAL*	G protein subunit alpha L
hsa-miR-10a-5p	*GPR63*	G protein-coupled receptor 63
hsa-miR-10a-5p	*H6PD*	Hexose-6-phosphate dehydrogenase/glucose 1-dehydrogenase
hsa-miR-10a-5p	*HLA-E*	Major histocompatibility complex, class I, E
hsa-miR-10a-5p	*ID4*	Inhibitor of DNA binding 4
hsa-miR-10a-5p	*IL12A*	Interleukin 12A
hsa-miR-10a-5p	*JHY*	Juntional cadherin complex regulator
hsa-miR-10a-5p	*KIAA1143*	KIAA1143
hsa-miR-10a-5p	*KLHDC8A*	Kelch domain containing 8A
hsa-miR-10a-5p	*KLHL6*	Kelch like family member 6

hsa-miR-10a-5p	*LCA5*	Lebercilin LCA5
hsa-miR-10a-5p	*LILRA2*	Leukocyte immunoglobulin like receptor A2
hsa-miR-10a-5p	*LIX1L*	Limb and CNS expressed 1 like
hsa-miR-10a-5p	*LRP3*	LDL receptor related protein 3
hsa-miR-10a-5p	*MMP14*	Matrix metallopeptidase 14
hsa-miR-10a-5p	*MOB3C*	MOB kinase activator 3C
hsa-miR-10a-5p	*MRC2*	Mannose receptor C type 2
hsa-miR-10a-5p	*NEK7*	NIMA related kinase 7
hsa-miR-10a-5p	*OAZ1*	Ornithine decarboxylase antizyme 1
hsa-miR-10a-5p	*PANX1*	Pannexin 1
hsa-miR-10a-5p	*PIK3CG*	Phosphatidylinositol-4,5-bisphosphate-3-kinase catalytic subunit gamma
hsa-miR-10a-5p	*PLSCR1*	Phospholipid scramblase 1
hsa-miR-10a-5p	*PTPRG*	Protein tyrosine phosphatase receptor type G
hsa-miR-10a-5p	*RAP2A*	RAP2A member of RAS oncogene family
hsa-miR-10a-5p	*RORA*	RAR related orphan receptor A
hsa-miR-10a-5p	*RPL15*	Ribosomal protein L15
hsa-miR-10a-5p	*RPS15A*	Ribosomal protein S15a
hsa-miR-10a-5p	*RPS29*	Ribosomal protein S29
hsa-miR-10a-5p	*RUNDC3B*	RUN domain containing 3B
hsa-miR-10a-5p	*SERPINE1*	Serpine family E member 1
hsa-miR-10a-5p	*SLC2A3*	Solute carrier family 2 member 3
hsa-miR-10a-5p	*SLC48A1*	Solute carrier family 48 member 1
hsa-miR-10a-5p	*SPARC*	Secreted protein acidic and cysteine rich
hsa-miR-10a-5p	*TGFB3*	Transforming growth factor beta 3
hsa-miR-10a-5p	*TMEM109*	Transmembrane protein 109
hsa-miR-10a-5p	*TPM4*	Tropomyosin 4
hsa-miR-10a-5p	*TUBA1A*	Tubulin alpha 1a

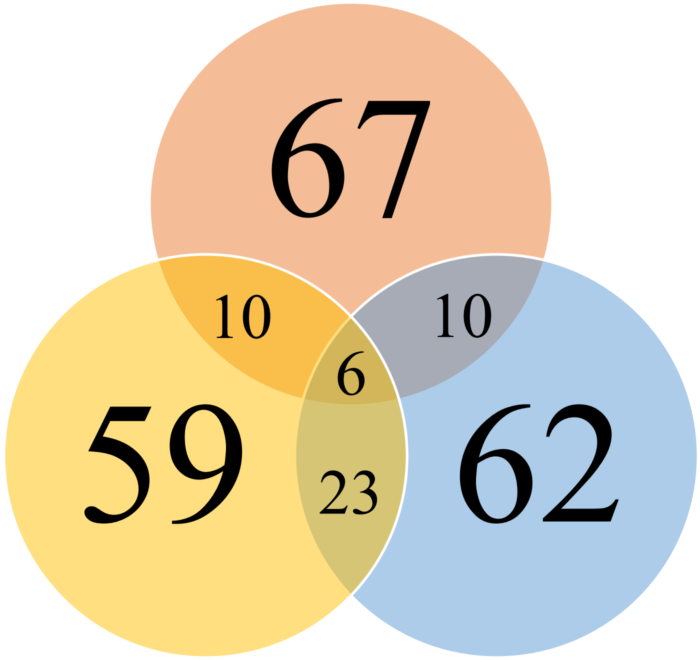

Figure 5-4. MiR-10a-5p potential target genes from MiRNA:mRNA target prediction software. MiRTarBase predicted 145 total target gene sites for miR-10a, with 67 being unique target genes (Red). TargetScan prediction found 59 unique potential target genes for miR-10a-5p (Yellow). MiRDB predicted 106 total target sites for miR-10a-5p on 62 unique genes (Blue). MiRTarBase and TargetScan shared 10 unique genes. MiRTarBase and miRDB shared 10 unique potential target genes. TargetScan and miRDB shared 23 unique potential miR-10-5p target genes. MiRTarBase, TargetScan, and miRDB shared 6 unique potential miR-10a-5p target genes.

Table 5-4. WebGesalt miR-10a.

ID: ACAGGGT,MIR-10A,MIR-10B; Name:			
size=123; overlap=20; expect=1.46; enrichmentRatio=13.67; PValue=0.000e+0; FDR=0.000e+0			
User ID	Gene Symbol	Gene Name	Entrez Gene
BDNF	*BDNF*	brain derived neurotrophic factor	627
ID4	*ID4*	inhibitor of DNA binding 4, HLH protein	3400
EPHA4	*EPHA4*	EPH receptor A4	2043
KLF11	*KLF11*	Kruppel like factor 11	8462
RAP2A	*RAP2A*	RAP2A, member of RAS oncogene family	5911
BACH2	*BACH2*	BTB domain and CNC homolog 2	60468
SLC38A2	*SLC38A2*	solute carrier family 38 member 2	54407
BCL6	*BCL6*	BCL6, transcription repressor	604
DOCK11	*DOCK11*	dedicator of cytokinesis 11	139818
GATA6	*GATA6*	GATA binding protein 6	2627
ITSN1	*ITSN1*	intersectin 1	6453
KCNA6	*KCNA6*	potassium voltage-gated channel subfamily A member 6	3742
NFASC	*NFASC*	neurofascin	23114
SOBP	*SOBP*	sine oculis binding protein homolog	55084
ARRDC3	*ARRDC3*	arrestin domain containing 3	57561
C14orf28	*C14orf28*	chromosome 14 open reading frame 28	122525
CELF2	*CELF2*	CUGBP Elav-like family member 2	10659
ELAVL2	*ELAVL2*	ELAV like RNA binding protein 2	1993
NFIX	*NFIX*	nuclear factor I X	4784
PALM2	*PALM2*	paralemmin 2	114299

Table 5-5. WebGesalt miR-10a pathways.

ID: GO:0005102; Name: signaling receptor binding			
size=1538; overlap=22; expect=11.14; enrichmentRatio=1.97; PValue=1.469e-3; FDR=4.871e-1			
User ID	Gene Symbol	Gene Name	Entrez Gene
ACVR2A	*ACVR2A*	activin A receptor type 2A	92
ARRDC3	*ARRDC3*	arrestin domain containing 3	57561
BAMBI	*BAMBI*	BMP and activin membrane bound inhibitor	25805
BDNF	*BDNF*	brain derived neurotrophic factor	627
DLG4	*DLG4*	discs large MAGUK scaffold protein 4	1742
EPHA4	*EPHA4*	EPH receptor A4	2043
FEM1B	*FEM1B*	fem-1 homolog B	10116
FHL2	*FHL2*	four and a half LIM domains 2	2274
FLRT2	*FLRT2*	fibronectin leucine rich transmembrane protein 2	23768
GNAL	*GNAL*	G protein subunit alpha L	2774
HLA-E	*HLA-E*	major histocompatibility complex, class I, E	3133
IL12A	*IL12A*	interleukin 12A	3592
IRS1	*IRS1*	insulin receptor substrate 1	3667
MMP14	*MMP14*	matrix metallopeptidase 14	4323
NEDD4	*NEDD4*	neural precursor cell expressed, developmentally down-regulated 4, E3 ubiquitin protein ligase	4734
PANX1	*PANX1*	pannexin 1	24145
PIK3CG	*PIK3CG*	phosphatidylinositol-4,5-bisphosphate 3-kinase catalytic subunit gamma	5294
PLSCR1	*PLSCR1*	phospholipid scramblase 1	5359
SERPINE1	*SERPINE1*	serpin family E member 1	5054
TGFB3	*TGFB3*	transforming growth factor beta 3	7043
TNFSF8	*TNFSF8*	TNF superfamily member 8	944
VDR	*VDR*	vitamin D receptor	7421
ID: hsa04218; Name: Cellular senescence			
size=160; overlap=5; expect=1.06; enrichmentRatio=4.71; PValue=4.245e-3; FDR=6.653e-1			
User ID	Gene Symbol	Gene Name	Entrez Gene
CDK6	*CDK6*	cyclin dependent kinase 6	1021
ETS1	*ETS1*	ETS proto-oncogene 1, transcription factor	2113
HLA-E	*HLA-E*	major histocompatibility complex, class I, E	3133
SERPINE1	*SERPINE1*	serpin family E member 1	5054
TGFB3	*TGFB3*	transforming growth factor beta 3	7043

ID: hsa04350; Name: TGF-beta signaling pathway			
size=84; overlap=4; expect=0.56; enrichmentRatio=7.17; PValue=2.347e-3; FDR=4.205e-1			
User ID	Gene Symbol	Gene Name	Entrez Gene
ACVR2A	*ACVR2A*	activin A receptor type 2A	92
BAMBI	*BAMBI*	BMP and activin membrane bound inhibitor	25805
ID4	*ID4*	inhibitor of DNA binding 4, HLH protein	3400
TGFB3	*TGFB3*	transforming growth factor beta 3	7043

Table 5-6: Putative miR-10a-5p target genes downregulated in OCCC with concurrent endometriosis within the receptor signaling pathway.

Gene Name	description	log2FoldChange	P_{adj}
ACVR2A	activin A receptor type 2A	-1.52	5.14E-05
ARRDC3	arrestin domain containing 3	-2.11	1.38E-05
BAMBI	BMP and activin membrane bound inhibitor	-2.57	1.03E-10
BDNF	brain derived neurotrophic factor	-2.42	4.93E-04
DLG4	discs large MAGUK scaffold protein 4	-1.55	7.17E-06
EPHA4	EPH receptor A4	-3.29	2.75E-13
FEM1B	fem-1 homolog B	-1.56	3.87E-09
FHL2	four and a half LIM domains 2	-2.70	1.60E-08
FLRT2	fibronectin leucine rich transmembrane protein 2	-3.15	5.94E-13
GNAL	G protein subunit alpha L	-3.60	3.56E-06
HLA-E	major histocompatibility complex, class I, E	-1.32	4.39E-03
IL12A	interleukin 12A	-1.82	4.61E-02
IRS1	insulin receptor substrate 1	-1.54	1.10E-02
MMP14	matrix metallopeptidase 14	-2.98	9.40E-06
NEDD4	NEDD4 E3 ubiquitin protein ligase	-1.48	6.79E-05
PANX1	pannexin 1	-2.03	2.86E-06
PIK3CG	phosphatidylinositol-4,5-bisphosphate 3-kinase catalytic subunit gamma	-2.49	2.24E-05
PLSCR1	phospholipid scramblase 1	-1.37	4.91E-02
SERPINE1	serpin family E member 1	-4.78	1.10E-06
TGFB3	transforming growth factor beta 3	-3.11	2.05E-12
TNFRSF8	TNF receptor superfamily member 8	-2.93	4.28E-03
VDR	vitamin D receptor	-2.12	4.67E-02

<u>MiR-10a-5p overexpression results in downregulation of genes involved in proliferation and cell cycle progression</u>

The 151 genes downregulated in OCCC with concurrent endometriosis, which were putative miR-10a-5p target genes, were manually annotated for functional roles in proliferation or cell cycle. To examine the association of miR-10a-5p expression on these hand-selected putative target genes, mature miR-10a-5p was overexpressed in OCCC cell lines and target gene expression was examined by qPCR. Overexpression of miR-10a resulted in a nearly 2-fold decrease in *PALM2-AKAP2* in SMOV-2 cells ($P < 0.01$, Figure 5-5A). A smaller, non-statistically significant effect was demonstrated in KK cells overexpressing miR-10a ($P = 0.12$, Figure 5-5B). *PALM2-AKAP2* is a newly named fusion gene with a yet unknown function, but it has been correlated with functions similar to the previously distinct *PALM2* and *AKAP2* genes, such as proliferation in colorectal cancer cell lines [413]. Similarly, decreased *AKAP2* decreased cellular proliferation in ovarian cancer and decreased proliferation through the regulation of *ERK1/2* [414, 415]. Overexpression of miR-10a-5p was associated with a 2.4-fold decrease in Cyclin dependent kinase 6 (*CDK6*) gene expression in both SMOV-2 and KK cells ($P < 0.05$, Figure 5-5A-B). *CDK6* is a critical molecule for cellular proliferation and cell cycle progression from G1 to S phase [416, 417]. Dysregulation of *CDK6* is common in cancers and has previously been implicated in dysfunctional proliferation and disease progression in ovarian carcinomas [418, 419]. Overexpression of miR-10a-5p was associated with a 2-fold decrease in *RAP2A*, member of *RAS* oncogene family (*RAP2A*) gene expression in SMOV-2 ($P < 0.01$, Figure 5-5A), and a 3-fold decrease in KK cells ($P < 0.001$, Figure 5-5B). *RAP2A* is involved in cellular proliferation, has been positively correlated with increased platinum resistance in gastric cancer cells, and is a downstream target of *TP53* in cell cycle regulation [420-422]. Overexpression of miR-10a-5p was associated with a more than 3-fold decrease in Serpin Family E Member 1 (*SERPINE1*) gene expression in KK cells (*P* = 0.01, Figure 5-5B). *SERPINE1* has been found to increase cancer cell proliferation through its regulation by miR-10a in clear cell renal carcinoma [323]. Overexpression of miR-10a-5p was associated with a non-statistically significant decrease in Ephrin type A receptor 4 (*EPHA4*) gene expression in SMOV-2 cells (*P* < 0.07, Figure 5-5A). *EPHA4* is a receptor involved in cancer cell proliferation in breast cancer cells through *AKT* signaling, where downregulation of *EPHA4* decreased proliferation and increasing *EPHA4* increased proliferation [423, 424]. *EPHA4* is not expressed in KK cells (data not shown).

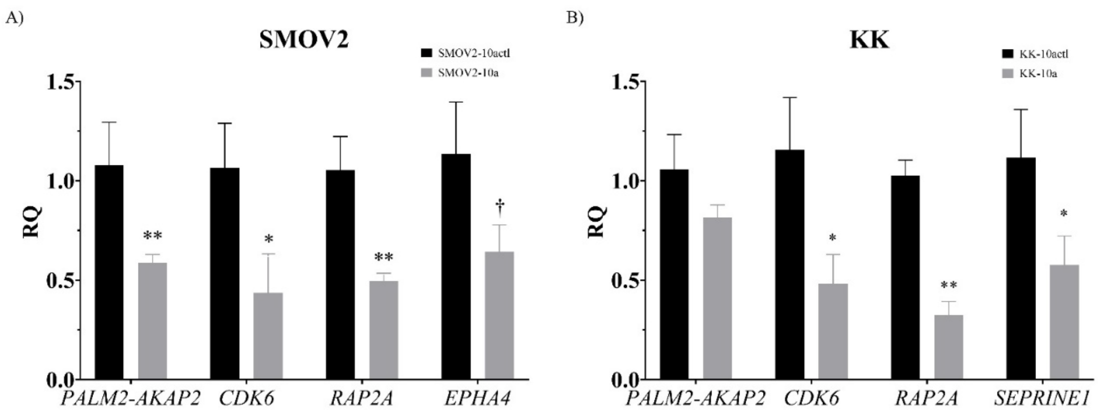

Figure 5-5. Putative miR-10a target genes, involved in cellular proliferation and the G1/S checkpoint, are downregulated with miR-10a-5p overexpression. Cells transfected with mature miRNA mimics for miR-10a (SMOV2-10a and KK-10a) were compared to cells transfected with negative control #1 (SMOV2-10actl and KK-10actl) for each cell line. A) SMOV-2 and B) KK gene expression panels. RQ, the relative quantity of gene of interest to *ACTB*, normalized to negative control #1. Expression is plotted as mean ± SEM. Each gene was run with $n = 6$ for each cell line and treatment group. ** $P < 0.001$, * $P < 0.05$, $^{\dagger}P < 0.07$ using unpaired Mann-Whitney or Welch's one-tailed t-test within cell lines.

5.3 Discussion

MiR-10a expression leads to variable effects on cancers that are tissue-specific [296-298, 301-321]. Some studies report that miR-10a acts as a tumor suppressor effects (*i.e.,* decreased proliferation, increased apoptosis, or clinical correlation to better treatment outcomes) [301-305], while other studies report oncogenic features of increased proliferation, metastasis, invasion, and decreased response to therapeutics *in vitro* or *in vivo* [306-321]. During our original analyses, we attempted to draw simple correlations between cell line miR-10a expression, common mutations (*i.e.*, *ARID1A* mutants), and cellular proliferation. However, we were unable to determine clear genotypic or phenotypic correlations for cell lines with lower and higher basal miR-10a expression. For example, when analyzing the mutational profiling results of the eleven cell lines in Table 2-3, seven out of eleven cell lines were profiled as *ARID1A* mutant cell lines (loss of function) [60, 80, 84]. Four of the cell lines in Table 2-3 are known as are published as *ARID1A* wildtype: ES-2, KK, RMG-I, and SKOV3 [60, 80, 84]. Three of these four *ARID1A* wild-type cell lines had higher expression of basal miR-10a, while the KK cell line had one of the lowest miR-10a expression levels. The seven ARID1A mutant cell lines varied in miR-10a expression, with OVAS and ES-2 as the highest to SMOV-2 exhibiting the lowest expression (Figure 4-3). Furthermore, the same variability between *ARID1A* mutation status and miR-10a basal expression also occurred when evaluating the doubling times of the cell lines. Although doubling times vary by cell culture protocol and conditions in laboratories (*i.e.,* preferred growth medium and supplements), a clear delineation of the doubling time of the cell lines used in Table 2-3 did not correlate with miR-10a expression. For example, using the reported doubling times for TOV-21G (25 hours), SKOV3 (27 hours), and ES-2 (19 hours) [80], TOV-21G had a low basal miR-10a, whereas SKOV3 and ES-2 had a higher basal expression of miR-10a even though their doubling times were not similar to one another.

In order to investigate the role of miR-10a on OCCC proliferation, we chose two cell lines with the lowest expression of miR-10a and no published contraindications to being an OCCC cell line: SMOV-2 and KK. Increasing miR-10a expression in SMOV-2 and KK cell lines resulted in a significant decrease in proliferation for both cell lines after 96 hours following transfection with miR-10a mimics. This time delay is likely due to the 40+ hour doubling time for SMOV-2 and KK cells. Interestingly, PI staining of the cells 24 hours after transfection showed early effects of miR-10a expression on the cell cycle. Both SMOV2-10a and KK-10a overexpressing cells showed a significant shift in the percentage of cells in the three phases of the cell cycle, as quantified by flow cytometry. The amount of cells in G_1 was significantly increased in both SMOV2-10a and KK-10a samples, with a decrease in the amount of cells (peaks) in S and G_2. This cell cycle shift suggests that cells are spending longer in G_1 or could potentially be shifting into a $G_{0/1}$ state of senescence as an effect of increased miR-10a. The percentage of cell debris was not changed by miR-10a expression, suggesting these cells are not undergoing apoptosis, but further testing with a Caspase-3 assay, for example, would provide better evidence on the effects of apoptosis. PI staining is unable to differentiate between G_1 and the senescent state of G_0; therefore, other assays such as beta-galactosidase staining would provide more insight into the true nature of miR-10a's effect on the cell cycle.

While increasing miR-10a expression in cells would result in a change in proliferation and cell cycle, targeting miRNAs clinically has previously been difficult

[425]. Due to the clinical difficulty of targeting miRNAs, finding a downstream target of miR-10a that could be clinically significant to the effect of miR-10a was pursued in our study. Using three target prediction software following the previously published protocol for identifying potential target genes [365], we identified 151 unique protein-coding genes as potential miR-10a targets using reciprocal expression in OCCC with concurrent endometriosis compared to endometrioma. Further analysis of these 151 genes using WebGestalt revealed that these genes were involved in receptor signaling pathways, proliferation, and cell cycle progression (Table 5-5). The 151 potential miR-10a target genes were manually annotated based on their functional roles in proliferation and cell cycle to highlight *PALM2-AKAP2*, *CDK6*, *RAP2A*, *EPHA4*, and *SERPINE1*. These genes were evaluated in SMOV2-10a and KK-10a cells and found to be significantly downregulated by miR-10a overexpression (Figure 5-3). Having these genes downregulated by miR-10a expression suggests them as direct factors in the change in proliferation and cell cycle. Overall, these findings provide insight into a mechanism for miR-10a in OCCC proliferation and cell cycle.

CHAPTER 6: DISCUSSION

The goal of this dissertation was to explore the transcriptomic contributions of concurrent endometriosis to OCCC to identify potential contributors to disease and clinically relevant biomarkers. We observed a positive relationship between miR-10a overexpression and chemoresistance *in vitro.* Furthermore, we identified a mechanism by which miR-10a regulates OCCC proliferation, and potential chemotherapeutic response involves disruption of the cell cycle (Figure 6-1). These results warrant further study in primary tissues and patient samples to corroborate miR-10a as a biomarker for chemotherapy response.

Transcriptomic Profiling of EOC

While multi-platform analyses are attempting to categorize epithelial ovarian cancers beyond histology to discover molecular features that can be targeted for therapeutic benefit [64, 98, 371], current first-line therapy for women with ovarian carcinomas remains similar for all histological subtypes and includes surgical debulking to remove maximum tumor tissue and six cycles of carboplatin and paclitaxel or neoadjuvant chemotherapy [134, 426]. Fortunately, 70% of women with high-grade serous ovarian carcinomas show a complete response to these standard regimens [427]. Unfortunately, up to 89% of women with OCCC show progression of disease with this standard protocol [150-152]. These epidemiological data highlight a critical need for further understanding of the molecular features of OCCC to improve treatment options and discoveries.

Towards this need for understanding the molecular underpinnings of ovarian cancer to develop novel therapeutic interventions, various -omics studies have been undertaken such as multi-platform epigenetic (*i.e.,* DNA methylation, histone binding), genomic (*i.e.,* whole genome sequencing, exome sequencing, targeted gene sequencing, copy number variant), transcriptomic (*i.e.,* bulk RNA, small RNA, target gene expression), and proteomic (*i.e.,* targeted immunohistochemistry, reverse phase protein array). Furthermore, many of the multi-platform studies utilized the much more abundant sample numbers from HGSOC [64].

Transcriptomic discoveries have contributed to new therapeutic interventions for women with EOC to add to the standard of care regimen of carboplatin and paclitaxel for some subtypes and stages of EOC (*i.e.,* stage II+ HGSOC) [134]. For example, bevacizumab, a monoclonal antibody targeting vascular endothelial growth factor (*VEGF*) [428], was approved as a new treatment option for women with ovarian cancer in 2014 for women with platinum-resistant, recurrent ovarian cancer [429, 430]. *VEGF* expression was first quantified in ascitic fluid of women with ovarian cancer in 1993 [431], and transcriptomically within ovarian tissue in 1994 [432]. Further approval of bevacizumab as part of first-line treatment for women with stage III+ EOC occurring in 2018 [433, 434]. Ovarian cancers typically overexpress VEGF [435] with the negative outcomes of increased angiogenesis and blood supply to the cancer cells [206]. While recent yet small population studies focusing on OCCC have found a survival benefit for women with advanced OCCC [436], unfortunately, most of the original clinical evidence and benefit of bevacizumab was contained to women with HGSOC [430, 437-439].

Currently, there are few publicly available transcriptomic datasets for OCCC listed in the gene expression omnibus (GEO), and some of them do not yet appear to be published as peer-reviewed articles (Supplementary Table 2-3). Moreover, many OCCC transcriptomic profiling studies utilize OCCC cell lines that do not represent women with OCCC and concurrent endometriosis [120, 374]. For example, Yamaguchi *et al.* [374] created an OCCC signature from OCCC cell lines and compared it to multiple published or publicly available OCCC datasets. Nagaraja *et al.* [120] integrated transcriptomic microarray data with small RNA data from next-generation sequencing of a panel of OCCC cell lines compared to primary cultures of normal ovarian surface epithelium. While up to 50% of OCCCs are associated with endometriosis [225, 376], most transcriptomic studies of primary tumors classified as OCCC do not characterize samples as coming from women with concurrent endometriosis, pathology-proven endometriosis or even a history of endometriosis [59, 129, 247, 250, 374, 375]. One of the few studies that delineated endometriosis status as part of their samples was from Bolton *et al.* where they performed the largest multi-platform sequencing of OCCC to date. They used both genomic (n = 421 samples) and transcriptomic (n = 211 samples) profiling [59]. While more than 10% of their samples of OCCC were classified as coming from women with endometriosis [59], they did not analyze data from OCCC with concurrent endometriosis independently from those without endometriosis. This lack of concurrent endometriosis analysis could have been due to the endometriosis being based on patient-reported history and only confirmed by histology on samples from one institution. One study that did delineate samples' endometriosis status, Shih *et al.* [129] included the following sample sets: endometriosis from women without OCCC, endometriosis adjacent to OCCC, atypical endometriosis, and OCCC. Their results showed that transcriptomic profiles from endometriosis adjacent to OCCC were most similar to atypical endometriosis. Similar to our results, they also showed that transcriptomic profiling of endometriosis samples from women without OCCC was distinct from the +OCCC samples [129]. However, Shih *et al.* [129] did not examine OCCC samples from women with concurrent endometriosis even though they used laser capture microdissection to retrieve their samples. They focused more on the separated endometriosis samples and the transcriptomic transformation from endometriosis to atypical endometriosis to OCCC.

Our study is unique for its inclusion of OCCC samples with pathologically-confirmed endometriosis from women with concurrent endometriosis. All OCCC with concurrent endometriosis samples were primary tumor tissue with the presence of concurrent endometriosis confirmed by pathology reports. Unfortunately, these strict inclusion criteria, as well as the limited availability of samples due to OCCC's rarity, restricted the sample size in our study. Future studies would be warranted to obtain matched samples of endometrioma and adjacent OCCC.

For another multi-platform transcriptomic approach, we also profiled small RNA molecules in OCCC with concurrent endometriosis. Small RNA sequencing of these samples identified miR-141-3p, miR-183-5p, and miR-10a-5p as the top three most upregulated miRNAs in OCCC with concurrent endometriosis. MiR-141-3p overexpression has been demonstrated in a panel of platinum-resistant cell ovarian cancer lines [440]. Further, increased expression of miR-141-3p was associated with increased cellular proliferation in esophageal cancer [441]. Like miR-141-3p, studies of miR-183-5p in ovarian carcinoma are limited, but bioinformatic analysis in high-grade serous ovarian carcinoma correlated miR-183-5p with platinum-resistance [442]. The specific role of these miRNAs in OCCC is currently unknown and will be crucial components in future studies. To our knowledge, this represents the first small RNA sequencing analysis of OCCC with concurrent endometriosis.

Previously, transcriptomic analysis with small RNAs has been oriented as a targeted therapeutic mechanism, with clinical trials unfortunately not progressing to Phase III commonly due to difficulty in delivery mechanisms causing off-target effects and severe toxicity profiles [443, 444]. However, non-invasive or minimally invasive laboratory testing (*i.e.,* urine and plasma samples) have been used to detect miRNA expression [328, 445], suggesting using miRNA expression as a biomarker of disease or therapeutic response marker is more feasible and an earlier step of understanding miR-10a expression in OCCC in future studies.

MiR-10a regulation of genes at critical pathways in OCCC and the cell cycle

Our transcriptomic profiling analyses revealed miR-10a-5p as the most abundant miRNA in OCCC with concurrent endometriosis, comprising 21% of the miRNA molecules. MiR-10a has been found to be upregulated in primary ductal breast carcinomas, squamous cell cervical carcinomas, acute myeloid leukemia, and pancreatic ductal adenocarcinomas and correlated with disease progression and platinum-resistance [311, 314, 319, 322, 327, 400-402, 446, 447]. Similar to other cancers, our study observed a strong, positive relationship between miR-10a-5p expression and platinum response in a panel of OCCC cell lines ($R^2 = 0.93$). Focusing on benign disease and ovarian function, previous studies have shown that miR-10a-5p expression is significantly lower in endometriomas compared to matched and unmatched eutopic endometrium [264, 448]. Further, increased expression of miR-10a-5p in granulosa cells resulted in decreased proliferation [449], consistent with our results in OCCC cell lines. Moreover, increased expression of miR-10a-5p in granulosa cells led to cell cycle deficiencies, mediated through indirect regulation of cyclin-dependent kinase 2 [449]. Dysregulated genes in the cell cycle and DNA repair pathways have been implicated in OCCC and associated with its disease progression and platinum-resistant phenotype. These genes include *RAP2A* [450-452], *CDK6* [418, 419, 453], *SERPINE1* [454, 455], and *EPHA4* [456-459] and are involved in disease progression, drug response, and are markers of progression. Overexpression of miR-10a-5p in OCCC cell lines showed an associated decrease in the expression of these genes, and although not directly tested in this study, provide support as being putative miR-10a-5p target genes as several published studies have shown direct effects or associated effects of miR-10a on *SERPINE1* [323] and *EPHA4* [459, 460] gene expression.

Our results led to a working hypothesis that miR-10a overexpression in OCCC prolongs G_1 or arrests cells in the $G_{0/1}$ phase. A limitation of the miR-10a overexpression data collection from our cell lines is the skewed interpretation of the results related to cell cycle/proliferation based on samples collected at different time points for cells with various doubling times. SMOV-2 and KK have long doubling times of 43 and 41 hours (Figure 5-2) that were lengthened to 85 and 48 hours in SMOV2-10a and KK-10a, respectively (Figure 5-2). Experimental design modifications could be done for future studies to increase the homogeneity between cell lines and collection times, such as cell cycle synchronization using pharmacological intervention (nocodazole) or serum starvation of the cell culture media.

Overall summary and working hypothesis

Figure 6-1 shows our working hypothesis of the role of miR-10a-5p effects on cell cycle progression in OCCC. In summary, we found a significant decrease in cellular proliferation with overexpression of miR-10a-5p in OCCC. This decrease in proliferation may be due to a deficit in the G1/S checkpoint as a significant increase in cell population in G_1 was seen in cell cycle analysis while also having a significant decrease in cells in both S and G_2 phases. Upon further evaluation of miR-10a target genes involved in proliferation, genes that regulated the G_1/S checkpoint were downregulated in SMOV-2 and KK cells transfected to overexpress miR-10a. More specifically, the miR-10a-5p target gene, *CDK6,* is well known for its regulation of a cell's progression to the S phase through its dimer with Cyclin-dependent kinase 4 (*CDK4*) [461]. Other genes, including *EPHA4* [424], *RAP2A* [422], and *SERPINE1* [462] have been implicated in cell cycle progression. Of particular interest to the increased number of cells in G_1 are *CDK6* and *EPHA4,* with downregulation of both being linked to cells remaining in G_0/G_1 [424, 463]. The increase in this population of cells is clinically significant for the cell cycle phases in which platinum and taxanes show efficacy [464, 465]. These drugs are commonly effective during the S and M phases, causing DNA and mitotic spindle damage, leading to cell death. However, if OCCC cells are overexpressing miR-10a and stuck in a senescent or earlier stage of the cell cycle for an extended period, they will be less likely to undergo damage and death from cytotoxic platinum and taxane agents, leading to resistant tumors. While future studies are needed to explore this hypothesis further, this study provides insight that miR-10a-5p is an impactful, potentially oncogenic molecule in OCCC that can lead to use as a potential biomarker and therapeutic target.

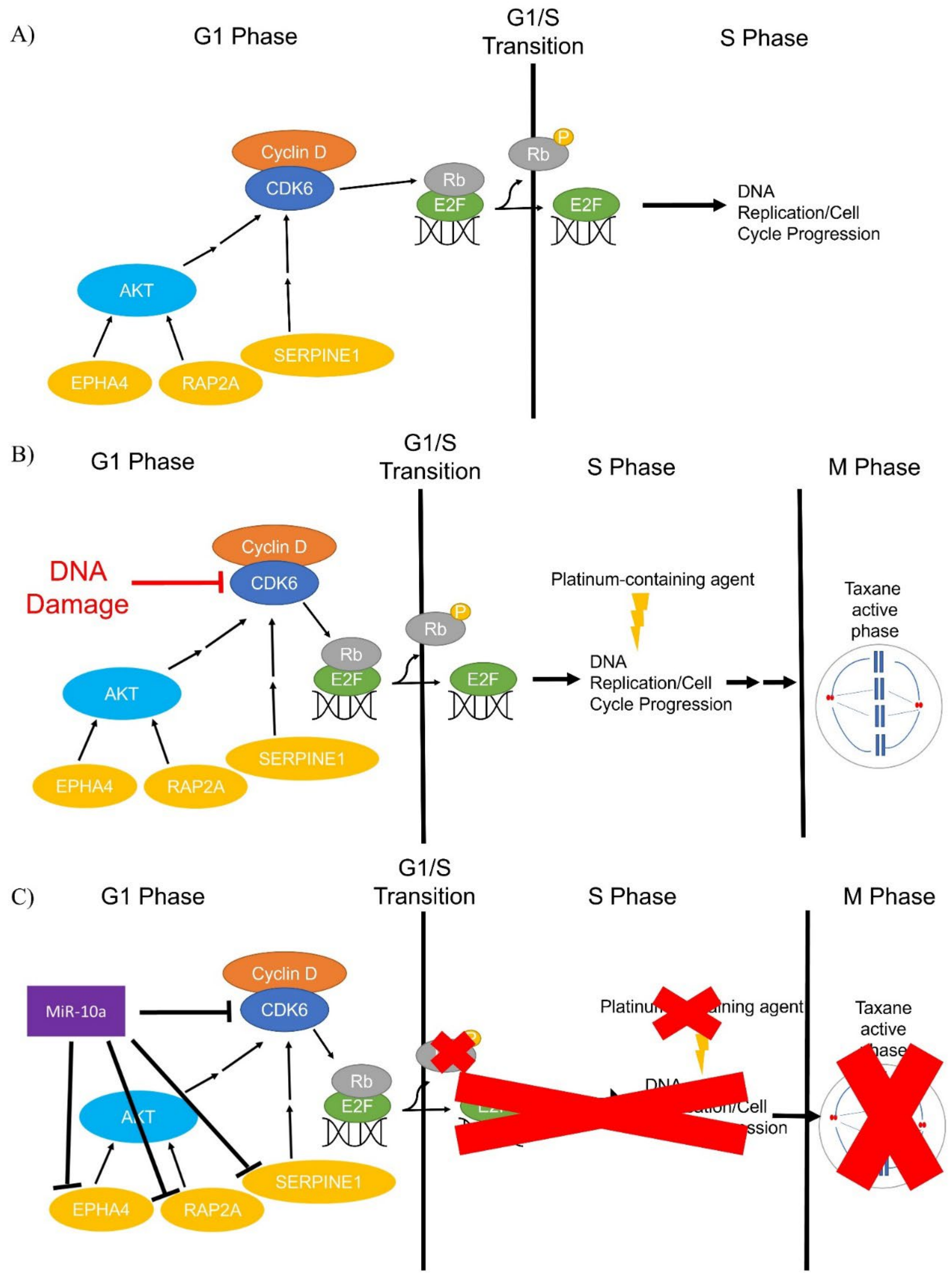

Figure 6-1. The working hypothesis for the mechanism of miR-10a-5p overexpression in OCCC G_0 or G_1/S Checkpoint. A) Simplified representation of cell cycle progression function in non-cancerous cells, whereby *CDK6* phosphorylates *Rb*

freeing *E2F* for DNA replication in the S phase. B) Infographic representation of cell cycle progression in non-malignant cells treated with platinum and/or taxane-containing agents. Cells will sustain DNA and/or microtubule damage resulting in no continued progression through the cell cycle and subsequent cell death. C) Represents the working hypothesis for cell cycle progression in miR-10a-5p overexpressing OCCC cells. MiR-10a-5p downregulates *CDK6* and other important regulators of the cell cycle slowing or halting phosphorylation of Rb leading to inactive or prolonged inactivation of E2F and transition to S Phase and DNA replication. Cells slowed in G_1 or senescing in G_0 miss the critical chemotherapeutic effects in the S and M phases (red “X”s).

APPENDIX

Supplementary Table 1. Clinical characteristics and experimental use of patient samples.

Tube ID	Tissue category	Tissue type	Tissue Source	Age	Endometrial cycle phase	Race Ethnicity	Surgical Indication	Location of endometriosis	OVCA Stage	%Tumor Cellularity	Experimental Use
CW44	Endometrioma	Ovarian cyst wall	Hawkins	30	Proliferative	Asian	Adnexal mass; pelvic pain	Cyst wall/ovarian endometrioma	NA	NA	Poly-A RNA sequencing; Small RNA sequencing
CW9	Endometrioma	Ovarian cyst wall	Hawkins	43	Proliferative	Latina	Adnexal mass; pelvic pain	Cyst wall/ovarian endometrioma	NA	NA	Poly-A RNA sequencing; Small RNA sequencing
LCW62	Endometrioma	Ovarian cyst wall	Hawkins	25	Proliferative	Asian	Adnexal mass; pelvic pain	Cyst wall/ovarian endometrioma; extensive peritoneal disease	NA	NA	Poly-A RNA sequencing; Small RNA sequencing
CW195	Endometrioma	Ovarian cyst wall	Hawkins	36	Unknown	Latina	Adnexal mass; pelvic pain	Cyst wall/ovarian endometrioma; extensive peritoneal disease	NA	NA	Poly-A RNA sequencing; Small RNA sequencing
CW145	Endometrioma	Ovarian cyst wall	Hawkins	29	Proliferative	Latina	Adnexal mass; pelvic pain	Cyst wall/ovarian endometrioma; extensive peritoneal disease	NA	NA	qPCR
CW153	Endometrioma	Ovarian cyst wall	Hawkins	21	Proliferative	Latina	Adnexal mass; pelvic pain; infertility	Cyst wall/ovarian endometrioma; extensive peritoneal disease	NA	NA	qPCR
CW2	Endometrioma	Ovarian cyst wall	Hawkins	42	Secretory	Latina	Adnexal mass; pelvic pain; AUB	Cyst wall/ovarian endometrioma	NA	NA	qPCR

CW119	Endometrioma	Ovarian cyst wall	Hawkins	42	Endometritis	Latina	Adnexal mass; pelvic pain	Cyst wall/ovarian endometrioma; extensive peritoneal disease	NA	NA	qPCR
CW98	Endometrioma	Ovarian cyst wall	Hawkins	23	Unknown	Non-Hispanic white	Adnexal mass; pelvic pain	Cyst wall/ovarian endometrioma; extensive peritoneal disease	NA	NA	qPCR
CW14	Endometrioma	Ovarian cyst wall	Hawkins	30	Proliferative	Non-Hispanic white	Adnexal mass; pelvic pain; infertility	Cyst wall/ovarian endometrioma; extensive peritoneal disease	NA	NA	qPCR
CW7	Endometrioma	Ovarian cyst wall	Hawkins	23	Proliferative	Non-Hispanic white	Adnexal mass; pelvic pain	Cyst wall/ovarian endometrioma; extensive peritoneal disease	NA	NA	qPCR
CW19	Endometrioma	Ovarian cyst wall	Hawkins	48	Interval	Latina	Adnexal mass; pelvic pain; infertility	Cyst wall/ovarian endometrioma; extensive peritoneal disease	NA	NA	qPCR
CW142	Endometrioma	Ovarian cyst wall	Hawkins	21	Unknown	Latina	Adnexal mass; pelvic pain	Cyst wall/ovarian endometrioma; extensive peritoneal disease	NA	NA	qPCR
CW99	Endometrioma	Ovarian cyst wall	Hawkins	41	Unknown	Latina	Adnexal mass; pelvic pain	Cyst wall/ovarian endometrioma	NA	NA	qPCR

CWM2	Endometrioma	Ovarian cyst wall	Hawkins	37	Prior hysterectomy	African American	Adnexal mass; pelvic pain	Cyst wall/ovarian endometrioma	NA	NA	qPCR
CW82a	Endometrioma	Ovarian cyst wall	Hawkins	31	IUD	Latina	Adnexal mass; pelvic pain	Cyst wall/ovarian endometrioma; extensive peritoneal disease	NA	NA	qPCR
2005-09-G923	Ovarian clear cell carcinoma (OCCC)	Ovary	NRG BB	63	Unknown	Unknown	Adnexal mass	none	IIB	50%	qPCR
UH1310-47	Ovarian clear cell carcinoma (OCCC)	Ovary	IUSCCC	39	Unknown	Non-Hispanic white	Adnexal mass	none	IA	50%	qPCR
UH0011-43	Ovarian clear cell carcinoma (OCCC)	Ovary	IUSCCC	52	Unknown	Non-Hispanic white	Adnexal mass	none	IA	50-80%	qPCR
UH0001-22	Ovarian clear cell carcinoma (OCCC)	Ovary	IUSCCC	79	Unknown	Non-Hispanic white	Adnexal mass	none	IA	50-80%	qPCR
UH9811-13	Ovarian clear cell carcinoma (OCCC)	Ovary	IUSCCC	59	Unknown	Non-Hispanic white	Adnexal mass	none	IA	50-80%	qPCR
UH9510-31	Ovarian clear cell carcinoma (OCCC)	Ovary	IUSCCC	72	Unknown	Non-Hispanic white	Adnexal mass	none	IA	50-80%	qPCR
UH9908-26	Ovarian clear cell carcinoma (OCCC)	Ovary	IUSCCC	52	Unknown	Non-Hispanic white	Adnexal mass	none	IIA	50-80%	qPCR
UH0602-38	Ovarian clear cell carcinoma (OCCC)	Ovary	IUSCCC	72	Unknown	African American	Adnexal mass	none	IIIC	50-80%	qPCR
2003-04-G261	Ovarian clear cell carcinoma (OCCC)	Ovary	NRG BB	54	NA	Unknown	Adnexal mass	none	IV	75%	qPCR
UH9510-07C	Ovarian clear cell carcinoma (OCCC)	Ovary	IUSCCC	53	Unknown	Non-Hispanic white	Adnexal mass	none	IV	50-80%	qPCR

2001-04-G618	Ovarian clear cell carcinoma with concurrent endometriosis (OCCC-ENDO)	Ovary	NRG BB	52	Unknown	Non-Hispanic white	Adnexal mass	Left ovary; Pelvic peritoneum	IA	>90%	Poly-A RNA sequencing; Small RNA sequencing; qPCR
2001-05-G002	Ovarian clear cell carcinoma with concurrent endometriosis (OCCC-ENDO)	Ovary	NRG BB	48	Proliferative	Unknown	Adnexal mass	Right and left ovary, pelvic peritoneum	IA	60%	Poly-A RNA sequencing; Small RNA sequencing; qPCR
2005-04-G741	Ovarian clear cell carcinoma with concurrent endometriosis (OCCC-ENDO)	Ovary	NRG BB	51	Atrophic	Unknown	Adnexal mass	Left ovary; sigmoid serosa; uterine serosa	IIB	80%	Poly-A RNA sequencing; Small RNA sequencing; qPCR
2003-03-G506	Ovarian clear cell carcinoma with concurrent endometriosis (OCCC-ENDO)	Ovary	NRG BB	50	Proliferative	Unknown	Adnexal mass	Right ovary, appendix	IIIC	80%	Poly-A RNA sequencing; Small RNA sequencing; qPCR
2003-02-G506	Ovarian clear cell carcinoma with concurrent endometriosis (OCCC-ENDO)	Ovary	NRG BB	55	Atrophic	Unknown	Adnexal mass	Right ovary; Left ovary; left fallopian tube; right fallopian tube	IA	60-70%	qPCR
2004-03-G712	Ovarian clear cell carcinoma with concurrent endometriosis (OCCC-ENDO)	Ovary	NRG BB	72	Inactive	Unknown	Adnexal mass	Right ovary, left ovary and tube uterine serosa	IA	>90%	qPCR
2008-03-G526	Ovarian clear cell carcinoma with concurrent endometriosis	Ovary	NRG BB	66	Atrophic	Unknown	Adnexal mass	Right ovary, uterine serosa	IIA	50%	qPCR

	(OCCC-ENDO)										
2005-01-G677	Ovarian clear cell carcinoma with concurrent endometriosis (OCCC-ENDO)	Ovary	NRG BB	45	Proliferative	Unknown	Adnexal mass	Pelvic peritoneum; uterine serosa	IIB	70%	qPCR
98-11-G630	Ovarian clear cell carcinoma with concurrent endometriosis (OCCC-ENDO)	Ovary	NRG BB	49	Unknown	Unknown	Adnexal mass	Right ovary	IIIA2	60-70%	qPCR

Supplementary Table 2. Gene Omnibus OCCC transcriptomic datasets cell lines.

GEO Accession	Sample Type	Total Samples	OCCC Samples	Endometriosis Samples	Platform	References
GSE101974	TOV-21G	22	22	0	Illumina HiSeq 2500 and Illumina NextSeq 500	[466]
GSE107201	TOV-21G	3	3	0	Illumina NextSeq 500	[467]
GSE110448	TOV-21G	2	2	0	Illumina NextSeq 500	[468]
GSE110449	TOV-21G	5	5	0	Illumina NextSeq 500	[468]
GSE113440	Extracellular vesicles from ES-2	6	6	0	Illumina HumanHT-12 V4.0 expression beadchip	[469]
GSE114332	ES-2, JHOC-5, and RMG-II	18	3	0	Illumina NextSeq 500	[470]
GSE122926	RMG-I and TOV-21G	12	4	0	Agilent-028004 SurePrint G3 Human GE 8x60K Microarray	[471]
GSE123426	OCI-C5x cell line and 11 clones	12	12	0	Illumina HiSeq 2000	[472]
GSE153440	Patient Derived Cell Lines: OCI-P5x and OCI-C5x	2	1	0	NanoString nCounter human PanCancer Pathways Panel	[473]
GSE16574	ES-2, KK, OVAS, OVISE, OVMANA, OVSAYO, OVTOKO, RMG-I, SMOV-2, and TOV-21G	40	34	0	Illumina HumanHT-12 V3.0 expression beadchip	[120]
GSE172016	TOV-21G	19	6	0	Illumina HiSeq 2500	[474]
GSE189552	OVISE, TOV-21G, ES-2, and JHOC-5	24	24	0	Illumina NovaSeq 6000	[475]
GSE200509	TOV-21G	6	3	0	Illumina NovaSeq 6000	[476]

GSE200852	FFPE and Frozen Primary Tissue and Immortalized Cell Lines (ES-2, TOV-21G, and SKOV3)	52	27	0	Illumina MiSeq	[477]
GSE214239	Patient Derived Extracellular Vesicles	8	4	0	Affymetrix Multispecies miRNA-4 Array	N/A
GSE25212	SKOV-3	16	16	0	Affymetrix Human Gene 1.0 ST Array	[478]
GSE27225	SKOV-3, TOV-21G, SKOV-2, IGROV-1, and ES-2	59	14	0	Human SMD Print_1360	[479]
GSE28472	IGROV-1 and SKOV-3	74	2	0	Derived from GPL7088 - CCDTM Hs_CCDTM36k	[480]
GSE29175	SKOV-3, JHOC-5, JHOC-7, JHOC-8, JHOC-9, OVISE, OVTOKO, RMG-1, RMG-2, RMG-5, TOV-21G, IGROV-1	38	13	0	Affymetrix Human Genome U133A 2.0 Array	[374]
GSE3001	KK, OVISE, OVTOKO, RMG-1, and SKOV-3	10	5	0	CodeLink Human 20K ver4.1	[481]
GSE30501	TOV-21G	6	6	0	Affymetrix Human Genome U133 Plus 2.0 Array	[482]
GSE34396	RMG-1	2	2	0	Agilent-014850 Whole Human Genome Microarray 4x44K G4112F	N/A

130

GSE36139	OVISE, OVTOKO, ES-2, IGROV-1, JHOC-5, EFO21, OAWA42, and OVMANA	1864	11	0	Affymetrix Human Genome U133 Plus 2.0 Array and Affymetrix Genome-Wide Human SNP 6.0 Array	[349]
GSE37290	RMG-2	20	20	0	Affymetrix Human Genome U133 Plus 2.0 Array	N/A
GSE39216	RMG-1	2	2	0	Human Cancer Array 11K	N/A
GSE40785	Primary Ovarian Cancer Tissue, SKOV-3, and RMG-1	37	12	0	llumina HumanHT-12 V4.0 expression beadchip	N/A
GSE40788	Primary Ovarian Tissue, SKOV-3, and RMG-1	103	7	0	Affymetrix Mapping 250K Sty2 SNP Array, Illumina HumanHT-12 V4.0 expression beadchip, and Affymetrix OncoScan™ FFPE Express	[388]
GSE49577	HOX424	101	50	0	Illumina HumanHT-12 V4.0 expression beadchip	[483, 484]
GSE52999	SKOV-3 and SKOV-3ip1	6	6	0	Illumina HumanHT-12 V3.0 expression beadchip	[485]
GSE53418	ES-2, SKOV-3, IGROV-1, TOV-21G	32	4	0	Affymetrix Human Exon 1.0 ST Array	[80]
GSE54979	OVISE	9	9	0	Illumina HumanHT-12 V4.0 expression beadchip	[486]

GSE60252	RMG-I	10	2	0	Affymetrix Human Gene 1.1 ST Array	N/A
GSE66729	Primary Ovarian Cancer Tissue, ES-2, IGROV-1, OVAS, OVMANA, OVTOKO, RMG-I, and TOV-21G	376	8	0	Illumina HiSeq 2000	[487]
GSE73637	IGROV-1, SKOV-3, ES-2, TOV-21G	52	12	0	Almac Ovarian Cancer Disease Specific Array	[389]
GSE82304	SKOV-3	6	6	0	Illumina HumanHT-12 V4.0 expression beadchip	[488]
GSE84405	TOV-21G	5	5	0	Illumina NextSeq 500	[489]
GSE90132	SKOV-3	12	8	0	Agilent-014850 Whole Human Genome Microarray 4x44K G4112F	[490]
GSE94304	ES-2, JHOC-5, JHOC-9, RMG-1, SKOV-3, TOV-21G	41	6	0	Illumina HiSeq 2000	[491]

132

Supplementary Table 3. Gene Omnibus OCCC transcriptomic datasets primary tumor samples.

GEO Accession	Sample Type	Total Samples	OCCC Samples	Endometriosis Samples	Platform	References
GSE121103	Frozen Primary Tissue	59	5	0	Illumina NextSeq 500 (Homo sapiens)	[492-494]
GSE128990	FFPE Primary Tissue	96	96	0	Nanostring nCounter Gene Expression Assay	[495]
GSE129617	Frozen Primary Tissue	25	25	0	Affymetrix Human Transcriptome Array 2.0	[116]
GSE14764	Frozen Primary Tissue	80	2	0	Affymetrix Human Genome U133A Array	[496]
GSE153440	Patient Derived Cell Lines	2	1	0	NanoString nCounter human PanCancer Pathways Panel	[473]
GSE157153	FFPE Primary Tissue with laser capture microdissection	66	17	37	Ion Torrent Proton	[129]
GSE160692	FFPE Primary Tissue	16	11	0	Illumina HiSeq 2000	[497]
GSE189553	Frozen Primary Tissue	23	11	0	Illumina HiSeq 2500	[475]
GSE19539	Frozen and OCT embedded tissue, lymphocytic DNA from blood samples	140	9	0	Affymetrix Human Gene 1.0 ST Array and Affymetrix Genome-Wide Human SNP 6.0 Array	[498]
GSE200852	FFPE and Frozen Primary Tissue and Immortalized Cell Lines (ES-2, TOV-21G, and SKOV3)	52	27	0	Illumina MiSeq	[477]
GSE2109	Primary Tissue	2158	2	0	Affymetrix Human Genome U133 Plus 2.0 Array	N/A
GSE212670	FFPE Primary Tissue	24	24	0	NanoString nCounter Human GX PanCancer Pathway Panel and Custom Probe Set	[499]

GSE214239	Extracellular Vesicles from Primary Tissue Samples	8	4	0	Affymetrix Multispecies miRNA-4 Array	N/A
GSE26193	Primary Tissue	107	6	0	Affymetrix Human Genome U133 Plus 2.0 Array	[62, 500-502]
GSE27223	Primary Tissue	49	5	0	Human SMD Print_1355, Human SMD Print_1360, Human SMD Print_1365, and Human SMD Print_1372	[479]
GSE29450	Frozen Primary Tissue with laser microdissection	20	10	0	Affymetrix Human Genome U133 Plus 2.0 Array	[503]
GSE30161	FFPE Primary Tissue	58	5	0	Affymetrix Human Genome U133 Plus 2.0 Array	[504]
GSE30274	Frozen Primary Tissue	56	12	0	Affymetrix Human Gene 1.0 ST Array	[505]
GSE30284	Frozen Primary Tissue	46	9	0	Affymetrix Human Gene 1.0 ST Array	[505]
GSE37394	FFPE Sections of Primary Tissue	67	15		Illumina HumanRef-8 WG-DASL v3.0	[506]
GSE39204	Patient Ascites	64	17		Affymetrix Human Genome U133 Plus 2.0 Array	[507, 508]
GSE40788	Primary Tissue and Ovarian Cancer Cell Lines	103	7	0	Affymetrix Mapping 250K Sty2 SNP Array, Illumina HumanHT-12 V4.0 expression beadchip, and Affymetrix OncoScan™ FFPE Express	[388]
GSE44104	Frozen Primary Tissue	60	12	0	Affymetrix Human Genome U133 Plus 2.0 Array	[509, 510]
GSE49888	Frozen Primary Tissue	19	2	0	Agilent-026652 Whole Human Genome Microarray 4x44K v2	N/A

135

GSE51088	Primary Tumors and Reference Pool	106	2	0	Agilent-012097 Human 1A Microarray (V2) G4110B	[511]
GSE53963	Primary Tumors and Reference Pool	106	2	0	Agilent-014850 Whole Human Genome Microarray 4x44K G4112F	[45]
GSE54807	FFPE Primary Tissue	11	5	0	Affymetrix Human Gene 1.0 ST Array	[512]
GSE55056	FFPE Primary Tissue	11	5	0	NanoString nCounter Human Cancer Reference Kit	[512]
GSE55512	Primary Tissue	12	2	0	Affymetrix Human Genome U133 Plus 2.0 Array	[508, 513]
GSE6008	Primary Tissue	103	8	0	Affymetrix Human Genome U133A Array	[514-518]
GSE63885	Frozen Primary Tissue	101	9	0	Affymetrix Human Genome U133 Plus 2.0 Array	[519, 520]
GSE65986	Primary Tissue	55	25	0	Affymetrix Human Genome U133 Plus 2.0 Array	[113, 521]
GSE66729	Primary Ovarian Cancer Tissue, ES-2, IGROV-1, OVAS, OVMANA, OVTOKO, RMG-I, and TOV-21G	376	8	0	Illumina HiSeq 2000	[487]
GSE6822	Primary Tissue	74	12	0	Affymetrix Human Full Length HuGeneFL Array	N/A
GSE68600	Primary Tissue	113	9	0	Affymetrix Human Full Length HuGeneFL Array	[522]
GSE73551	Primary Tissue	50	12	0	Almac Ovarian Cancer Disease Specific Array	[389]
GSE73614	Primary Tissue	107	24	0	Agilent-014850 Whole Human Genome Microarray 4x44K G4112F	[94]

GSE74357	Primary Tissue	529	3	0	Agilent-014850 Whole Human Genome Microarray 4x44K G4112F	[523]
GSE82007	Primary Tissue	61	3	0	Hs-ATC7.6k-v5px_16Bx22Cx22R	[524]
GSE8841	Primary Tissue	83	16	0	Agilent Human 1 cDNA Microarray (G4100A)	[525]
GSE8842	Primary Tissue	83	16	0	Agilent Human 1 cDNA Microarray (G4100A)	[525]

BIBLIOGRAPHY

1. Siegel, R.L., et al., *Cancer statistics, 2023.* CA Cancer J Clin, 2023. **73**(1): p. 17-48.
2. Giaquinto, A.N., et al., *Breast Cancer Statistics, 2022.* CA Cancer J Clin, 2022. **72**(6): p. 524-541.
3. Goff, B.A., *Ovarian Cancer Is Not So Silent.* Obstetrics & Gynecology, 2022. **139**(2): p. 155-156.
4. Andersen, M.R., et al., *Combining a symptoms index with CA 125 to improve detection of ovarian cancer.* Cancer, 2008. **113**(3): p. 484-9.
5. Goff, B.A., et al., *Ovarian carcinoma diagnosis.* Cancer, 2000. **89**(10): p. 2068-75.
6. Goff, B.A., et al., *Development of an ovarian cancer symptom index: possibilities for earlier detection.* Cancer, 2007. **109**(2): p. 221-7.
7. Eltabbakh, G.H., P.R. Yadav, and A. Morgan, *Clinical picture of women with early stage ovarian cancer.* Gynecol Oncol, 1999. **75**(3): p. 476-9.
8. Lataifeh, I., et al., *Presenting symptoms of epithelial ovarian cancer.* Aust N Z J Obstet Gynaecol, 2005. **45**(3): p. 211-4.
9. Vine, M.F., et al., *Characterization of prediagnostic symptoms among primary epithelial ovarian cancer cases and controls.* Gynecol Oncol, 2003. **90**(1): p. 75-82.
10. Webb, P.M., et al., *Symptoms and diagnosis of borderline, early and advanced epithelial ovarian cancer.* Gynecol Oncol, 2004. **92**(1): p. 232-9.
11. Chan, J.K., et al., *Symptoms of Women With High-Risk Early-Stage Ovarian Cancer.* Obstet Gynecol, 2022. **139**(2): p. 157-162.
12. Lowe, K.A., et al., *The temporal stability of the Symptom Index among women at high-risk for ovarian cancer.* Gynecol Oncol, 2009. **114**(2): p. 225-30.
13. Williams, P., P. Murchie, and C. Bond, *Patient and primary care delays in the diagnostic pathway of gynaecological cancers: a systematic review of influencing factors.* Br J Gen Pract, 2019. **69**(679): p. e106-e111.
14. Brain, K.E., et al., *Ovarian cancer symptom awareness and anticipated delayed presentation in a population sample.* BMC Cancer, 2014. **14**: p. 171.
15. Sud, A., et al., *Effect of delays in the 2-week-wait cancer referral pathway during the COVID-19 pandemic on cancer survival in the UK: a modelling study.* The Lancet Oncology, 2020. **21**(8): p. 1035-1044.
16. Sud, A., et al., *Effect of delays in the 2-week-wait cancer referral pathway during the COVID-19 pandemic on cancer survival in the UK: a modelling study.* Lancet Oncol, 2020. **21**(8): p. 1035-1044.
17. Givler, D.N. and A. Givler, *Health Screening*, in *StatPearls*. 2023: Treasure Island (FL).
18. Guirguis-Blake, J.M., et al., in *Screening for Gynecologic Conditions With Pelvic Examination: A Systematic Review for the U.S. Preventive Services Task Force*. 2017: Rockville (MD).
19. Ebell, M.H., et al., *A systematic review of the bimanual examination as a test for ovarian cancer.* Am J Prev Med, 2015. **48**(3): p. 350-6.

20. Moss, E.L., J. Hollingworth, and T.M. Reynolds, *The role of CA125 in clinical practice.* J Clin Pathol, 2005. **58**(3): p. 308-12.
21. van Nagell, J.R., Jr., et al., *Long-term survival of women with epithelial ovarian cancer detected by ultrasonographic screening.* Obstet Gynecol, 2011. **118**(6): p. 1212-1221.
22. Pinsky, P.F., et al., *Extended mortality results for ovarian cancer screening in the PLCO trial with median 15years follow-up.* Gynecol Oncol, 2016. **143**(2): p. 270-275.
23. Buys, S.S., et al., *Effect of screening on ovarian cancer mortality: the Prostate, Lung, Colorectal and Ovarian (PLCO) cancer screening randomized controlled trial.* Jama, 2011. **305**(22): p. 2295-2303.
24. Menon, U., et al., *Risk Algorithm Using Serial Biomarker Measurements Doubles the Number of Screen-Detected Cancers Compared With a Single-Threshold Rule in the United Kingdom Collaborative Trial of Ovarian Cancer Screening.* J Clin Oncol, 2015. **33**(18): p. 2062-71.
25. Menon, U., et al., *Ovarian cancer population screening and mortality after long-term follow-up in the UK Collaborative Trial of Ovarian Cancer Screening (UKCTOCS): a randomised controlled trial.* Lancet, 2021. **397**(10290): p. 2182-2193.
26. Bast, R.C., Jr., et al., *Reactivity of a monoclonal antibody with human ovarian carcinoma.* J Clin Invest, 1981. **68**(5): p. 1331-7.
27. Bast, R.C., Jr., et al., *A radioimmunoassay using a monoclonal antibody to monitor the course of epithelial ovarian cancer.* N Engl J Med, 1983. **309**(15): p. 883-7.
28. Rosen, D.G., et al., *Potential markers that complement expression of CA125 in epithelial ovarian cancer.* Gynecol Oncol, 2005. **99**(2): p. 267-77.
29. Fritsche, H.A. and R.C. Bast, *CA 125 in ovarian cancer: advances and controversy.* Clin Chem, 1998. **44**(7): p. 1379-80.
30. Patsner, B., *Preoperative serum CA-125 levels in early stage ovarian cancer.* Eur J Gynaecol Oncol, 1990. **11**(5): p. 319-21.
31. Woolas, R.P., et al., *Elevation of multiple serum markers in patients with stage I ovarian cancer.* J Natl Cancer Inst, 1993. **85**(21): p. 1748-51.
32. Kobel, M., et al., *Ovarian carcinoma subtypes are different diseases: implications for biomarker studies.* PLoS Med, 2008. **5**(12): p. e232.
33. Meden, H. and A. Fattahi-Meibodi, *CA 125 in benign gynecological conditions.* Int J Biol Markers, 1998. **13**(4): p. 231-7.
34. Force, U.S.P.S.T., et al., *Screening for Ovarian Cancer: US Preventive Services Task Force Recommendation Statement.* JAMA, 2018. **319**(6): p. 588-594.
35. Berek, J.S., et al., *Cancer of the ovary, fallopian tube, and peritoneum: 2021 update.* Int J Gynaecol Obstet, 2021. **155 Suppl 1**(Suppl 1): p. 61-85.
36. Torre, L.A., et al., *Ovarian cancer statistics, 2018.* CA Cancer J Clin, 2018. **68**(4): p. 284-296.
37. Ray-Coquard, I., et al., *Non-epithelial ovarian cancer: ESMO Clinical Practice Guidelines for diagnosis, treatment and follow-up.* Ann Oncol, 2018. **29**(Suppl 4): p. iv1-iv18.

38. Veneris, J.T., P. Mahajan, and A.L. Frazier, *Contemporary management of ovarian germ cell tumors and remaining controversies.* Gynecol Oncol, 2020. **158**(2): p. 467-475.
39. Bast, R.C., Jr., et al., *Holland-Frei Cancer Medicine*. 2017, Newark, UNITED STATES: John Wiley & Sons, Incorporated.
40. Kim, J., et al., *Cell Origins of High-Grade Serous Ovarian Cancer.* Cancers (Basel), 2018. **10**(11).
41. Seidman, J.D., et al., *The histologic type and stage distribution of ovarian carcinomas of surface epithelial origin.* Int J Gynecol Pathol, 2004. **23**(1): p. 41-4.
42. Machida, H., et al., *Trends and characteristics of epithelial ovarian cancer in Japan between 2002 and 2015: A JSGO-JSOG joint study.* Gynecol Oncol, 2019. **153**(3): p. 589-596.
43. Kobel, M., et al., *Differences in tumor type in low-stage versus high-stage ovarian carcinomas.* Int J Gynecol Pathol, 2010. **29**(3): p. 203-11.
44. Peres, L.C., et al., *Invasive Epithelial Ovarian Cancer Survival by Histotype and Disease Stage.* J Natl Cancer Inst, 2019. **111**(1): p. 60-68.
45. Konecny, G.E., et al., *Prognostic and therapeutic relevance of molecular subtypes in high-grade serous ovarian cancer.* J Natl Cancer Inst, 2014. **106**(10).
46. Konecny, G.E., B. Winterhoff, and C. Wang, *Gene-expression signatures in ovarian cancer: Promise and challenges for patient stratification.* Gynecol Oncol, 2016. **141**(2): p. 379-385.
47. Hui, P. and N. Buza, *Atlas of Intraoperative Frozen Section Diagnosis in Gynecologic Pathology*. 2015, Cham, SWITZERLAND: Springer International Publishing AG.
48. Nofech-Mozes, S., et al., *Immunophenotyping of serous carcinoma of the female genital tract.* Mod Pathol, 2008. **21**(9): p. 1147-55.
49. Kobel, M., et al., *An Immunohistochemical Algorithm for Ovarian Carcinoma Typing.* Int J Gynecol Pathol, 2016. **35**(5): p. 430-41.
50. Hollis, R.L., et al., *Distinct histopathological features are associated with molecular subtypes and outcome in low grade serous ovarian carcinoma.* Sci Rep, 2023. **13**(1): p. 7681.
51. Soslow, R.A., et al., *Morphologic patterns associated with BRCA1 and BRCA2 genotype in ovarian carcinoma.* Mod Pathol, 2012. **25**(4): p. 625-36.
52. Kurman, R.J. and M. Shih Ie, *The Dualistic Model of Ovarian Carcinogenesis: Revisited, Revised, and Expanded.* Am J Pathol, 2016. **186**(4): p. 733-47.
53. Köbel, M., et al., *Molecular Analysis of Mixed Endometrial Carcinomas Shows Clonality in Most Cases.* Am J Surg Pathol, 2016. **40**(2): p. 166-180.
54. Tsuchiya, A., et al., *Expression profiling in ovarian clear cell carcinoma: identification of hepatocyte nuclear factor-1 beta as a molecular marker and a possible molecular target for therapy of ovarian clear cell carcinoma.* Am J Pathol, 2003. **163**(6): p. 2503-12.
55. Gadducci, A., et al., *Clear cell carcinoma of the ovary: Epidemiology, pathological and biological features, treatment options and clinical outcomes.* Gynecol Oncol, 2021.

56. Seidman, J.D., R.J. Kurman, and B.M. Ronnett, *Primary and metastatic mucinous adenocarcinomas in the ovaries: incidence in routine practice with a new approach to improve intraoperative diagnosis.* Am J Surg Pathol, 2003. **27**(7): p. 985-93.
57. Meagher, N.S., et al., *A combination of the immunohistochemical markers CK7 and SATB2 is highly sensitive and specific for distinguishing primary ovarian mucinous tumors from colorectal and appendiceal metastases.* Mod Pathol, 2019. **32**(12): p. 1834-1846.
58. Handley, K.F., et al., *Classification of High-Grade Serous Ovarian Cancer Using Tumor Morphologic Characteristics.* JAMA Netw Open, 2022. **5**(10): p. e2236626.
59. Bolton, K.L., et al., *Molecular Subclasses of Clear Cell Ovarian Carcinoma and Their Impact on Disease Behavior and Outcomes.* Clin Cancer Res, 2022. **28**(22): p. 4947-4956.
60. Barnes, B.M., et al., *Distinct transcriptional programs stratify ovarian cancer cell lines into the five major histological subtypes.* Genome Med, 2021. **13**(1): p. 140.
61. Stur, E., et al., *Spatially resolved transcriptomics of high-grade serous ovarian carcinoma.* iScience, 2022. **25**(3): p. 103923.
62. Kieffer, Y., et al., *Clinical Interest of Combining Transcriptomic and Genomic Signatures in High-Grade Serous Ovarian Cancer.* Front Genet, 2020. **11**: p. 219.
63. Murakami, R., et al., *Establishment of a Novel Histopathological Classification of High-Grade Serous Ovarian Carcinoma Correlated with Prognostically Distinct Gene Expression Subtypes.* Am J Pathol, 2016. **186**(5): p. 1103-13.
64. Cancer Genome Atlas Research, N., *Integrated genomic analyses of ovarian carcinoma.* Nature, 2011. **474**(7353): p. 609-15.
65. Tothill, R.W., et al., *Novel molecular subtypes of serous and endometrioid ovarian cancer linked to clinical outcome.* Clin Cancer Res, 2008. **14**(16): p. 5198-208.
66. Tan, T.Z., et al., *Functional genomics identifies five distinct molecular subtypes with clinical relevance and pathways for growth control in epithelial ovarian cancer.* EMBO Mol Med, 2013. **5**(7): p. 1051-66.
67. Wang, K., et al., *Monitoring gene expression profile changes in ovarian carcinomas using cDNA microarray.* Gene, 1999. **229**(1-2): p. 101-8.
68. Ono, K., et al., *Identification by cDNA microarray of genes involved in ovarian carcinogenesis.* Cancer Res, 2000. **60**(18): p. 5007-11.
69. Welsh, J.B., et al., *Analysis of gene expression profiles in normal and neoplastic ovarian tissue samples identifies candidate molecular markers of epithelial ovarian cancer.* Proc Natl Acad Sci U S A, 2001. **98**(3): p. 1176-81.
70. Hao, D., et al., *Integrated Analysis Reveals Tubal- and Ovarian-Originated Serous Ovarian Cancer and Predicts Differential Therapeutic Responses.* Clin Cancer Res, 2017. **23**(23): p. 7400-7411.
71. Lawrenson, K., et al., *Integrated molecular profiling studies to characterize the cellular origins of high-grade serous ovarian cancer.* BioRxiv, 2018: p. 330597.
72. Zhang, Z., et al., *Molecular Subtyping of Serous Ovarian Cancer Based on Multi-omics Data.* Sci Rep, 2016. **6**: p. 26001.

73. Chen, G.M., et al., *Consensus on Molecular Subtypes of High-Grade Serous Ovarian Carcinoma.* Clin Cancer Res, 2018. **24**(20): p. 5037-5047.
74. Leong, H.S., et al., *Efficient molecular subtype classification of high-grade serous ovarian cancer.* J Pathol, 2015. **236**(3): p. 272-7.
75. Shih, A.J., et al., *Identification of grade and origin specific cell populations in serous epithelial ovarian cancer by single cell RNA-seq.* PLoS One, 2018. **13**(11): p. e0206785.
76. Shih, A.J., et al., *Correction: Identification of grade and origin specific cell populations in serous epithelial ovarian cancer by single cell RNA-seq.* PLoS One, 2018. **13**(12): p. e0208778.
77. Cook, D.P. and B.C. Vanderhyden, *Ovarian cancer and the evolution of subtype classifications using transcriptional profilingdagger.* Biol Reprod, 2019. **101**(3): p. 645-658.
78. Ye, S., et al., *Integrative genomic and transcriptomic analysis reveals immune subtypes and prognostic markers in ovarian clear cell carcinoma.* Br J Cancer, 2022. **126**(8): p. 1215-1223.
79. Hollis, R.L., *Molecular characteristics and clinical behaviour of epithelial ovarian cancers.* Cancer Lett, 2023. **555**: p. 216057.
80. Beaufort, C.M., et al., *Ovarian cancer cell line panel (OCCP): clinical importance of in vitro morphological subtypes.* PLoS One, 2014. **9**(9): p. e103988.
81. Pamula-Pilat, J., et al., *Gene expression profiles in three histologic types, clear-cell, endometrioid and serous ovarian carcinomas.* J Biol Regul Homeost Agents, 2014. **28**(4): p. 659-74.
82. Zorn, K.K., et al., *Gene expression profiles of serous, endometrioid, and clear cell subtypes of ovarian and endometrial cancer.* Clin Cancer Res, 2005. **11**(18): p. 6422-30.
83. Heinzelmann-Schwarz, V.A., et al., *A distinct molecular profile associated with mucinous epithelial ovarian cancer.* Br J Cancer, 2006. **94**(6): p. 904-13.
84. Domcke, S., et al., *Evaluating cell lines as tumour models by comparison of genomic profiles.* Nat Commun, 2013. **4**: p. 2126.
85. Castellvi, J., et al., *Phosphorylated 4E binding protein 1: a hallmark of cell signaling that correlates with survival in ovarian cancer.* Cancer, 2006. **107**(8): p. 1801-11.
86. Kobel, M., et al., *IGF2BP3 (IMP3) expression is a marker of unfavorable prognosis in ovarian carcinoma of clear cell subtype.* Mod Pathol, 2009. **22**(3): p. 469-75.
87. Kalloger, S.E., et al., *Calculator for ovarian carcinoma subtype prediction.* Mod Pathol, 2011. **24**(4): p. 512-21.
88. Wiegand, K.C., et al., *Loss of BAF250a (ARID1A) is frequent in high-grade endometrial carcinomas.* J Pathol, 2011. **224**(3): p. 328-33.
89. Lu, F.I., et al., *Prevalence of loss of expression of DNA mismatch repair proteins in primary epithelial ovarian tumors.* Int J Gynecol Pathol, 2012. **31**(6): p. 524-31.

90. Sfakianos, G.P., et al., *Validation of ovarian cancer gene expression signatures for survival and subtype in formalin fixed paraffin embedded tissues.* Gynecol Oncol, 2013. **129**(1): p. 159-64.
91. Sieh, W., et al., *Hormone-receptor expression and ovarian cancer survival: an Ovarian Tumor Tissue Analysis consortium study.* Lancet Oncol, 2013. **14**(9): p. 853-62.
92. Zhang, X., et al., *Profile of differentially expressed miRNAs in high-grade serous carcinoma and clear cell ovarian carcinoma, and the expression of miR-510 in ovarian carcinoma.* Mol Med Rep, 2015. **12**(6): p. 8021-31.
93. Webb, J.R., et al., *PD-L1 expression is associated with tumor-infiltrating T cells and favorable prognosis in high-grade serous ovarian cancer.* Gynecol Oncol, 2016. **141**(2): p. 293-302.
94. Winterhoff, B., et al., *Molecular classification of high grade endometrioid and clear cell ovarian cancer using TCGA gene expression signatures.* Gynecol Oncol, 2016. **141**(1): p. 95-100.
95. Wang, C., et al., *Expression signature distinguishing two tumour transcriptome classes associated with progression-free survival among rare histological types of epithelial ovarian cancer.* Br J Cancer, 2016. **114**(12): p. 1412-20.
96. Tassi, R.A., et al., *FOXM1 expression is significantly associated with chemotherapy resistance and adverse prognosis in non-serous epithelial ovarian cancer patients.* J Exp Clin Cancer Res, 2017. **36**(1): p. 63.
97. Mackenzie, R., et al., *Morphologic and Molecular Characteristics of Mixed Epithelial Ovarian Cancers.* Am J Surg Pathol, 2015. **39**(11): p. 1548-57.
98. Fridley, B.L., et al., *Transcriptomic Characterization of Endometrioid, Clear Cell, and High-Grade Serous Epithelial Ovarian Carcinoma.* Cancer Epidemiol Biomarkers Prev, 2018. **27**(9): p. 1101-1109.
99. Nagasawa, S., et al., *Systematic Identification of Characteristic Genes of Ovarian Clear Cell Carcinoma Compared with High-Grade Serous Carcinoma Based on RNA-Sequencing.* Int J Mol Sci, 2019. **20**(18).
100. Calura, E., et al., *Transcriptional Characterization of Stage I Epithelial Ovarian Cancer: A Multicentric Study.* Cells, 2019. **8**(12).
101. Matei, D., et al., *Gene expression in epithelial ovarian carcinoma.* Oncogene, 2002. **21**(41): p. 6289-98.
102. Worley, M.J., Jr., et al., *Molecular changes in endometriosis-associated ovarian clear cell carcinoma.* Eur J Cancer, 2015. **51**(13): p. 1831-42.
103. Lopacinska-Jorgensen, J., et al., *Integrated microRNA and mRNA signatures associated with overall survival in epithelial ovarian cancer.* PLoS One, 2021. **16**(7): p. e0255142.
104. Vazquez-Garcia, I., et al., *Ovarian cancer mutational processes drive site-specific immune evasion.* Nature, 2022. **612**(7941): p. 778-786.
105. Vang, R., et al., *Molecular Alterations of TP53 are a Defining Feature of Ovarian High-Grade Serous Carcinoma: A Rereview of Cases Lacking TP53 Mutations in The Cancer Genome Atlas Ovarian Study.* Int J Gynecol Pathol, 2016. **35**(1): p. 48-55.

106. Zehir, A., et al., *Mutational landscape of metastatic cancer revealed from prospective clinical sequencing of 10,000 patients.* Nat Med, 2017. **23**(6): p. 703-713.
107. Bonome, T., et al., *Expression profiling of serous low malignant potential, low-grade, and high-grade tumors of the ovary.* Cancer Res, 2005. **65**(22): p. 10602-12.
108. Canet, B., et al., *Ovarian clear cell carcinomas: RHO GTPases may contribute to explain their singular biologic behavior.* Hum Pathol, 2011. **42**(6): p. 833-9.
109. Kobel, M., et al., *A limited panel of immunomarkers can reliably distinguish between clear cell and high-grade serous carcinoma of the ovary.* Am J Surg Pathol, 2009. **33**(1): p. 14-21.
110. Espinosa, I., et al., *Gene expression analysis identifies two groups of ovarian high-grade serous carcinomas with different prognosis.* Mod Pathol, 2011. **24**(6): p. 846-54.
111. Anglesio, M.S., et al., *IL6-STAT3-HIF signaling and therapeutic response to the angiogenesis inhibitor sunitinib in ovarian clear cell cancer.* Clin Cancer Res, 2011. **17**(8): p. 2538-48.
112. Quattrocchi, L., et al., *Expression of angiogenic chemokines in ovarian clear cell carcinoma.* J Obstet Gynaecol Res, 2013. **39**(1): p. 297-304.
113. Makii, C., et al., *MDM2 is a potential therapeutic target and prognostic factor for ovarian clear cell carcinomas with wild type TP53.* Oncotarget, 2016. **7**(46): p. 75328-75338.
114. Vilming Elgaaen, B., et al., *Global miRNA expression analysis of serous and clear cell ovarian carcinomas identifies differentially expressed miRNAs including miR-200c-3p as a prognostic marker.* BMC Cancer, 2014. **14**: p. 80.
115. Miao, Y., et al., *Annexin IV is differentially expressed in clear cell carcinoma of the ovary.* Int J Gynecol Cancer, 2009. **19**(9): p. 1545-9.
116. Tan, T.Z., et al., *Analysis of gene expression signatures identifies prognostic and functionally distinct ovarian clear cell carcinoma subtypes.* EBioMedicine, 2019. **50**: p. 203-210.
117. Zhou, H., et al., *Distinct gene expression profiles associated with clinical outcomes in patients with ovarian clear cell carcinoma and high-grade serous ovarian carcinoma.* J Ovarian Res, 2020. **13**(1): p. 38.
118. Kuo, K.T., et al., *DNA copy numbers profiles in affinity-purified ovarian clear cell carcinoma.* Clin Cancer Res, 2010. **16**(7): p. 1997-2008.
119. Tsuda, H., et al., *Identification of overexpression and amplification of ABCF2 in clear cell ovarian adenocarcinomas by cDNA microarray analyses.* Clin Cancer Res, 2005. **11**(19 Pt 1): p. 6880-8.
120. Nagaraja, A.K., et al., *A link between mir-100 and FRAP1/mTOR in clear cell ovarian cancer.* Mol Endocrinol, 2010. **24**(2): p. 447-63.
121. Matsumura, N., et al., *Sorafenib efficacy in ovarian clear cell carcinoma revealed by transcriptome profiling.* Cancer Sci, 2010. **101**(12): p. 2658-63.
122. Sung, C.O., et al., *Integrative analysis of copy number alteration and gene expression profiling in ovarian clear cell adenocarcinoma.* Cancer Genet, 2013. **206**(5): p. 145-53.

123. Chandler, R.L., et al., *Global gene expression profiling of a mouse model of ovarian clear cell carcinoma caused by ARID1A and PIK3CA mutations implicates a role for inflammatory cytokine signaling.* Genom Data, 2015. **5**: p. 329-32.
124. Abou-Taleb, H., et al., *Comprehensive assessment of the expression of the SWI/SNF complex defines two distinct prognostic subtypes of ovarian clear cell carcinoma.* Oncotarget, 2016. **7**(34): p. 54758-54770.
125. Azar, W.J., et al., *Noncanonical IL6 Signaling-Mediated Activation of YAP Regulates Cell Migration and Invasion in Ovarian Clear Cell Cancer.* Cancer Res, 2020. **80**(22): p. 4960-4971.
126. Tamura, R., et al., *Proposing a molecular classification associated with hypercoagulation in ovarian clear cell carcinoma.* Gynecol Oncol, 2021. **163**(2): p. 327-333.
127. Suryawanshi, S., et al., *Plasma microRNAs as novel biomarkers for endometriosis and endometriosis-associated ovarian cancer.* Clin Cancer Res, 2013. **19**(5): p. 1213-24.
128. Wiegand, K.C., et al., *ARID1A mutations in endometriosis-associated ovarian carcinomas.* N Engl J Med, 2010. **363**(16): p. 1532-43.
129. Shin, H.Y., et al., *Tetraspanin 1 promotes endometriosis leading to ovarian clear cell carcinoma.* Mol Oncol, 2021. **15**(4): p. 987-1004.
130. Cybulska, P., et al., *Molecular profiling and molecular classification of endometrioid ovarian carcinomas.* Gynecol Oncol, 2019. **154**(3): p. 516-523.
131. Dion, L., et al., *The Landscape and Therapeutic Implications of Molecular Profiles in Epithelial Ovarian Cancer.* J Clin Med, 2020. **9**(7).
132. Kurman, R.J. and I.M. Shih, *Molecular pathogenesis and extraovarian origin of epithelial ovarian cancer-Shifting the paradigm.* Human Pathology, 2011. **42**(7): p. 918-931.
133. Rojas, V., et al., *Molecular Characterization of Epithelial Ovarian Cancer: Implications for Diagnosis and Treatment.* Int J Mol Sci, 2016. **17**(12).
134. Network, N.C.C. *Ovarian Cancer (Version 1.2024)*. April 17, 2024]; Available from: https://www.nccn.org/professionals/physician_gls/pdf/ovarian.pdf.
135. Kelland, L., *The resurgence of platinum-based cancer chemotherapy.* Nat Rev Cancer, 2007. **7**(8): p. 573-84.
136. Omura, G., et al., *A randomized trial of cyclophosphamide and doxorubicin with or without cisplatin in advanced ovarian carcinoma. A Gynecologic Oncology Group Study.* Cancer, 1986. **57**(9): p. 1725-30.
137. Omura, G.A., et al., *A randomized comparison of melphalan versus melphalan plus hexamethylmelamine versus adriamycin plus cyclophosphamide in ovarian carcinoma.* Cancer, 1983. **51**(5): p. 783-9.
138. Bowtell, D.D., et al., *Rethinking ovarian cancer II: reducing mortality from high-grade serous ovarian cancer.* Nat Rev Cancer, 2015. **15**(11): p. 668-79.
139. Lippert, T.H., H.J. Ruoff, and M. Volm, *Intrinsic and acquired drug resistance in malignant tumors. The main reason for therapeutic failure.* Arzneimittelforschung, 2008. **58**(6): p. 261-4.

140. Alatise, K.L., S. Gardner, and A. Alexander-Bryant, *Mechanisms of Drug Resistance in Ovarian Cancer and Associated Gene Targets.* Cancers (Basel), 2022. **14**(24).
141. Freimund, A.E., et al., *Mechanisms of Drug Resistance in High-Grade Serous Ovarian Cancer.* Hematol Oncol Clin North Am, 2018. **32**(6): p. 983-996.
142. Lindemann, K., et al., *Response rates to second-line platinum-based therapy in ovarian cancer patients challenge the clinical definition of platinum resistance.* Gynecol Oncol, 2018. **150**(2): p. 239-246.
143. Cooke, S.L. and J.D. Brenton, *Evolution of platinum resistance in high-grade serous ovarian cancer.* Lancet Oncol, 2011. **12**(12): p. 1169-74.
144. Jayson, G.C., et al., *Ovarian cancer.* Lancet, 2014. **384**(9951): p. 1376-88.
145. McGuire, W.P., et al., *Cyclophosphamide and cisplatin compared with paclitaxel and cisplatin in patients with stage III and stage IV ovarian cancer.* N Engl J Med, 1996. **334**(1): p. 1-6.
146. Ozols, R.F., et al., *Phase III trial of carboplatin and paclitaxel compared with cisplatin and paclitaxel in patients with optimally resected stage III ovarian cancer: a Gynecologic Oncology Group study.* J Clin Oncol, 2003. **21**(17): p. 3194-200.
147. Paoletti, X., et al., *Assessment of Progression-Free Survival as a Surrogate End Point of Overall Survival in First-Line Treatment of Ovarian Cancer: A Systematic Review and Meta-analysis.* JAMA Network Open, 2020. **3**(1): p. e1918939-e1918939.
148. Pfisterer, J., et al., *Gemcitabine plus carboplatin compared with carboplatin in patients with platinum-sensitive recurrent ovarian cancer: an intergroup trial of the AGO-OVAR, the NCIC CTG, and the EORTC GCG.* J Clin Oncol, 2006. **24**(29): p. 4699-707.
149. Parmar, M.K., et al., *Paclitaxel plus platinum-based chemotherapy versus conventional platinum-based chemotherapy in women with relapsed ovarian cancer: the ICON4/AGO-OVAR-2.2 trial.* Lancet, 2003. **361**(9375): p. 2099-106.
150. Itamochi, H., et al., *Low proliferation activity may be associated with chemoresistance in clear cell carcinoma of the ovary.* Obstet Gynecol, 2002. **100**(2): p. 281-7.
151. Itamochi, H., J. Kigawa, and N. Terakawa, *Mechanisms of chemoresistance and poor prognosis in ovarian clear cell carcinoma.* Cancer Sci, 2008. **99**(4): p. 653-8.
152. Sugiyama, T., et al., *Randomized Phase III Trial of Irinotecan Plus Cisplatin Compared With Paclitaxel Plus Carboplatin As First-Line Chemotherapy for Ovarian Clear Cell Carcinoma: JGOG3017/GCIG Trial.* J Clin Oncol, 2016. **34**(24): p. 2881-7.
153. Sugiyama, T., et al., *Clinical characteristics of clear cell carcinoma of the ovary: a distinct histologic type with poor prognosis and resistance to platinum-based chemotherapy.* Cancer, 2000. **88**(11): p. 2584-9.
154. Shu, C.A., et al., *Ovarian clear cell carcinoma, outcomes by stage: the MSK experience.* Gynecol Oncol, 2015. **139**(2): p. 236-41.

155. Goff, B.A., et al., *Clear cell carcinoma of the ovary: a distinct histologic type with poor prognosis and resistance to platinum-based chemotherapy in stage III disease.* Gynecol Oncol, 1996. **60**(3): p. 412-7.
156. Al-Barrak, J., et al., *Exploring palliative treatment outcomes in women with advanced or recurrent ovarian clear cell carcinoma.* Gynecol Oncol, 2011. **122**(1): p. 107-10.
157. Ku, F.C., et al., *Clear cell carcinomas of the ovary have poorer outcomes compared with serous carcinomas: Results from a single-center Taiwanese study.* J Formos Med Assoc, 2018. **117**(2): p. 117-125.
158. Liu, H., et al., *Prognosis of ovarian clear cell cancer compared with other epithelial cancer types: A population-based analysis.* Oncol Lett, 2020. **19**(3): p. 1947-1957.
159. Ceppi, L., et al., *Early-stage clear cell ovarian cancer compared to high-grade histological subtypes: An outcome exploratory analysis in two oncology centers.* Gynecol Oncol, 2021. **160**(1): p. 64-70.
160. Zondervan, K.T., C.M. Becker, and S.A. Missmer, *Endometriosis.* N Engl J Med, 2020. **382**(13): p. 1244-1256.
161. *Practice bulletin no. 114: management of endometriosis.* Obstet Gynecol, 2010. **116**(1): p. 223-236.
162. Agarwal, S.K., et al., *Clinical diagnosis of endometriosis: a call to action.* Am J Obstet Gynecol, 2019. **220**(4): p. 354 e1-354 e12.
163. Culley, L., et al., *The social and psychological impact of endometriosis on women's lives: a critical narrative review.* Hum Reprod Update, 2013. **19**(6): p. 625-39.
164. Moradi, M., et al., *Impact of endometriosis on women's lives: a qualitative study.* BMC Womens Health, 2014. **14**: p. 123.
165. Kvaskoff, M., et al., *Endometriosis: a high-risk population for major chronic diseases?* Hum Reprod Update, 2015. **21**(4): p. 500-16.
166. Soliman, A.M., et al., *The Effect of Endometriosis Symptoms on Absenteeism and Presenteeism in the Workplace and at Home.* J Manag Care Spec Pharm, 2017. **23**(7): p. 745-754.
167. Soliman, A.M., et al., *Real-World Evaluation of Direct and Indirect Economic Burden Among Endometriosis Patients in the United States.* Adv Ther, 2018. **35**(3): p. 408-423.
168. Surrey, E., et al., *Impact of Endometriosis Diagnostic Delays on Healthcare Resource Utilization and Costs.* Adv Ther, 2020. **37**(3): p. 1087-1099.
169. Nnoaham, K.E., et al., *Impact of endometriosis on quality of life and work productivity: a multicenter study across ten countries.* Fertil Steril, 2011. **96**(2): p. 366-373 e8.
170. Hudelist, G., et al., *Diagnostic delay for endometriosis in Austria and Germany: causes and possible consequences.* Hum Reprod, 2012. **27**(12): p. 3412-6.
171. Fourquet, J., et al., *Characteristics of women with endometriosis from the USA and Puerto Rico.* J Endometr Pelvic Pain Disord, 2015. **7**(4): p. 129-135.
172. Staal, A.H., M. van der Zanden, and A.W. Nap, *Diagnostic Delay of Endometriosis in the Netherlands.* Gynecol Obstet Invest, 2016. **81**(4): p. 321-4.

173. Soliman, A.M., M. Fuldeore, and M.C. Snabes, *Factors Associated with Time to Endometriosis Diagnosis in the United States.* J Womens Health (Larchmt), 2017. **26**(7): p. 788-797.
174. Morassutto, C., et al., *Incidence and Estimated Prevalence of Endometriosis and Adenomyosis in Northeast Italy: A Data Linkage Study.* PLoS One, 2016. **11**(4): p. e0154227.
175. Harada, T., *Endometriosis: pathogenesis and treatment*. 2014: Springer.
176. Crause, R.W. and D.C. Schrön, *Disputatio inauguralis medica de ulceribus uteri*. 1690: Literis Krebsianis.
177. von Rokitansky, K.F., *Ueber uterusdrüsen-neubildung in uterus-und ovarial-sarcomen*. 1860: Druck von Carl Ueberreuter.
178. Sampson, J.A., *Peritoneal endometriosis due to the menstrual dissemination of endometrial tissue into the peritoneal cavity.* American Journal of Obstetrics and Gynecology, 1927. **14**: p. 422.
179. Sampson, J.A., *Heterotopic or misplaced endometrial tissue*. 1925.
180. Filby, C.E., et al., *Cellular Origins of Endometriosis: Towards Novel Diagnostics and Therapeutics.* Semin Reprod Med, 2020. **38**(2-03): p. 201-215.
181. Gruenwald, P., *Origin of endometriosis from the mesenchyme of the celomic walls.* American Journal of Obstetrics and Gynecology, 1942. **44**(3): p. 470-474.
182. Signorile, P.G., R. Viceconte, and A. Baldi, *New Insights in Pathogenesis of Endometriosis.* Front Med (Lausanne), 2022. **9**: p. 879015.
183. Nisolle, M. and J. Donnez, *Peritoneal endometriosis, ovarian endometriosis, and adenomyotic nodules of the rectovaginal septum are three different entities.* Fertil Steril, 1997. **68**(4): p. 585-96.
184. Von Recklinghausen, F., *Adenomyomas and cystadenomas of the wall of the uterus and tube: their origin as remnants of the wolffian body.* Wien Klin Wochenschr, 1896. **8**(530): p. 897-903.
185. WW, R., *Aberrant portion of the Mullerian duct found in an ovary.* Johns Hopkins Hospital Bulletin, 1899. **10**: p. 8-10.
186. Sampson, J.A., *Metastatic or Embolic Endometriosis, due to the Menstrual Dissemination of Endometrial Tissue into the Venous Circulation.* Am J Pathol, 1927. **3**(2): p. 93-110 43.
187. Endometriosis Initiative, G., *A Call for New Theories on the Pathogenesis and Pathophysiology of Endometriosis.* J Minim Invasive Gynecol, 2024.
188. Speroff, L. and M.A. Fritz, *Clinical Gynecologic Endocrinology and Infertility*. Seventh ed. 2005: Lippincott Williams & Wilkins.
189. Johnson, N.P., et al., *World Endometriosis Society consensus on the classification of endometriosis.* Hum Reprod, 2017. **32**(2): p. 315-324.
190. Zondervan, K.T., et al., *Endometriosis.* Nat Rev Dis Primers, 2018. **4**(1): p. 9.
191. Becker, C.M., et al., *World Endometriosis Research Foundation Endometriosis Phenome and Biobanking Harmonisation Project: I. Surgical phenotype data collection in endometriosis research.* Fertil Steril, 2014. **102**(5): p. 1213-22.
192. Vitonis, A.F., et al., *World Endometriosis Research Foundation Endometriosis Phenome and Biobanking Harmonization Project: II. Clinical and covariate phenotype data collection in endometriosis research.* Fertil Steril, 2014. **102**(5): p. 1223-32.

193. Rahmioglu, N., et al., *World Endometriosis Research Foundation Endometriosis Phenome and Biobanking Harmonization Project: III. Fluid biospecimen collection, processing, and storage in endometriosis research.* Fertil Steril, 2014. **102**(5): p. 1233-43.
194. Fassbender, A., et al., *World Endometriosis Research Foundation Endometriosis Phenome and Biobanking Harmonisation Project: IV. Tissue collection, processing, and storage in endometriosis research.* Fertil Steril, 2014. **102**(5): p. 1244-53.
195. International Working Group of Aagl, E.E., et al., *An international terminology for endometriosis, 2021().* Hum Reprod Open, 2021. **2021**(4): p. hoab029.
196. Pedrassani, M., et al., *Superficial Endometriosis at Ultrasound Examination-A Diagnostic Criteria Proposal.* Diagnostics (Basel), 2023. **13**(11).
197. Kristjansdottir, A., V. Rafnsson, and R.T. Geirsson, *Comprehensive evaluation of the incidence and prevalence of surgically diagnosed pelvic endometriosis in a complete population.* Acta Obstet Gynecol Scand, 2023. **102**(10): p. 1329-1337.
198. Saavalainen, L., et al., *Trends in the incidence rate, type and treatment of surgically verified endometriosis - a nationwide cohort study.* Acta Obstet Gynecol Scand, 2018. **97**(1): p. 59-67.
199. Hoyle, A.T. and Y. Puckett, *Endometrioma*, in *StatPearls*. 2024: Treasure Island (FL).
200. Bausic, A., et al., *Transvaginal Ultrasound vs. Magnetic Resonance Imaging (MRI) Value in Endometriosis Diagnosis.* Diagnostics (Basel), 2022. **12**(7).
201. Imperiale, L., et al., *Three Types of Endometriosis: Pathogenesis, Diagnosis and Treatment. State of the Art.* J Clin Med, 2023. **12**(3).
202. *Revised American Society for Reproductive Medicine classification of endometriosis: 1996.* Fertil Steril, 1997. **67**(5): p. 817-21.
203. Tuttlies, F., et al., *[ENZIAN-score, a classification of deep infiltrating endometriosis].* Zentralbl Gynakol, 2005. **127**(5): p. 275-81.
204. Adamson, G.D. and D.J. Pasta, *Endometriosis fertility index: the new, validated endometriosis staging system.* Fertil Steril, 2010. **94**(5): p. 1609-15.
205. Abrao, M.S., et al., *AAGL 2021 Endometriosis Classification: An Anatomy-based Surgical Complexity Score.* J Minim Invasive Gynecol, 2021. **28**(11): p. 1941-1950 e1.
206. Hanahan, D. and R.A. Weinberg, *Hallmarks of cancer: the next generation.* Cell, 2011. **144**(5): p. 646-74.
207. Flores, I., et al., *Molecular profiling of experimental endometriosis identified gene expression patternsin common with human disease.* Fertility and Sterility, 2007. **87**(5): p. 1180-1199.
208. Van Gorp, T., et al., *Endometriosis and the development of malignant tumours of the pelvis. A review of literature.* Best Pract Res Clin Obstet Gynaecol, 2004. **18**(2): p. 349-71.
209. Swiersz, L.M., *Role of endometriosis in cancer and tumor development.* Ann N Y Acad Sci, 2002. **955**: p. 281-92; discussion 293-5, 396-406.
210. Artemova, D., et al., *Endometriosis and Cancer: Exploring the Role of Macrophages.* Int J Mol Sci, 2021. **22**(10).

211. Zou, Y., et al., *The presence of KRAS, PPP2R1A and ARID1A mutations in 101 Chinese samples with ovarian endometriosis.* Mutat Res, 2018. **809**: p. 1-5.
212. Lac, V., et al., *Iatrogenic endometriosis harbors somatic cancer-driver mutations.* Hum Reprod, 2019. **34**(1): p. 69-78.
213. Suda, K., et al., *Clonal lineage from normal endometrium to ovarian clear cell carcinoma through ovarian endometriosis.* Cancer Sci, 2020. **111**(8): p. 3000-3009.
214. Suda, K., et al., *Clonal Expansion and Diversification of Cancer-Associated Mutations in Endometriosis and Normal Endometrium.* Cell Rep, 2018. **24**(7): p. 1777-1789.
215. Anglesio, M.S., et al., *Multifocal endometriotic lesions associated with cancer are clonal and carry a high mutation burden.* J Pathol, 2015. **236**(2): p. 201-9.
216. Samartzis, E.P., et al., *Loss of ARID1A/BAF250a-expression in endometriosis: a biomarker for risk of carcinogenic transformation?* Mod Pathol, 2012. **25**(6): p. 885-92.
217. Praetorius, T.H., et al., *Molecular analysis suggests oligoclonality and metastasis of endometriosis lesions across anatomically defined subtypes.* Fertil Steril, 2022. **118**(3): p. 524-534.
218. Bulun, S.E., Y. Wan, and D. Matei, *Epithelial Mutations in Endometriosis: Link to Ovarian Cancer.* Endocrinology, 2019. **160**(3): p. 626-638.
219. Anglesio, M.S., et al., *Cancer-Associated Mutations in Endometriosis without Cancer.* N Engl J Med, 2017. **376**(19): p. 1835-1848.
220. Ishikawa, M., et al., *Affinity-purified DNA-based mutation profiles of endometriosis-related ovarian neoplasms in Japanese patients.* Oncotarget, 2018. **9**(19): p. 14754-14763.
221. Kim, S.I., et al., *Genomic landscape of ovarian clear cell carcinoma via whole exome sequencing.* Gynecol Oncol, 2018. **148**(2): p. 375-382.
222. Shibuya, Y., et al., *Identification of somatic genetic alterations in ovarian clear cell carcinoma with next generation sequencing.* Genes Chromosomes Cancer, 2018. **57**(2): p. 51-60.
223. Taylor, H.S., A.M. Kotlyar, and V.A. Flores, *Endometriosis is a chronic systemic disease: clinical challenges and novel innovations.* Lancet, 2021. **397**(10276): p. 839-852.
224. Jones, S., et al., *Frequent mutations of chromatin remodeling gene ARID1A in ovarian clear cell carcinoma.* Science, 2010. **330**(6001): p. 228-31.
225. Stamp, J.P., et al., *BAF250a Expression in Atypical Endometriosis and Endometriosis-Associated Ovarian Cancer.* Int J Gynecol Cancer, 2016. **26**(5): p. 825-32.
226. Arimoto, T., et al., *Genome-wide cDNA microarray analysis of gene-expression profiles involved in ovarian endometriosis.* Int J Oncol, 2003. **22**(3): p. 551-60.
227. Kao, L.C., et al., *Expression profiling of endometrium from women with endometriosis reveals candidate genes for disease-based implantation failure and infertility.* Endocrinology, 2003. **144**(7): p. 2870-81.
228. Matsuzaki, S., et al., *DNA microarray analysis of gene expression profiles in deep endometriosis using laser capture microdissection.* Mol Hum Reprod, 2004. **10**(10): p. 719-28.

229. Borrelli, G.M., et al., *(Partial) Loss of BAF250a (ARID1A) in rectovaginal deep-infiltrating endometriosis, endometriomas and involved pelvic sentinel lymph nodes.* Mol Hum Reprod, 2016. **22**(5): p. 329-37.
230. Pearce, C.L., et al., *Association between endometriosis and risk of histological subtypes of ovarian cancer: a pooled analysis of case-control studies.* Lancet Oncol, 2012. **13**(4): p. 385-94.
231. Saavalainen, L., et al., *Risk of Gynecologic Cancer According to the Type of Endometriosis.* Obstet Gynecol, 2018. **131**(6): p. 1095-1102.
232. Hermens, M., et al., *Incidence of endometrioid and clear-cell ovarian cancer in histological proven endometriosis: the ENOCA population-based cohort study.* Am J Obstet Gynecol, 2020. **223**(1): p. 107 e1-107 e11.
233. Fukunaga, M., et al., *Ovarian atypical endometriosis: its close association with malignant epithelial tumours.* Histopathology, 1997. **30**(3): p. 249-55.
234. Siufi Neto, J., et al., *Cellular, histologic, and molecular changes associated with endometriosis and ovarian cancer.* J Minim Invasive Gynecol, 2014. **21**(1): p. 55-63.
235. Varga, J., et al., *Predictive factors of endometriosis progression into ovarian cancer.* J Ovarian Res, 2022. **15**(1): p. 5.
236. Anglesio, M.S. and P.J. Yong, *Endometriosis-associated Ovarian Cancers.* Clin Obstet Gynecol, 2017. **60**(4): p. 711-727.
237. Wilbur, M.A., et al., *Cancer Implications for Patients with Endometriosis.* Semin Reprod Med, 2017. **35**(1): p. 110-116.
238. Lee, A.W., et al., *Evidence of a genetic link between endometriosis and ovarian cancer.* Fertil Steril, 2016. **105**(1): p. 35-43 e1-10.
239. Kim, H.S., et al., *Risk and prognosis of ovarian cancer in women with endometriosis: a meta-analysis.* Br J Cancer, 2014. **110**(7): p. 1878-90.
240. Wang, C., et al., *The Association between Endometriosis, Tubal Ligation, Hysterectomy and Epithelial Ovarian Cancer: Meta-Analyses.* Int J Environ Res Public Health, 2016. **13**(11): p. 1138.
241. Vercellini, P., et al., *Endometriosis: pathogenesis and treatment.* Nat Rev Endocrinol, 2014. **10**(5): p. 261-75.
242. Grandi, G., et al., *The Association between Endometriomas and Ovarian Cancer: Preventive Effect of Inhibiting Ovulation and Menstruation during Reproductive Life.* Biomed Res Int, 2015. **2015**: p. 751571.
243. Sato, N., et al., *Loss of heterozygosity on 10q23.3 and mutation of the tumor suppressor gene PTEN in benign endometrial cyst of the ovary: possible sequence progression from benign endometrial cyst to endometrioid carcinoma and clear cell carcinoma of the ovary.* Cancer Res, 2000. **60**(24): p. 7052-6.
244. Yamamoto, S., et al., *Loss of ARID1A protein expression occurs as an early event in ovarian clear-cell carcinoma development and frequently coexists with PIK3CA mutations.* Mod Pathol, 2012. **25**(4): p. 615-24.
245. Stewart, C.J., et al., *KRAS mutations in ovarian low-grade endometrioid adenocarcinoma: association with concurrent endometriosis.* Hum Pathol, 2012. **43**(8): p. 1177-83.

246. Zhang, C., et al., *Distinct molecular pathways in ovarian endometrioid adenocarcinoma with concurrent endometriosis.* Int J Cancer, 2018. **143**(10): p. 2505-2515.
247. Suryawanshi, S., et al., *Complement pathway is frequently altered in endometriosis and endometriosis-associated ovarian cancer.* Clin Cancer Res, 2014. **20**(23): p. 6163-74.
248. Wu, R.L., et al., *Comparative Analysis of Differentially Expressed miRNAs and their Downstream mRNAs in Ovarian Cancer and its Associated Endometriosis.* J Cancer Sci Ther, 2015. **7**(7): p. 258-265.
249. Yang, L., et al., *Comprehensive Analysis of the Transcriptome-Wide m6A Methylome in Endometrioid Ovarian Cancer.* Front Oncol, 2022. **12**: p. 844613.
250. Mortlock, S., et al., *A multi-level investigation of the genetic relationship between endometriosis and ovarian cancer histotypes.* Cell Rep Med, 2022. **3**(3): p. 100542.
251. Pavaleanu, I., et al., *Insights into molecular pathways of endometriosis and endometriosis-related ovarian carcinoma.* Rom J Morphol Embryol, 2020. **61**(3): p. 739-749.
252. Rahmioglu, N., et al., *The genetic basis of endometriosis and comorbidity with other pain and inflammatory conditions.* Nat Genet, 2023. **55**(3): p. 423-436.
253. Lee, R.C., R.L. Feinbaum, and V. Ambros, *The C. elegans heterochronic gene lin-4 encodes small RNAs with antisense complementarity to lin-14.* Cell, 1993. **75**(5): p. 843-54.
254. Bartel, D.P., *MicroRNAs: genomics, biogenesis, mechanism, and function.* Cell, 2004. **116**(2): p. 281-97.
255. Friedman, R.C., et al., *Most mammalian mRNAs are conserved targets of microRNAs.* Genome Res, 2009. **19**(1): p. 92-105.
256. Lewis, B.P., et al., *Prediction of mammalian microRNA targets.* Cell, 2003. **115**(7): p. 787-98.
257. Lai, E.C., C. Wiel, and G.M. Rubin, *Complementary miRNA pairs suggest a regulatory role for miRNA:miRNA duplexes.* RNA, 2004. **10**(2): p. 171-5.
258. Lau, N.C., et al., *An abundant class of tiny RNAs with probable regulatory roles in Caenorhabditis elegans.* Science, 2001. **294**(5543): p. 858-62.
259. Iorio, M.V. and C.M. Croce, *Causes and consequences of microRNA dysregulation.* Cancer J, 2012. **18**(3): p. 215-22.
260. Mall, C., et al., *Stability of miRNA in human urine supports its biomarker potential.* Biomark Med, 2013. **7**(4): p. 623-31.
261. Michael, A., et al., *Exosomes from human saliva as a source of microRNA biomarkers.* Oral Dis, 2010. **16**(1): p. 34-8.
262. Wang, K., et al., *Comparing the MicroRNA spectrum between serum and plasma.* PLoS One, 2012. **7**(7): p. e41561.
263. Condrat, C.E., et al., *miRNAs as Biomarkers in Disease: Latest Findings Regarding Their Role in Diagnosis and Prognosis.* Cells, 2020. **9**(2).
264. Hawkins, S.M., et al., *Functional microRNA involved in endometriosis.* Mol Endocrinol, 2011. **25**(5): p. 821-32.
265. Moustafa, S., et al., *Accurate diagnosis of endometriosis using serum microRNAs.* Am J Obstet Gynecol, 2020.

266. Ohlsson Teague, E.M., et al., *MicroRNA-regulated pathways associated with endometriosis.* Mol Endocrinol, 2009. **23**(2): p. 265-75.
267. Burney, R.O., et al., *MicroRNA expression profiling of eutopic secretory endometrium in women with versus without endometriosis.* Mol Hum Reprod, 2009. **15**(10): p. 625-31.
268. Zhao, Z.Z., et al., *Evaluation of polymorphisms in predicted target sites for micro RNAs differentially expressed in endometriosis.* Mol Hum Reprod, 2011. **17**(2): p. 92-103.
269. Petracco, R., et al., *MicroRNA 135 regulates HOXA10 expression in endometriosis.* J Clin Endocrinol Metab, 2011. **96**(12): p. E1925-33.
270. Liu, S., et al., *Expression of miR-126 and Crk in endometriosis: miR-126 may affect the progression of endometriosis by regulating Crk expression.* Arch Gynecol Obstet, 2012. **285**(4): p. 1065-72.
271. Wang, W.T., et al., *Circulating microRNAs identified in a genome-wide serum microRNA expression analysis as noninvasive biomarkers for endometriosis.* J Clin Endocrinol Metab, 2013. **98**(1): p. 281-9.
272. Jia, S.Z., et al., *Plasma miR-17-5p, miR-20a and miR-22 are down-regulated in women with endometriosis.* Hum Reprod, 2013. **28**(2): p. 322-30.
273. Schneider, C., et al., *Targeting of syndecan-1 by micro-ribonucleic acid miR-10b modulates invasiveness of endometriotic cells via dysregulation of the proteolytic milieu and interleukin-6 secretion.* Fertil Steril, 2013. **99**(3): p. 871-881 e1.
274. Abe, W., et al., *miR-196b targets c-myc and Bcl-2 expression, inhibits proliferation and induces apoptosis in endometriotic stromal cells.* Hum Reprod, 2013. **28**(3): p. 750-61.
275. Adammek, M., et al., *MicroRNA miR-145 inhibits proliferation, invasiveness, and stem cell phenotype of an in vitro endometriosis model by targeting multiple cytoskeletal elements and pluripotency factors.* Fertil Steril, 2013. **99**(5): p. 1346-1355 e5.
276. Shen, L., et al., *MicroRNA23a and microRNA23b deregulation derepresses SF-1 and upregulates estrogen signaling in ovarian endometriosis.* J Clin Endocrinol Metab, 2013. **98**(4): p. 1575-82.
277. Laudanski, P., et al., *MicroRNAs expression profiling of eutopic proliferative endometrium in women with ovarian endometriosis.* Reprod Biol Endocrinol, 2013. **11**: p. 78.
278. Wang, Y., et al., *MiR-195 inhibits proliferation and growth and induces apoptosis of endometrial stromal cells by targeting FKN.* Int J Clin Exp Pathol, 2013. **6**(12): p. 2824-34.
279. Shi, X.Y., et al., *Downregulation of miR-183 inhibits apoptosis and enhances the invasive potential of endometrial stromal cells in endometriosis.* Int J Mol Med, 2014. **33**(1): p. 59-67.
280. Hsu, C.Y., et al., *miRNA-199a-5p regulates VEGFA in endometrial mesenchymal stem cells and contributes to the pathogenesis of endometriosis.* J Pathol, 2014. **232**(3): p. 330-43.
281. Santamaria, X. and H. Taylor, *MicroRNA and gynecological reproductive diseases.* Fertil Steril, 2014. **101**(6): p. 1545-51.

282. Filigheddu, N., et al., *Differential expression of microRNAs between eutopic and ectopic endometrium in ovarian endometriosis.* J Biomed Biotechnol, 2010. **2010**: p. 369549.
283. Saare, M., et al., *Challenges in endometriosis miRNA studies - From tissue heterogeneity to disease specific miRNAs.* Biochim Biophys Acta Mol Basis Dis, 2017. **1863**(9): p. 2282-2292.
284. Logan, M. and S.M. Hawkins, *Role of microRNAs in cancers of the female reproductive tract: insights from recent clinical and experimental discovery studies.* Clin Sci (Lond), 2015. **128**(3): p. 153-80.
285. Nam, E.J., et al., *MicroRNA expression profiles in serous ovarian carcinoma.* Clin Cancer Res, 2008. **14**(9): p. 2690-5.
286. Lee, C.H., et al., *MicroRNA profiling of BRCA1/2 mutation-carrying and non-mutation-carrying high-grade serous carcinomas of ovary.* PLoS One, 2009. **4**(10): p. e7314.
287. White, N.M., et al., *Three dysregulated miRNAs control kallikrein 10 expression and cell proliferation in ovarian cancer.* Br J Cancer, 2010. **102**(8): p. 1244-53.
288. Miles, G.D., et al., *Identifying microRNA/mRNA dysregulations in ovarian cancer.* BMC Res Notes, 2012. **5**: p. 164.
289. Peng, D.X., et al., *Prognostic implications of microRNA-100 and its functional roles in human epithelial ovarian cancer.* Oncol Rep, 2012. **27**(4): p. 1238-44.
290. Li, J., et al., *Tiam1, negatively regulated by miR-22, miR-183 and miR-31, is involved in migration, invasion and viability of ovarian cancer cells.* Oncol Rep, 2012. **27**(6): p. 1835-42.
291. Liu, Z., et al., *MiR-182 overexpression in tumourigenesis of high-grade serous ovarian carcinoma.* J Pathol, 2012. **228**(2): p. 204-15.
292. Kozomara, A. and S. Griffiths-Jones, *miRBase: annotating high confidence microRNAs using deep sequencing data.* Nucleic Acids Res, 2014. **42**(Database issue): p. D68-73.
293. Kozomara, A., M. Birgaoanu, and S. Griffiths-Jones, *miRBase: from microRNA sequences to function.* Nucleic Acids Res, 2019. **47**(D1): p. D155-D162.
294. Griffiths-Jones, S., et al., *miRBase: microRNA sequences, targets and gene nomenclature.* Nucleic Acids Res, 2006. **34**(Database issue): p. D140-4.
295. Mansfield, J.H., et al., *MicroRNA-responsive 'sensor' transgenes uncover Hox-like and other developmentally regulated patterns of vertebrate microRNA expression.* Nat Genet, 2004. **36**(10): p. 1079-83.
296. Jiajie, T., et al., *Conserved miR-10 family represses proliferation and induces apoptosis in ovarian granulosa cells.* Sci Rep, 2017. **7**: p. 41304.
297. Hassel, D., et al., *MicroRNA-10 regulates the angiogenic behavior of zebrafish and human endothelial cells by promoting vascular endothelial growth factor signaling.* Circ Res, 2012. **111**(11): p. 1421-33.
298. Jonsson, M.E., et al., *Comprehensive analysis of microRNA expression in regionalized human neural progenitor cells reveals microRNA-10 as a caudalizing factor.* Development, 2015. **142**(18): p. 3166-77.
299. Keller, A., et al., *miRNATissueAtlas2: an update to the human miRNA tissue atlas.* Nucleic Acids Res, 2022. **50**(D1): p. D211-D221.

300. Lund, A.H., *miR-10 in development and cancer.* Cell Death Differ, 2010. **17**(2): p. 209-14.
301. Mu, H., et al., *MiR-10a functions as a tumor suppressor in prostate cancer via targeting KDM4A.* J Cell Biochem, 2019. **120**(4): p. 4987-4997.
302. Ke, K. and T. Lou, *MicroRNA-10a suppresses breast cancer progression via PI3K/Akt/mTOR pathway.* Oncol Lett, 2017. **14**(5): p. 5994-6000.
303. Zhang, J., et al., *S-equol inhibits proliferation and promotes apoptosis of human breast cancer MCF-7 cells via regulating miR-10a-5p and PI3K/AKT pathway.* Arch Biochem Biophys, 2019. **672**: p. 108064.
304. Khan, S., et al., *MicroRNA-10a is reduced in breast cancer and regulated in part through retinoic acid.* BMC Cancer, 2015. **15**: p. 345.
305. Wang, B., et al., *LncRNA PCED1B-AS1 knockdown inhibits osteosarcoma via methylation-mediated miR-10a downregulation.* J Orthop Surg Res, 2022. **17**(1): p. 464.
306. Xiong, Z., B. Jiang, and G. Li, *Downregulation of miR-10a inhibits cutaneous squamous cell carcinoma cell proliferation, migration, and invasion by targeting Syndecan-1.* Int J Clin Exp Pathol, 2020. **13**(10): p. 2502-2512.
307. Gu, Y., et al., *Upregulation of miRNA-10a-5p promotes tumor progression in cervical cancer by suppressing UBE2I signaling.* J Obstet Gynaecol, 2023. **43**(1): p. 2171283.
308. Zhang, X., et al., *Extracellular vesicles-encapsulated microRNA-10a-5p shed from cancer-associated fibroblast facilitates cervical squamous cell carcinoma cell angiogenesis and tumorigenicity via Hedgehog signaling pathway.* Cancer Gene Ther, 2021. **28**(5): p. 529-542.
309. Zhai, L., et al., *MicroRNA-10a-5p suppresses cancer proliferation and division in human cervical cancer by targeting BDNF.* Exp Ther Med, 2017. **14**(6): p. 6147-6151.
310. Zeng, T. and G. Li, *MicroRNA10a enhances the metastatic potential of cervical cancer cells by targeting phosphatase and tensin homologue.* Mol Med Rep, 2014. **10**(3): p. 1377-82.
311. Long, M.J., et al., *MicroRNA-10a targets CHL1 and promotes cell growth, migration and invasion in human cervical cancer cells.* Cancer Lett, 2012. **324**(2): p. 186-96.
312. Lu, X., et al., *Down-regulation of microRNA-10a mediates the anti-tumor effect of icaritin in A549 cells via the PTEN/AKT and ERK pathway.* Gen Physiol Biophys, 2019. **38**(6): p. 525-533.
313. Bao, M., et al., *Serum miR-10a-5p and miR-196a-5p as non-invasive biomarkers in non-small cell lung cancer.* Int J Clin Exp Pathol, 2018. **11**(2): p. 773-780.
314. Yu, T., et al., *MiRNA-10a is upregulated in NSCLC and may promote cancer by targeting PTEN.* Oncotarget, 2015. **6**(30): p. 30239-50.
315. Bryant, A., et al., *miR-10a is aberrantly overexpressed in Nucleophosmin1 mutated acute myeloid leukaemia and its suppression induces cell death.* Mol Cancer, 2012. **11**: p. 8.
316. Tu, J., et al., *MicroRNA-10a promotes granulosa cells tumor development via PTEN-AKT/Wnt regulatory axis.* Cell Death Dis, 2018. **9**(11): p. 1076.

317. Wang, C., W. Yin, and H. Liu, *MicroRNA-10a promotes epithelial-to-mesenchymal transition and stemness maintenance of pancreatic cancer stem cells via upregulating the Hippo signaling pathway through WWC2 inhibition.* J Cell Biochem, 2020.
318. Fei, X., et al., *Hsa-miR-10a-5p promotes pancreatic cancer growth by BDNF/SEMA4C pathway.* J Biol Regul Homeost Agents, 2020. **34**(3): p. 927-934.
319. Xiong, G., et al., *MiR-10a-5p targets TFAP2C to promote gemcitabine resistance in pancreatic ductal adenocarcinoma.* J Exp Clin Cancer Res, 2018. **37**(1): p. 76.
320. Ohuchida, K., et al., *MicroRNA-10a is overexpressed in human pancreatic cancer and involved in its invasiveness partially via suppression of the HOXA1 gene.* Ann Surg Oncol, 2012. **19**(7): p. 2394-402.
321. Weiss, F.U., et al., *Retinoic acid receptor antagonists inhibit miR-10a expression and block metastatic behavior of pancreatic cancer.* Gastroenterology, 2009. **137**(6): p. 2136-45 e1-7.
322. Zeng, T. and G. Li, *MicroRNA-10a enhances the metastatic potential of cervical cancer cells by targeting phosphatase and tensin homologue.* Mol Med Rep, 2014. **10**(3): p. 1377-82.
323. Liu, R.J., et al., *BAP1-Related ceRNA (NEAT1/miR-10a-5p/SERPINE1) Promotes Proliferation and Migration of Kidney Cancer Cells.* Front Oncol, 2022. **12**: p. 852515.
324. Vu, T.T., et al., *miR-10a as a therapeutic target and predictive biomarker for MDM2 inhibition in acute myeloid leukemia.* Leukemia, 2021. **35**(7): p. 1933-1948.
325. Huang, T., et al., *miR-10a increases the cisplatin resistance of lung adenocarcinoma circulating tumor cells via targeting PIK3CA in the PI3K/Akt pathway.* Oncol Rep, 2020. **43**(6): p. 1906-1914.
326. Sun, W., et al., *MicroRNA-10a silencing reverses cisplatin resistance in the A549/cisplatin human lung cancer cell line via the transforming growth factor-β/Smad2/STAT3/STAT5 pathway.* Mol Med Rep, 2015. **11**(5): p. 3854-9.
327. Pogribny, I.P., et al., *Alterations of microRNAs and their targets are associated with acquired resistance of MCF-7 breast cancer cells to cisplatin.* Int J Cancer, 2010. **127**(8): p. 1785-94.
328. Benson, E.A., et al., *Carboplatin with Decitabine Therapy, in Recurrent Platinum Resistant Ovarian Cancer, Alters Circulating miRNAs Concentrations: A Pilot Study.* PLoS One, 2015. **10**(10): p. e0141279.
329. Collins, K.E., et al., *Transcriptomic analyses of ovarian clear-cell carcinoma with concurrent endometriosis.* Front Endocrinol (Lausanne), 2023. **14**: p. 1162786.
330. Chen, S., et al., *fastp: an ultra-fast all-in-one FASTQ preprocessor.* Bioinformatics, 2018. **34**(17): p. i884-i890.
331. Kim, D., B. Langmead, and S.L. Salzberg, *HISAT: a fast spliced aligner with low memory requirements.* Nat Methods, 2015. **12**(4): p. 357-60.
332. Langmead, B. and S.L. Salzberg, *Fast gapped-read alignment with Bowtie 2.* Nat Methods, 2012. **9**(4): p. 357-9.
333. Liao, Y., G.K. Smyth, and W. Shi, *featureCounts: an efficient general purpose program for assigning sequence reads to genomic features.* Bioinformatics, 2014. **30**(7): p. 923-30.

334. Frankish, A., et al., *GENCODE reference annotation for the human and mouse genomes.* Nucleic Acids Res, 2019. **47**(D1): p. D766-D773.
335. Frankish, A., et al., *Gencode 2021.* Nucleic Acids Res, 2021. **49**(D1): p. D916-D923.
336. Friedlander, M.R., et al., *Discovering microRNAs from deep sequencing data using miRDeep.* Nat Biotechnol, 2008. **26**(4): p. 407-15.
337. Langmead, B., et al., *Ultrafast and memory-efficient alignment of short DNA sequences to the human genome.* Genome Biol, 2009. **10**(3): p. R25.
338. Love, M.I., W. Huber, and S. Anders, *Moderated estimation of fold change and dispersion for RNA-seq data with DESeq2.* Genome Biol, 2014. **15**(12): p. 550.
339. Banu, S.K., et al., *Gene expression profiles and functional characterization of human immortalized endometriotic epithelial and stromal cells.* Fertil Steril, 2008. **90**(4): p. 972-87.
340. ; Available from: https://www.sigmaaldrich.com/US/en/technical-documents/protocol/genomics/qpcr/qpcr-efficiency-determination.
341. Bustin, S.A., et al., *Primer sequence disclosure: a clarification of the MIQE guidelines.* Clin Chem, 2011. **57**(6): p. 919-21.
342. Yu, Z., et al., *Functional analysis of miR-34c as a putative tumor suppressor in high-grade serous ovarian cancer.* Biol Reprod, 2014. **91**(5): p. 113.
343. Livak, K.J. and T.D. Schmittgen, *Analysis of relative gene expression data using real-time quantitative PCR and the 2(-Delta Delta C(T)) Method.* Methods, 2001. **25**(4): p. 402-8.
344. Faul, F., et al., *G*Power 3: a flexible statistical power analysis program for the social, behavioral, and biomedical sciences.* Behav Res Methods, 2007. **39**(2): p. 175-91.
345. Faul, F., et al., *Statistical power analyses using G*Power 3.1: tests for correlation and regression analyses.* Behav Res Methods, 2009. **41**(4): p. 1149-60.
346. Subramanian, A., et al., *Gene set enrichment analysis: a knowledge-based approach for interpreting genome-wide expression profiles.* Proc Natl Acad Sci U S A, 2005. **102**(43): p. 15545-50.
347. Liberzon, A., et al., *The Molecular Signatures Database (MSigDB) hallmark gene set collection.* Cell Syst, 2015. **1**(6): p. 417-425.
348. Liberzon, A., et al., *Molecular signatures database (MSigDB) 3.0.* Bioinformatics, 2011. **27**(12): p. 1739-40.
349. Barretina, J., et al., *The Cancer Cell Line Encyclopedia enables predictive modelling of anticancer drug sensitivity.* Nature, 2012. **483**(7391): p. 603-7.
350. Lu, X., et al., *SSMD: a semi-supervised approach for a robust cell type identification and deconvolution of mouse transcriptomics data.* Brief Bioinform, 2021. **22**(4).
351. Wan, C., et al., *LTMG: a novel statistical modeling of transcriptional expression states in single-cell RNA-Seq data.* Nucleic Acids Res, 2019. **47**(18): p. e111.
352. Lau, D.H., et al., *Multifactorial mechanisms associated with broad cross-resistance of ovarian carcinoma cells selected by cyanomorpholino doxorubicin.* Cancer Res, 1991. **51**(19): p. 5181-7.

353. Lau, D.H., K.L. Ross, and B.I. Sikic, *Paradoxical increase in DNA cross-linking in a human ovarian carcinoma cell line resistant to cyanomorpholino doxorubicin.* Cancer Res, 1990. **50**(13): p. 4056-60.
354. Provencher, D.M., et al., *Characterization of four novel epithelial ovarian cancer cell lines.* In Vitro Cell Dev Biol Anim, 2000. **36**(6): p. 357-61.
355. Alley, M.C., et al., *Feasibility of drug screening with panels of human tumor cell lines using a microculture tetrazolium assay.* Cancer Res, 1988. **48**(3): p. 589-601.
356. Yu, D., et al., *Enhanced c-erbB-2/neu expression in human ovarian cancer cells correlates with more severe malignancy that can be suppressed by E1A.* Cancer Res, 1993. **53**(4): p. 891-8.
357. Gorai, I., et al., *Establishment and characterization of two human ovarian clear cell adenocarcinoma lines from metastatic lesions with different properties.* Gynecol Oncol, 1995. **57**(1): p. 33-46.
358. Morisawa, T., et al., *[Establishment and characterization of a new SCC antigen producing cell line (HCS-2) from a carcinoma of the uterine cervix].* Hum Cell, 1988. **1**(3): p. 308-14.
359. Sasa, H., et al., *[Establishment and characterization of a CA125-producing human ovarian clear cell carcinoma cell line].* Hum Cell, 1993. **6**(4): p. 279-86.
360. Yonamine, K., K. Hayashi, and T. Iida, *Establishment and characterization of human ovarian clear cell adenocarcinoma cell line (SMOV-2), and its cytotoxity by anticancer agents.* Hum Cell, 1999. **12**(3): p. 139-48.
361. Eva, A., et al., *Cellular genes analogous to retroviral onc genes are transcribed in human tumour cells.* Nature, 1982. **295**(5845): p. 116-9.
362. Li, M., et al., *Integrated analysis of DNA methylation and gene expression reveals specific signaling pathways associated with platinum resistance in ovarian cancer.* BMC Med Genomics, 2009. **2**: p. 34.
363. Fogh, J., J.M. Fogh, and T. Orfeo, *One hundred and twenty-seven cultured human tumor cell lines producing tumors in nude mice.* J Natl Cancer Inst, 1977. **59**(1): p. 221-6.
364. Nozawa, S., et al., *Establishment of a human ovarian clear cell carcinoma cell line (RMG-I) and its single cell cloning--with special reference to the stem cell of the tumor.* Hum Cell, 1988. **1**(4): p. 426-35.
365. Creighton, C.J., et al., *A bioinformatics tool for linking gene expression profiling results with public databases of microRNA target predictions.* RNA, 2008. **14**(11): p. 2290-6.
366. Lewis, B.P., C.B. Burge, and D.P. Bartel, *Conserved seed pairing, often flanked by adenosines, indicates that thousands of human genes are microRNA targets.* Cell, 2005. **120**(1): p. 15-20.
367. Agarwal, V., et al., *Predicting effective microRNA target sites in mammalian mRNAs.* Elife, 2015. **4**.
368. Liu, W. and X. Wang, *Prediction of functional microRNA targets by integrative modeling of microRNA binding and target expression data.* Genome Biol, 2019. **20**(1): p. 18.
369. Chen, Y. and X. Wang, *miRDB: an online database for prediction of functional microRNA targets.* Nucleic Acids Res, 2020. **48**(D1): p. D127-D131.

370. Huang, H.Y., et al., *miRTarBase update 2022: an informative resource for experimentally validated miRNA-target interactions.* Nucleic Acids Res, 2022. **50**(D1): p. D222-D230.
371. Bast, R.C., Jr., et al., *Critical questions in ovarian cancer research and treatment: Report of an American Association for Cancer Research Special Conference.* Cancer, 2019. **125**(12): p. 1963-1972.
372. Ayhan, A., et al., *Loss of ARID1A expression is an early molecular event in tumor progression from ovarian endometriotic cyst to clear cell and endometrioid carcinoma.* Int J Gynecol Cancer, 2012. **22**(8): p. 1310-5.
373. Wendel, J.R.H., X. Wang, and S.M. Hawkins, *The Endometriotic Tumor Microenvironment in Ovarian Cancer.* Cancers (Basel), 2018. **10**(8): p. E261.
374. Yamaguchi, K., et al., *Identification of an ovarian clear cell carcinoma gene signature that reflects inherent disease biology and the carcinogenic processes.* Oncogene, 2010. **29**(12): p. 1741-52.
375. Marquez, R.T., et al., *Patterns of gene expression in different histotypes of epithelial ovarian cancer correlate with those in normal fallopian tube, endometrium, and colon.* Clin Cancer Res, 2005. **11**(17): p. 6116-26.
376. Jimbo, H., et al., *Prevalence of ovarian endometriosis in epithelial ovarian cancer.* Int J Gynaecol Obstet, 1997. **59**(3): p. 245-50.
377. Prat, J., et al., *Abridged republication of FIGO's staging classification for cancer of the ovary, fallopian tube, and peritoneum.* Eur J Gynaecol Oncol, 2015. **36**(4): p. 367-9.
378. Chen, Y. and P.S. Meltzer, *Gene expression analysis via multidimensional scaling.* Curr Protoc Bioinformatics, 2005. **Chapter 7**: p. Unit 7 11.
379. Yamamoto, S., et al., *Cumulative alterations of p27-related cell-cycle regulators in the development of endometriosis-associated ovarian clear cell adenocarcinoma.* Histopathology, 2010. **56**(6): p. 740-9.
380. Hever, A., et al., *Human endometriosis is associated with plasma cells and overexpression of B lymphocyte stimulator.* Proc Natl Acad Sci U S A, 2007. **104**(30): p. 12451-6.
381. Chand, A.L., et al., *Laser capture microdissection and cDNA array analysis of endometrium identify CCL16 and CCL21 as epithelial-derived inflammatory mediators associated with endometriosis.* Reprod Biol Endocrinol, 2007. **5**: p. 18.
382. Lawson, C., et al., *Abnormal interleukin 1 receptor types I and II gene expression in eutopic and ectopic endometrial tissues of women with endometriosis.* J Reprod Immunol, 2008. **77**(1): p. 75-84.
383. Zhao, H., et al., *A cross-study gene set enrichment analysis identifies critical pathways in endometriosis.* Reprod Biol Endocrinol, 2009. **7**: p. 94.
384. Anglesio, M.S., et al., *Type-specific cell line models for type-specific ovarian cancer research.* PLoS One, 2013. **8**(9): p. e72162.
385. Papp, E., et al., *Integrated Genomic, Epigenomic, and Expression Analyses of Ovarian Cancer Cell Lines.* Cell Rep, 2018. **25**(9): p. 2617-2633.
386. McCabe, A., et al., *Investigating the suitability of in vitro cell lines as models for the major subtypes of epithelial ovarian cancer.* Front Cell Dev Biol, 2023. **11**: p. 1104514.

387. Parker, R.J., et al., *Acquired cisplatin resistance in human ovarian cancer cells is associated with enhanced repair of cisplatin-DNA lesions and reduced drug accumulation.* J Clin Invest, 1991. **87**(3): p. 772-7.
388. Ince, T.A., et al., *Characterization of twenty-five ovarian tumour cell lines that phenocopy primary tumours.* Nat Commun, 2015. **6**: p. 7419.
389. Blayney, J.K., et al., *Prior knowledge transfer across transcriptional data sets and technologies using compositional statistics yields new mislabelled ovarian cell line.* Nucleic Acids Res, 2016. **44**(17): p. e137.
390. Benard, J., et al., *Characterization of a human ovarian adenocarcinoma line, IGROV1, in tissue culture and in nude mice.* Cancer Res, 1985. **45**(10): p. 4970-9.
391. Caumanns, J.J., et al., *Integrative Kinome Profiling Identifies mTORC1/2 Inhibition as Treatment Strategy in Ovarian Clear Cell Carcinoma.* Clin Cancer Res, 2018. **24**(16): p. 3928-3940.
392. Itamochi, H., et al., *Establishment and characterization of a novel ovarian clear cell adenocarcinoma cell line, TU-OC-1, with a mutation in the PIK3CA gene.* Hum Cell, 2013. **26**(3): p. 121-7.
393. Zhang, X., et al., *Identification of Three Potential Prognostic Genes in Platinum-Resistant Ovarian Cancer via Integrated Bioinformatics Analysis.* Cancer Manag Res, 2021. **13**: p. 8629-8646.
394. Shaw, T.J., et al., *Characterization of intraperitoneal, orthotopic, and metastatic xenograft models of human ovarian cancer.* Mol Ther, 2004. **10**(6): p. 1032-42.
395. Wang, X., M. Ivan, and S.M. Hawkins, *The role of MicroRNA molecules and MicroRNA-regulating machinery in the pathogenesis and progression of epithelial ovarian cancer.* Gynecol Oncol, 2017. **147**(2): p. 481-487.
396. Ditto, A., et al., *Validation of MiROvaR, a microRNA-based predictor of early relapse in early stage epithelial ovarian cancer as a new strategy to optimise patients' prognostic assessment.* Eur J Cancer, 2022. **161**: p. 55-63.
397. Bagnoli, M., et al., *Development and validation of a microRNA-based signature (MiROvaR) to predict early relapse or progression of epithelial ovarian cancer: a cohort study.* Lancet Oncol, 2016. **17**(8): p. 1137-1146.
398. Wyman, S.K., et al., *Repertoire of microRNAs in epithelial ovarian cancer as determined by next generation sequencing of small RNA cDNA libraries.* PLoS One, 2009. **4**(4): p. e5311.
399. Dahiya, N., et al., *MicroRNA expression and identification of putative miRNA targets in ovarian cancer.* PLoS One, 2008. **3**(6): p. e2436.
400. Chang, C.H., et al., *The prognostic significance of RUNX2 and miR-10a/10b and their inter-relationship in breast cancer.* J Transl Med, 2014. **12**: p. 257.
401. Sun, W., et al., *MicroRNA-10a silencing reverses cisplatin resistance in the A549/cisplatin human lung cancer cell line via the transforming growth factor-beta/Smad2/STAT3/STAT5 pathway.* Mol Med Rep, 2015. **11**(5): p. 3854-9.
402. Lee, J.W., et al., *Altered MicroRNA expression in cervical carcinomas.* Clin Cancer Res, 2008. **14**(9): p. 2535-42.
403. Huang, T., et al., *miR10a increases the cisplatin resistance of lung adenocarcinoma circulating tumor cells via targeting PIK3CA in the PI3K/Akt pathway.* Oncol Rep, 2020. **43**(6): p. 1906-1914.

404. Utsunomiya, H., et al., *Paclitaxel-platinum combination chemotherapy for advanced or recurrent ovarian clear cell adenocarcinoma: a multicenter trial.* Int J Gynecol Cancer, 2006. **16**(1): p. 52-6.
405. Takano, M., et al., *Clear cell carcinoma of the ovary: a retrospective multicentre experience of 254 patients with complete surgical staging.* Br J Cancer, 2006. **94**(10): p. 1369-74.
406. Ho, C.M., et al., *Pure-type clear cell carcinoma of the ovary as a distinct histological type and improved survival in patients treated with paclitaxel-platinum-based chemotherapy in pure-type advanced disease.* Gynecol Oncol, 2004. **94**(1): p. 197-203.
407. Pectasides, D., et al., *Advanced stage clear-cell epithelial ovarian cancer: the Hellenic Cooperative Oncology Group experience.* Gynecol Oncol, 2006. **102**(2): p. 285-91.
408. Zhu, H., M. Kang, and X. Bai, *TCF21 regulates miR-10a-5p/LIN28B signaling to block the proliferation and invasion of melanoma cells.* PLoS One, 2021. **16**(8): p. e0255971.
409. Yuan, Z. and W. Wang, *LncRNA SNHG4 regulates miR-10a/PTEN to inhibit the proliferation of acute myeloid leukemia cells.* Hematology, 2020. **25**(1): p. 160-164.
410. Zhu, M., et al., *CircRNA circSEPT9 Downregulates miR-10a through Methylation to Promote Cell Proliferation in Laryngeal Squamous Cell Carcinoma.* Crit Rev Eukaryot Gene Expr, 2021. **31**(6): p. 17-22.
411. He, L. and G.J. Hannon, *MicroRNAs: small RNAs with a big role in gene regulation.* Nat Rev Genet, 2004. **5**(7): p. 522-31.
412. Wang, J., et al., *WebGestalt 2017: a more comprehensive, powerful, flexible and interactive gene set enrichment analysis toolkit.* Nucleic Acids Res, 2017. **45**(W1): p. W130-W137.
413. Bracker, T.U., et al., *Efficacy of MS-275, a selective inhibitor of class I histone deacetylases, in human colon cancer models.* Int J Oncol, 2009. **35**(4): p. 909-20.
414. Li, X., et al., *AKAP2 is upregulated in ovarian cancer, and promotes growth and migration of cancer cells.* Mol Med Rep, 2017. **16**(4): p. 5151-5156.
415. Wang, B., et al., *AKAP2 overexpression modulates growth plate chondrocyte functions through ERK1/2 signaling.* Bone, 2021. **146**: p. 115875.
416. Meyerson, M. and E. Harlow, *Identification of G1 kinase activity for cdk6, a novel cyclin D partner.* Mol Cell Biol, 1994. **14**(3): p. 2077-86.
417. Romero-Pozuelo, J., et al., *Cdk4 and Cdk6 Couple the Cell-Cycle Machinery to Cell Growth via mTORC1.* Cell Rep, 2020. **31**(2): p. 107504.
418. Cao, J., et al., *Exosomal miR-21-5p contributes to ovarian cancer progression by regulating CDK6.* Hum Cell, 2021. **34**(4): p. 1185-1196.
419. Duan, L., et al., *MuiR-182-5p functions as a tumor suppressor to sensitize human ovarian cancer cells to cisplatin through direct targeting the cyclin dependent kinase 6 (CDK6).* J BUON, 2020. **25**(5): p. 2279-2286.
420. Wang, T., et al., *Rap2A/p-ERK1/2 is involved in glioma proliferation and migration.* Curr Mol Med, 2022.
421. Zhang, J., et al., *Knockdown of RAP2A gene expression suppresses cisplatin resistance in gastric cancer cells.* Oncol Lett, 2020. **19**(1): p. 350-358.

422. Wu, J.X., et al., *Rap2a is a novel target gene of p53 and regulates cancer cell migration and invasion.* Cell Signal, 2015. **27**(6): p. 1198-207.
423. Dong, Y., et al., *MicroRNA-335 suppresses the proliferation, migration, and invasion of breast cancer cells by targeting EphA4.* Mol Cell Biochem, 2018. **439**(1-2): p. 95-104.
424. Ding, L., et al., *EphA4 promotes cell proliferation and cell adhesion-mediated drug resistance via the AKT pathway in multiple myeloma.* Tumour Biol, 2017. **39**(3): p. 1010428317694298.
425. Segal, M. and F.J. Slack, *Challenges identifying efficacious miRNA therapeutics for cancer.* Expert Opin Drug Discov, 2020. **15**(9): p. 987-992.
426. Armstrong, D.K., et al., *NCCN Guidelines Insights: Ovarian Cancer, Version 1.2019.* J Natl Compr Canc Netw, 2019. **17**(8): p. 896-909.
427. Bast, R.C., Jr., B. Hennessy, and G.B. Mills, *The biology of ovarian cancer: new opportunities for translation.* Nat Rev Cancer, 2009. **9**(6): p. 415-28.
428. Presta, L.G., et al., *Humanization of an anti-vascular endothelial growth factor monoclonal antibody for the therapy of solid tumors and other disorders.* Cancer research, 1997. **57**(20): p. 4593-4599.
429. Pujade-Lauraine, E., et al., *Bevacizumab combined with chemotherapy for platinum-resistant recurrent ovarian cancer: The AURELIA open-label randomized phase III trial.* J Clin Oncol, 2014. **32**(13): p. 1302-8.
430. Aghajanian, C., et al., *OCEANS: a randomized, double-blind, placebo-controlled phase III trial of chemotherapy with or without bevacizumab in patients with platinum-sensitive recurrent epithelial ovarian, primary peritoneal, or fallopian tube cancer.* J Clin Oncol, 2012. **30**(17): p. 2039-45.
431. Yeo, K.T., et al., *Vascular permeability factor (vascular endothelial growth factor) in guinea pig and human tumor and inflammatory effusions.* Cancer Res, 1993. **53**(12): p. 2912-8.
432. Olson, T.A., et al., *Vascular permeability factor gene expression in normal and neoplastic human ovaries.* Cancer Res, 1994. **54**(1): p. 276-80.
433. Tewari, K.S., et al., *Final Overall Survival of a Randomized Trial of Bevacizumab for Primary Treatment of Ovarian Cancer.* J Clin Oncol, 2019. **37**(26): p. 2317-2328.
434. Colomban, O., et al., *Bevacizumab for Newly Diagnosed Ovarian Cancers: Best Candidates Among High-Risk Disease Patients (ICON-7).* JNCI Cancer Spectr, 2020. **4**(3): p. pkaa026.
435. Paley, P.J., et al., *Vascular endothelial growth factor expression in early stage ovarian carcinoma.* Cancer: Interdisciplinary International Journal of the American Cancer Society, 1997. **80**(1): p. 98-106.
436. Tate, S., et al., *Bevacizumab in First-Line Chemotherapy Improves Progression-Free Survival for Advanced Ovarian Clear Cell Carcinoma.* Cancers (Basel), 2021. **13**(13).
437. Coleman, R.L., et al., *Bevacizumab and paclitaxel-carboplatin chemotherapy and secondary cytoreduction in recurrent, platinum-sensitive ovarian cancer (NRG Oncology/Gynecologic Oncology Group study GOG-0213): a multicentre, open-label, randomised, phase 3 trial.* Lancet Oncol, 2017. **18**(6): p. 779-791.

438. Perren, T.J., et al., *A phase 3 trial of bevacizumab in ovarian cancer.* N Engl J Med, 2011. **365**(26): p. 2484-96.
439. Burger, R.A., et al., *Incorporation of bevacizumab in the primary treatment of ovarian cancer.* N Engl J Med, 2011. **365**(26): p. 2473-83.
440. Ying, H.C., et al., *MicroRNA signatures of platinum-resistance in ovarian cancer.* Eur J Gynaecol Oncol, 2015. **36**(1): p. 16-20.
441. Phatak, P., et al., *MicroRNA-141-3p regulates cellular proliferation, migration, and invasion in esophageal cancer by targeting tuberous sclerosis complex 1.* Mol Carcinog, 2021. **60**(2): p. 125-137.
442. Qi, X., et al., *Network vulnerability-based and knowledge-guided identification of microRNA biomarkers indicating platinum resistance in high-grade serous ovarian cancer.* Clin Transl Med, 2019. **8**(1): p. 28.
443. Momin, M.Y., et al., *The Challenges and Opportunities in the Development of MicroRNA Therapeutics: A Multidisciplinary Viewpoint.* Cells, 2021. **10**(11).
444. Seyhan, A.A., *Trials and Tribulations of MicroRNA Therapeutics.* Int J Mol Sci, 2024. **25**(3).
445. Aftab, M., et al., *Urine miRNA signature as a potential non-invasive diagnostic and prognostic biomarker in cervical cancer.* Sci Rep, 2021. **11**(1): p. 10323.
446. Ujifuku, K., et al., *miR-195, miR-455-3p and miR-10a(*) are implicated in acquired temozolomide resistance in glioblastoma multiforme cells.* Cancer Lett, 2010. **296**(2): p. 241-8.
447. Slaby, O., et al., *MicroRNAs in colorectal cancer: translation of molecular biology into clinical application.* Mol Cancer, 2009. **8**: p. 102.
448. Haikalis, M.E., et al., *MicroRNA expression pattern differs depending on endometriosis lesion type.* Biol Reprod, 2018. **98**(5): p. 623-633.
449. Li, D., et al., *miR-10a-5p inhibits chicken granulosa cells proliferation and Progesterone(P4) synthesis by targeting MAPRE1 to suppress CDK2.* Theriogenology, 2022. **192**: p. 97-108.
450. Han, Y., et al., *lncRNA FLVCR1-AS1 drives colorectal cancer progression via modulation of the miR-381/RAP2A axis.* Mol Med Rep, 2021. **23**(2).
451. Wang, X., R. Meng, and Q.M. Hu, *LINC00319-Mediated miR-3127 Repression Enhances Bladder Cancer Progression Through Upregulation of RAP2A.* Front Genet, 2020. **11**: p. 180.
452. Wu, F., et al., *The Suppression of miR-199a-3p by Promoter Methylation Contributes to Papillary Thyroid Carcinoma Aggressiveness by Targeting RAP2a and DNMT3a.* Front Cell Dev Biol, 2020. **8**: p. 594528.
453. Weiner-Gorzel, K., et al., *Overexpression of the microRNA miR-433 promotes resistance to paclitaxel through the induction of cellular senescence in ovarian cancer cells.* Cancer Med, 2015. **4**(5): p. 745-58.
454. Pan, J.X., et al., *Aberrant SERPINE1 DNA methylation is involved in carboplatin induced epithelial-mesenchymal transition in epithelial ovarian cancer.* Arch Gynecol Obstet, 2017. **296**(6): p. 1145-1152.
455. Zhao, C. and Z. Liu, *MicroRNA 617 Targeting SERPINE1 Inhibited the Progression of Oral Squamous Cell Carcinoma.* Mol Cell Biol, 2021. **41**(6): p. e0056520.

456. Giaginis, C., et al., *Ephrin (Eph) receptor A1, A4, A5 and A7 expression in human non-small cell lung carcinoma: associations with clinicopathological parameters, tumor proliferative capacity and patients' survival.* BMC Clin Pathol, 2014. **14**(1): p. 8.
457. Kori, M. and K. Yalcin Arga, *Potential biomarkers and therapeutic targets in cervical cancer: Insights from the meta-analysis of transcriptomics data within network biomedicine perspective.* PLoS One, 2018. **13**(7): p. e0200717.
458. Saintigny, P., et al., *Global evaluation of Eph receptors and ephrins in lung adenocarcinomas identifies EphA4 as an inhibitor of cell migration and invasion.* Mol Cancer Ther, 2012. **11**(9): p. 2021-32.
459. Yan, Y., et al., *MicroRNA-10a is involved in the metastatic process by regulating Eph tyrosine kinase receptor A4-mediated epithelial-mesenchymal transition and adhesion in hepatoma cells.* Hepatology, 2013. **57**(2): p. 667-77.
460. Luo, L., et al., *Exosomal MicroRNA-10a Is Associated with Liver Regeneration in Rats through Downregulation of EphA4.* Chin Med J (Engl), 2018. **131**(4): p. 454-460.
461. Goel, S., J.S. Bergholz, and J.J. Zhao, *Targeting CDK4 and CDK6 in cancer.* Nat Rev Cancer, 2022. **22**(6): p. 356-372.
462. Szoltysek, K., et al., *RRAD, IL4I1, CDKN1A, and SERPINE1 genes are potentially co-regulated by NF-kappaB and p53 transcription factors in cells exposed to high doses of ionizing radiation.* BMC Genomics, 2018. **19**(1): p. 813.
463. Goel, S., et al., *CDK4/6 inhibition triggers anti-tumour immunity.* Nature, 2017. **548**(7668): p. 471-475.
464. Horwitz, S.B., et al., *Taxol: mechanisms of action and resistance.* Ann N Y Acad Sci, 1986. **466**: p. 733-44.
465. Basourakos, S.P., et al., *Combination Platinum-based and DNA Damage Response-targeting Cancer Therapy: Evolution and Future Directions.* Curr Med Chem, 2017. **24**(15): p. 1586-1606.
466. Kelso, T.W.R., et al., *Chromatin accessibility underlies synthetic lethality of SWI/SNF subunits in ARID1A-mutant cancers.* Elife, 2017. **6**.
467. Fukumoto, T., et al., *Repurposing Pan-HDAC Inhibitors for ARID1A-Mutated Ovarian Cancer.* Cell Rep, 2018. **22**(13): p. 3393-3400.
468. Wu, S., et al., *SWI/SNF catalytic subunits' switch drives resistance to EZH2 inhibitors in ARID1A-mutated cells.* Nat Commun, 2018. **9**(1): p. 4116.
469. Salem, M., et al., *miR-590-3p Promotes Ovarian Cancer Growth and Metastasis via a Novel FOXA2-Versican Pathway.* Cancer Res, 2018. **78**(15): p. 4175-4190.
470. Reyes, A.L.P., et al., *GENAVi: a shiny web application for gene expression normalization, analysis and visualization.* BMC Genomics, 2019. **20**(1): p. 745.
471. Baldi, S., et al., *ARID1A downregulation promotes cell proliferation and migration of colon cancer via VIM activation and CDH1 suppression.* J Cell Mol Med, 2022. **26**(24): p. 5984-5997.
472. Naffar-Abu Amara, S., et al., *Transient commensal clonal interactions can drive tumor metastasis.* Nat Commun, 2020. **11**(1): p. 5799.
473. Lui, G.Y.L., et al., *BET, SRC, and BCL2 family inhibitors are synergistic drug combinations with PARP inhibitors in ovarian cancer.* EBioMedicine, 2020. **60**: p. 102988.

474. McCorkle, J.R., et al., *Lapatinib and poziotinib overcome ABCB1-mediated paclitaxel resistance in ovarian cancer.* PLoS One, 2021. **16**(8): p. e0254205.
475. Akasu-Nagayoshi, Y., et al., *PHOSPHATE exporter XPR1/SLC53A1 is required for the tumorigenicity of epithelial ovarian cancer.* Cancer Sci, 2022. **113**(6): p. 2034-2043.
476. Wang, C.K., et al., *MEX3A Mediates p53 Degradation to Suppress Ferroptosis and Facilitate Ovarian Cancer Tumorigenesis.* Cancer Res, 2023. **83**(2): p. 251-263.
477. Yoshida, K., et al., *Expression of the chrXq27.3 miRNA cluster in recurrent ovarian clear cell carcinoma and its impact on cisplatin resistance.* Oncogene, 2021. **40**(7): p. 1255-1268.
478. Bard-Chapeau, E.A., et al., *Ecotopic viral integration site 1 (EVI1) regulates multiple cellular processes important for cancer and is a synergistic partner for FOS protein in invasive tumors.* Proc Natl Acad Sci U S A, 2012. **109**(6): p. 2168-73.
479. Houshdaran, S., et al., *DNA methylation profiles of ovarian epithelial carcinoma tumors and cell lines.* PLoS One, 2010. **5**(2): p. e9359.
480. Ascierto, M.L., et al., *Permissivity of the NCI-60 cancer cell lines to oncolytic Vaccinia Virus GLV-1h68.* BMC Cancer, 2011. **11**: p. 451.
481. Komatsu, M., et al., *Prediction of individual response to platinum/paclitaxel combination using novel marker genes in ovarian cancers.* Mol Cancer Ther, 2006. **5**(3): p. 767-75.
482. Song, H., et al., *PAX2 Expression in Ovarian Cancer.* Int J Mol Sci, 2013. **14**(3): p. 6090-105.
483. Koussounadis, A., et al., *Chemotherapy-induced dynamic gene expression changes in vivo are prognostic in ovarian cancer.* Br J Cancer, 2014. **110**(12): p. 2975-84.
484. Koussounadis, A., et al., *Dynamic modulation of phosphoprotein expression in ovarian cancer xenograft models.* BMC Cancer, 2016. **16**: p. 205.
485. Pradeep, S., et al., *Hematogenous metastasis of ovarian cancer: rethinking mode of spread.* Cancer Cell, 2014. **26**(1): p. 77-91.
486. Bitler, B.G., et al., *Synthetic lethality by targeting EZH2 methyltransferase activity in ARID1A-mutated cancers.* Nat Med, 2015. **21**(3): p. 231-8.
487. Balbin, O.A., et al., *The landscape of antisense gene expression in human cancers.* Genome Res, 2015. **25**(7): p. 1068-79.
488. Sharrow, A.C., et al., *Characterization of aldehyde dehydrogenase 1 high ovarian cancer cells: Towards targeted stem cell therapy.* Gynecol Oncol, 2016. **142**(2): p. 341-8.
489. Bitler, B.G., et al., *ARID1A-mutated ovarian cancers depend on HDAC6 activity.* Nat Cell Biol, 2017. **19**(8): p. 962-973.
490. Faddaoui, A., et al., *Suppression of the grainyhead transcription factor 2 gene (GRHL2) inhibits the proliferation, migration, invasion and mediates cell cycle arrest of ovarian cancer cells.* Cell Cycle, 2017. **16**(7): p. 693-706.
491. Medrano, M., et al., *Interrogation of Functional Cell-Surface Markers Identifies CD151 Dependency in High-Grade Serous Ovarian Cancer.* Cell Rep, 2017. **18**(10): p. 2343-2358.

492. Lin, X., et al., *Super-Enhancer-Associated LncRNA UCA1 Interacts Directly with AMOT to Activate YAP Target Genes in Epithelial Ovarian Cancer.* iScience, 2019. **17**: p. 242-255.
493. Corona, R.I., et al., *Non-coding somatic mutations converge on the PAX8 pathway in ovarian cancer.* Nat Commun, 2020. **11**(1): p. 2020.
494. Nakamura, K., et al., *Functional analysis of the 1p34.3 risk locus implicates GNL2 in high-grade serous ovarian cancer.* Am J Hum Genet, 2022. **109**(1): p. 116-135.
495. Heong, V., et al., *A multi-ethnic analysis of immune-related gene expression signatures in patients with ovarian clear cell carcinoma.* J Pathol, 2021. **255**(3): p. 285-295.
496. Denkert, C., et al., *A prognostic gene expression index in ovarian cancer - validation across different independent data sets.* J Pathol, 2009. **218**(2): p. 273-80.
497. Alldredge, J., et al., *Transcriptome Analysis of Ovarian and Uterine Clear Cell Malignancies.* Front Oncol, 2020. **10**: p. 598579.
498. Ramakrishna, M., et al., *Identification of candidate growth promoting genes in ovarian cancer through integrated copy number and expression analysis.* PLoS One, 2010. **5**(4): p. e9983.
499. Yin, M., et al., *Differential molecular pathway expression according to chemotherapeutic response in ovarian clear cell carcinoma.* BMC Womens Health, 2023. **23**(1): p. 298.
500. Gentric, G., et al., *PML-Regulated Mitochondrial Metabolism Enhances Chemosensitivity in Human Ovarian Cancers.* Cell Metab, 2019. **29**(1): p. 156-173 e10.
501. Mateescu, B., et al., *miR-141 and miR-200a act on ovarian tumorigenesis by controlling oxidative stress response.* Nat Med, 2011. **17**(12): p. 1627-35.
502. Mieulet, V., et al., *Stiffness increases with myofibroblast content and collagen density in mesenchymal high grade serous ovarian cancer.* Sci Rep, 2021. **11**(1): p. 4219.
503. Stany, M.P., et al., *Identification of novel therapeutic targets in microdissected clear cell ovarian cancers.* PLoS One, 2011. **6**(7): p. e21121.
504. Ferriss, J.S., et al., *Multi-gene expression predictors of single drug responses to adjuvant chemotherapy in ovarian carcinoma: predicting platinum resistance.* PLoS One, 2012. **7**(2): p. e30550.
505. Huang, R.Y., et al., *Histotype-specific copy-number alterations in ovarian cancer.* BMC Med Genomics, 2012. **5**: p. 47.
506. Arildsen, N.S., et al., *Involvement of Chromatin Remodeling Genes and the Rho GTPases RhoB and CDC42 in Ovarian Clear Cell Carcinoma.* Front Oncol, 2017. **7**: p. 109.
507. Abiko, K., et al., *PD-L1 on tumor cells is induced in ascites and promotes peritoneal dissemination of ovarian cancer through CTL dysfunction.* Clin Cancer Res, 2013. **19**(6): p. 1363-74.
508. Ukita, M., et al., *CXCL13-producing CD4+ T cells accumulate in the early phase of tertiary lymphoid structures in ovarian cancer.* JCI Insight, 2022. **7**(12).

509. Wu, Y.H., et al., *COL11A1 promotes tumor progression and predicts poor clinical outcome in ovarian cancer.* Oncogene, 2014. **33**(26): p. 3432-40.
510. Wu, Y.H., et al., *COL11A1 confers chemoresistance on ovarian cancer cells through the activation of Akt/c/EBPbeta pathway and PDK1 stabilization.* Oncotarget, 2015. **6**(27): p. 23748-63.
511. Karlan, B.Y., et al., *POSTN/TGFBI-associated stromal signature predicts poor prognosis in serous epithelial ovarian cancer.* Gynecol Oncol, 2014. **132**(2): p. 334-42.
512. Tyekucheva, S., et al., *Comparing Platforms for Messenger RNA Expression Profiling of Archival Formalin-Fixed, Paraffin-Embedded Tissues.* J Mol Diagn, 2015. **17**(4): p. 374-81.
513. Abiko, K., et al., *IFN-gamma from lymphocytes induces PD-L1 expression and promotes progression of ovarian cancer.* Br J Cancer, 2015. **112**(9): p. 1501-9.
514. Hendrix, N.D., et al., *Fibroblast growth factor 9 has oncogenic activity and is a downstream target of Wnt signaling in ovarian endometrioid adenocarcinomas.* Cancer Res, 2006. **66**(3): p. 1354-62.
515. Bommer, G.T., et al., *IRS1 regulation by Wnt/beta-catenin signaling and varied contribution of IRS1 to the neoplastic phenotype.* J Biol Chem, 2010. **285**(3): p. 1928-38.
516. Wu, R., et al., *Mouse model of human ovarian endometrioid adenocarcinoma based on somatic defects in the Wnt/beta-catenin and PI3K/Pten signaling pathways.* Cancer Cell, 2007. **11**(4): p. 321-33.
517. Wu, R., et al., *Impact of oviductal versus ovarian epithelial cell of origin on ovarian endometrioid carcinoma phenotype in the mouse.* J Pathol, 2016. **240**(3): p. 341-351.
518. Liu, Y., et al., *DNA methylation inhibition increases T cell KIR expression through effects on both promoter methylation and transcription factors.* Clin Immunol, 2009. **130**(2): p. 213-24.
519. Lisowska, K.M., et al., *Gene expression analysis in ovarian cancer - faults and hints from DNA microarray study.* Front Oncol, 2014. **4**: p. 6.
520. Lisowska, K.M., et al., *Unsupervised analysis reveals two molecular subgroups of serous ovarian cancer with distinct gene expression profiles and survival.* J Cancer Res Clin Oncol, 2016. **142**(6): p. 1239-52.
521. Uehara, Y., et al., *Correction: Integrated Copy Number and Expression Analysis Identifies Profiles of Whole-Arm Chromosomal Alterations and Subgroups with Favorable Outcome in Ovarian Clear Cell Carcinomas.* PLoS One, 2015. **10**(7): p. e0132751.
522. Schwartz, D.R., et al., *Gene expression in ovarian cancer reflects both morphology and biological behavior, distinguishing clear cell from other poor-prognosis ovarian carcinomas.* Cancer Res, 2002. **62**(16): p. 4722-9.
523. Way, G.P., et al., *Comprehensive Cross-Population Analysis of High-Grade Serous Ovarian Cancer Supports No More Than Three Subtypes.* G3 (Bethesda), 2016. **6**(12): p. 4097-4103.
524. Jazaeri, A.A., et al., *Gene expression profiles of BRCA1-linked, BRCA2-linked, and sporadic ovarian cancers.* J Natl Cancer Inst, 2002. **94**(13): p. 990-1000.

525. Marchini, S., et al., *Analysis of gene expression in early-stage ovarian cancer.* Clin Cancer Res, 2008. **14**(23): p. 7850-60.

CURRICULUM VITAE

Kaitlyn Elizabeth Collins

Current Position:
MD/PhD student, 3rd year Medical Student, Medical Scientist Training Program, Indiana University School of Medicine, Indianapolis, IN, USA

Education

Graduate
Indiana University
Indianapolis, IN
Ph.D.
Graduation: August 2024

Graduate
Indiana University School of Medicine
Indianapolis, IN
Medical Scientist Training Program
M.D. candidate
Intended Graduation: May 2026

Undergraduate
Indiana University College of Arts and Sciences
Bloomington, IN
Degree: Bachelor of Science in Biology and Neuroscience with High Distinction
Minors: Chemistry, Psychology, History, and an Honors Notation
Date of Completion: May 2016

Academic Positions

April 2018- August 2024 Hawkins Lab, Indiana	Medical Scientist Training Program, Graduate Student, University School of Medicine • Mentor: Shannon Hawkins, M.D., Ph.D.
August 2016-April 2018, July 2024- present	Medical Scientist Training Program, Medical Student, Indiana University School of Medicine • Mentors: Maureen Harrington, Ph.D. and Raghu Mirmira, M.D., Ph.D. Brittney-Shea Herbert, Ph.D. and Benjamin Gaston, M.D.
June 2014- July 2016	Undergraduate Research Assistant, Indiana University, Bloomington, IN • Mentor: Cara Wellman, Ph.D.

January-December 2014 Undergraduate Research Assistant, Indiana University, Bloomington, IN

- Mentors: Karin James, Ph.D. and Lisa Byrge, Ph.D.

Honors and Awards

2016 University Honors Graduate, Hutton Honor College, Indiana University Bloomington

2016 University Honors Graduate, College of Arts and Sciences, Biology Honors Thesis,
Indiana University Bloomington

2012-2016 IU Excellence Scholarship recipient, Indiana University Bloomington

2016 Phi Beta Kappa, Gamma of Indiana

2013-2016 Dean's List, 7 Semesters, Indiana University Bloomington

Mentoring Experience

2018-present American Physician Scientist Association, mentor to undergraduate students

2018-2024 Hawkins Lab, mentor or co-mentor to 5 Summer Research Program (SRP) students, 4 medical students, 2 undergraduate students, and 1 medical resident

2020-present Growth through Guidance, Mentor to local high school students interested in careers and science and medicine

Professional Affiliations

2016-present Member, Phi Beta Kappa

2016-present Member, American Medical Association

2016-2017 IU School of Medicine Northwest Service Learning Committee, MS1 Co-Chair

2017-present Combined Degree Student Council of IU School of Medicine, Class of 2024 Representative

2018-present American College of Obstetrics and Gynecology

2018-present American Physician Scientist Association

2019-2023 Society for the Study of Reproduction, Trainee and Public Affair Representative

Posters and Abstracts

1. Bollinger, J.L., **Collins, K.E**., Patel, R., Wellman, C.L. Sex differences in- and stress effects on- microglial activation in brain regions critical for emotion regulation. Society for Neuroscience 46th Annual Meeting, 2016.
2. **Collins, K.E.**, Wang, X., Zhang C., Rusch D, Buechlein A., Creighton C.J., Hawkins, S.M. Transcriptomic profiling and bioinformatic analysis of

endometriosis-associated ovarian clear cell carcinoma. Society for the Study of Reproduction 52nd Annual Meeting, 2019. P225.

3. **Collins, K.E.**, Wang, X., Nephew, K.P., Creighton C.J., Jones, D.E., Hawkins, S.M. MiR-10a Overexpression and Chemoresistance in Ovarian Clear Cell Carcinoma. Society for the Study of Reproduction 53rd Annual Meeting, 2020. Abstract #2025.
4. **Collins, K.E.**, Wang, X., Nephew, K.P., Creighton C.J., Hawkins, S.M. MiR-10a targets chemoresistance genes in ovarian clear cell carcinoma. Indiana University Simon Comprehensive Cancer Center Research Day, 2021. Poster #10.
5. **Collins, K.E.**, Wang, X., Nephew, K.P., Creighton C.J., Hawkins, S.M. MiR-10a targets chemoresistance genes in ovarian clear cell carcinoma. Society for the Study of Reproduction 54rd Annual Meeting, 2021. Poster #211.
6. Davis, N.B., **Collins, K.E.,** Hawkins, S.M. Function of miR-10a Overexpression in Ovarian Clear Cell Carcinoma. Indiana University Medical Student Program for Research and Scholarship Poster Session, 2022. N.B. Davis was mentored in the Hawkins Lab by K.E. Collins through the Cancer in the Under-Privileged Indigent or Disadvantaged (CUPID) Program and Indiana University Simon Comprehensive Cancer Center.
7. Wickware, S., **Collins, K.,** Wendel, J., Hawkins, S. *Arid1a* Expression in Early Whole Mice Ovaries. Indiana University Simon Cancer Center Summer Research Program Poster Session, 2022. S. Wickware was mentored in the Hawkins Lab by K. Collins through the American Cancer Society Diversity in Cancer Research (DICR) Program and Indiana University Simon Comprehensive Cancer Center.
8. **Collins, K.E.**, Wang, X., Wickware, S., Martinez, M., Klymenko, Y., Wendel, J., Kersey, J., Emerson, R., Zhang, C., Hawkins, S.M. Characterization of Cellular Senescence in a Mouse Model of Spontaneous Ovarian Endometrioma. Society for Reproductive Investigation 70th Annual Meeting, 2023. Abstract #1422.
9. **Collins, K.E.**, Wang, X., Wickware, S., Martinez, M., Klymenko, Y., Wendel, J., Kersey, J., Emerson, R., Zhang, C., Hawkins, S.M. Characterization of Cellular Senescence in a Mouse Model of Spontaneous Ovarian Endometrioma. Society for Reproductive Investigation 70th Annual Meeting, 2023. Abstract #1416.

Publications

1. Bollinger JL, **Collins KE**, Patel R, Wellman CL. Behavioral stress alters corticolimbic microglia in a sex- and brain region-specific manner. PLoS One. 2017;12(12):e0187631. Epub 2017/12/02. doi: 10.1371/journal.pone.0187631. PubMed PMID: 29194444; PMCID: PMC5711022.
2. Pandita P, Wang X, Jones DE, **Collins K**, Hawkins SM. Unique Molecular Features in High-Risk Histology Endometrial Cancers. Cancers (Basel). 2019;11(11):1665. Epub 2019/11/14. doi: 10.3390/cancers11111665. PubMed PMID: 31717878; PMCID: PMC6896116.
3. Peipert LJ, **Collins KE**, Zhao Q, Peipert JF. Copper intrauterine device and incident sexually transmitted infections. Am J Obstet Gynecol. 2021

Nov;225(5):579-580. doi: 10.1016/j.ajog.2021.07.026. Epub 2021 Sep 3. PMID: 34363781.

4. **Collins KE**, Wang X, Klymenko Y, Davis NB, Martinez MC, Zhang C, So K, Buechlein A, Rusch DB, Creighton CJ, Hawkins SM. Transcriptomic Analyses of Ovarian Clear-Cell Carcinoma with Concurrent Endometriosis. Frontiers. 2023 (pre-print).

Prior Research Support

Cancer Biology Training Award, IUSCC Collins (PI)
11/1/2019-10/31/2020

Transcriptomic profiling and bioinformatics analysis to determine unique molecular underpinnings of miR-10a in ovarian clear cell carcinoma within the endometriotic tumor microenvironment

The overall goal of this research project is to determine the impact of miR-10a on chemoresistance in ovarian clear cell carcinoma.

Role: PI